

**INVESTIGATING THE EFFECTS OF VARIOUS
REINFORCEMENTS ON THE BEARING CAPACITY OF
HIGHWAY PAVEMENT**

**KARAYOLU ÜST YAPISININ TAŞIMA KAPASİTESİNE
ÇEŞİTLİ DONATILARIN ETKİLERİNİN İNCELENMESİ**

VOLKAN BÜYÜKAKIN

ASST. PROF. DR. ELİF ÇİÇEK

Supervisor

Submitted to

Graduate School of Science and Engineering of Hacettepe University

as a Partial Fulfillment to the Requirements

for be Award of the Degree of Master of Science

in Civil Engineering.

2020

ÖZET

KARAYOLU ÜST YAPISININ TAŞIMA KAPASİTESİNE ÇEŞİTLİ DONATILARIN ETKİLERİNİN İNCELENMESİ

Volkan BÜYÜKAKIN

Yüksek Lisans, İnşaat Mühendisliği Bölümü

Tez Danışmanı: Dr. Elif ÇİÇEK

Temmuz 2020, 112 sayfa

Genellikle yol taşıma kapasitesini arttırmak amacıyla, temel ve alt temel tabaka kalınlıkları arttırılabilmektedir. Fakat bu yöntem yolun maliyetini önemli ölçüde etkilemektedir. Bu nedenle bu çalışmada, çeşitli donatı tipleri kullanılarak daha sağlam bir yol inşası sağlanarak, maliyete etkileri incelenmektedir. Çalışma iki ana bölümden oluşmaktadır. İlk bölümde geotekstil, geogrid, ve lif donatıların yolun taşıma kapasitesi üzerindeki etkileri ve zeminin davranışını nasıl değiştirdiği California Bearing Ratio (CBR) testleri ile incelenmiştir. Hazırlanan numunelerde donatılar farklı derinliklerde, adetlerde ve kombinasyonlarda test edilerek, zemin içerisinde en verimli yerleştirme şekli saptanmaya çalışılmıştır. Ayrıca donatılar mikroskop altında incelenerek, örgü biçimlerinin ve yüzeylerinin yolun taşıma kapasitesine etkileri tartışılmıştır. Buna ek olarak, donatıların performansları birbirleriyle karşılaştırılarak taşıma kapasitesini en çok arttıran malzemeler tespit edilmiştir. İkinci bölümde ise, otoyol ve taşıma standartlarını belirleyen AASHTO (American Association of State Highway and Transportation Officials)'nun belirlemiş olduğu esnek yol tasarım kriterlerine göre, kaplamasız bir yol tasarlanmıştır. Temel ve alt temel tabaka kalınlıkları, donatılı ve donatısız durumlar için

hesaplanmış ve karşılaştırılmıştır. Daha sonra ise zemin ve donatı maliyetleri de hesaba katılarak, modeller fiyat ve performans açısından değerlendirilmiştir. Sonuç olarak, farklı donatılı yol model örneklerinde davranışların değiştiği gözlemlenmiş, oturma arttıkça donatıların yolun taşıma kapasitesini önemli ölçüde arttırdığı ve gereken tabaka kalınlıklarını azaltarak inşaat maliyetini düşürdüğü tespit edilmiştir. Fiyat ve performans kriterleri birlikte düşünüldüğünde, en verimli sonuçlar ince geotekstil donatıyla güçlendirilmiş modellerde gözlemlenmiştir.

Anahtar Kelimeler: CBR, Lif, Geosentetik, Geotekstil, Geogrid, Maliyet Analizi

ABSTRACT

INVESTIGATING THE EFFECTS OF VARIOUS REINFORCEMENTS ON THE BEARING CAPACITY OF HIGHWAY PAVEMENT

Volkan BÜYÜKAKIN

Master of Science, Department of Civil Engineering

Supervisor: Asst. Prof. Dr. Elif ÇİÇEK

July 2020, 112 pages

Generally, in order to increase the road bearing capacity, base and subbase layer thicknesses can be increased. However, this method significantly affects the cost of the road. For this reason, this study examines the effects on cost by providing a more robust road construction by using various reinforcement types. The study consists of two main parts. In the first part, the effects of geotextiles, geogrids, and fiber reinforcements on the bearing capacity of the road and how the soil changes its behavior were examined with California Bearing Ratio (CBR) tests. In the prepared samples, reinforcements were tested in different depths, quantities and combinations, and the most efficient placement method was determined in the soil. In addition, the effects of knitting patterns and surfaces on the bearing capacity of the road were discussed by examining the reinforcements under a microscope. Also, by comparing the performances of the reinforcements with each other, the materials that increase the bearing capacity most were determined. In the second part, an uncoated road is designed according to the flexible road design criteria determined by AASHTO (American Association of State Highway and Transportation Officials), which sets the highway and transportation standards. Base

and subbase layer thicknesses were calculated for reinforced and unreinforced conditions and compared. Then, considering the soil and reinforcement costs, the models were evaluated in terms of price and performance. As a result, it was observed that the behaviors changed in different reinforced road model samples, and as the settlement increased, it was determined that the reinforcements significantly increased the bearing capacity of the road and decreased the construction cost by decreasing the required layer thicknesses. Considering the price and performance criteria together, the most efficient results were observed in models reinforced with thin geotextile reinforcement.

Keywords: CBR, Fiber, Geosynthetic, Geotextile, Geogrid, Cost Analysis

TEŐEKKÜR

Yüksek lisans eğitimim ve tez çalışmam sırasında kıymetli bilgilerini ve tecrübelerini benimle paylaşarak bana destek olan danışman hocam sayın Dr. Elif ÇİÇEK'e ve tez jürimde bulunarak değerli görüşleriyle vizyonumu genişletmeme katkıda bulunan sayın Prof. Dr. M. Vefa AKPINAR, Prof. Dr. Semra İDE, Prof. Dr. Serhat KÜÇÜKALİ ve Doç. Dr. A. Ufuk ŞAHİN'e teşekkürlerimi ve saygılarımı sunarım. Ayrıca, tezimde kullanmış olduğum mikroskobik görüntüleri elde etmemde bana yardımcı olan sayın Dr. Banu Şebnem ÖNDER'e ve deney çalışmalarımnda laboratuvarını kullandığım Onur Taahhüt Taşımacılık İnşaat Tic. ve San. A.Ş.'ye teşekkürü borç bilirim.

Son olarak, çalışmalarım boyunca en zor zamanlarımda tüm sevgisi ve hoşgörüsüyle yanımda olarak sabrını ve desteğini benden bir an bile esirgemeyen Esra KILIÇ'a ve hayatım boyunca her zaman önümü açan, zorluklar karşısında bana pes etmemeyi öğreten, fedakârlıklarıyla beni bugüne getiren ve koşulsuz sevgisiyle hep yanımda olan canım anneme sonsuz teşekkür ederim.

TABLE OF CONTENTS

TEŞEKKÜR	v
TABLE OF CONTENTS	vi
LIST OF FIGURES.....	viii
LIST OF TABLES	xi
SYMBOLS AND ABBREVIATIONS	xiii
1. INTRODUCTION.....	1
2. LITERATURE REVIEW.....	3
2.1. General Information About Pavement Design	3
2.2. General Information About Reinforcements.....	5
2.2.1 Geosynthetic Reinforcements	6
2.2.1.1. Geotextiles.....	7
2.2.1.2. Geogrids	11
2.2.2. Fiber Reinforcements	14
2.2.2.1. Natural Fibers	14
2.2.2.2. Synthetic Fibers.....	17
3. MATERIALS & METHODS.....	29
3.1. Materials.....	29
3.1.1. Soil	29
3.1.1.1. Sieve Analysis	30
3.1.1.2. Friction Angle	31
3.1.1.3. Optimum Moisture Content (Modified Proctor Test)	32
3.1.1.4. Relative Density	35
3.1.2. Reinforcements.....	38
3.1.2.1. Geotextiles.....	38
3.1.2.2. Geogrids	42
3.1.2.3. Fibers	43
3.2. Methods	44

3.2.1. California Bearing Ratio Testing Program	44
3.2.1.1. Geotextile Reinforced Pavement Tests	48
3.2.1.2. Geogrid Reinforced Pavement Tests	49
3.2.1.3. Fiber Reinforced Pavement Tests	50
3.2.1.4. Geotextile and Fiber Combined Pavement Tests.....	52
3.2.2. Microscopy Analysis	52
3.2.3. Cost Analysis	52
4. RESULTS AND DISCUSSION	57
4.1. Test Results.....	57
4.1.1. Unreinforced Test	57
4.1.2. Geotextile Reinforced Pavement Tests.....	58
4.1.3. Geogrid Reinforced Pavement Tests	80
4.1.4. Fiber Reinforced Pavement Tests	84
4.1.5. Geotextile and Fiber Combined Pavement Tests.....	94
4.2. Pavement Thickness and Cost Analysis Results.....	99
4.2.1. Pavement Thickness Results.....	99
4.2.2. Cost Estimation Results	101
5. CONCLUSION.....	109
6. REFERENCES	113

LIST OF FIGURES

Figure 2.1	A road embankment reinforced with geosynthetic	7
Figure 2.2	Geotextile reinforcement application.....	8
Figure 2.3	Geogrid application.....	12
Figure 2.4	Straw fibers.	15
Figure 2.5	Corn silk fibers.....	17
Figure 2.6	Glass fibers.....	17
Figure 2.7	Polypropylene fibers	18
Figure 2.8	Steel fibers.....	18
Figure 3.1	The quarry testing pavement soil obtained	29
Figure 3.2	Conducting the sieve analysis.....	30
Figure 3.3	Grain size distribution of soil.....	30
Figure 3.4	Friction angle of the testing soil.....	32
Figure 3.5	Modified Proctor test sample.	33
Figure 3.6	Modified Proctor Test Results (Dry Unit Weight vs. Water Content).	35
Figure 3.7	Soil sample under microscope	37
Figure 3.8	Surface textures of geotextiles; (a) Geotextile 1, (b) Geotextile 2, (c) Geotextile 3	39
Figure 3.9	Surface textures of geotextiles; (a) Geotextile 4, (b) Geotextile 5, (c) Geotextile 6.....	40
Figure 3.10	Surface textures of geotextiles; (a) Geotextile 7, (b) Geotextile 8, (c) Geotextile 9.....	40
Figure 3.11	Surface textures of geotextiles; (a) Geotextile 10, (b) Geotextile 11	41
Figure 3.12	Surface textures of geotextiles; (a) Geotextile 12, (b) Geotextile 13, (c) Geotextile 14.....	41
Figure 3.13	Images of geogrids; (a) Geogrid 1, (b) Geogrid 2, (c) Geogrid 3.....	42
Figure 3.14	Fiber types used in the study; (a) Fiber 1, (b) Fiber 2, (c) Fiber 3, (d) Fiber 4, (e) Fiber 5, (f) Fiber 6	44
Figure 3.15	Compacting soil samples with 4.5 kg rammer.....	45
Figure 3.16	Compacted samples in the curing pool	46
Figure 3.17	Different locations of reinforcements that were placed in molds; (a) unreinforced sample, (b) bottom reinforcement, (c) top reinforcement, (d)	

reinforcement, (e) two-layered reinforcement and (f) three-layered reinforcement	48
Figure 3.18 A geotextile reinforcement placed between soil layers	49
Figure 3.19 A geogrid placed between compacted soil layers.....	50
Figure 3.20 Fiber reinforcement placement; (a) 1% content by total mass at h/4 depth, (b) 1% content by total mass mixed in soil	51
Figure 3.21 Synthetic fiber reinforcements that were placed between soil layers at h/4 depth	51
Figure 3.22 Fiber reinforcements and soil after mixed by hand	51
Figure 4.1 Stress-penetration graph of unreinforced pavement.....	58
Figure 4.2 Comparison of the stress-penetration curves of Geotextile 1 on different placement conditions	59
Figure 4.3 Comparison of the stress-penetration curves with different quantities of Geotextile 1 reinforced pavement.....	61
Figure 4.4 Comparison of the stress-penetration curves of Geotextile 2 reinforced pavements	63
Figure 4.5 Comparison of the stress-penetration curves of Geotextile 3 reinforced pavements	65
Figure 4.6 Microscope images for geotextiles; (a) Geotextile 1, (b) Geotextile 2, (c) Geotextile 3.	68
Figure 4.7 Comparison of the stress-penetration curves of Geotextile 4, 5 and 6 reinforced pavements	69
Figure 4.8 Microscope images for geotextiles; (a) Geotextile 4, (b) Geotextile 5, (c) Geotextile 6.	71
Figure 4.9 Comparison of the stress-penetration curves of Geotextile 7, 8, 9, 10 and 11 reinforced pavements.....	72
Figure 4.10 Microscope images for geotextiles; (a) Geotextile 7, (b) Geotextile 8, (c) Geotextile 9.	74
Figure 4.11 Microscope image for Geotextile 10	74
Figure 4.12 Comparison of the stress-penetration curves of Geotextile 12, 13 and 14 reinforced pavements.....	75
Figure 4.13 Microscope images for geotextiles; (a) Geotextile 12, (b) Geotextile 13, (c) Geotextile 14.	77

Figure 4.14 Soil layers and geotextiles that were extracted from the mold after CBR Test	77
Figure 4.15 Condition of a geotextile reinforcement after CBR Test.	78
Figure 4.16 Comparison of the stress-penetration curves of Geogrid 1, 2 and 3 reinforced pavements	80
Figure 4.17 Images of Geogrid 1 under microscope.	82
Figure 4.18 Images of Geogrid 2 under microscope.	83
Figure 4.19 Images of Geogrid 3 under microscope	83
Figure 4.20 Comparison of the stress-penetration curves of Fiber 1, 2, 3, 4, 5 and 6 reinforced pavements as layer without mixing	84
Figure 4.21 Image of Fiber 1 under microscope	86
Figure 4.22 Image of Fiber 6 under microscope	87
Figure 4.23 Comparison of the stress-penetration curves of Fiber 1, 2, 3, 4, 5 and 6 reinforced pavements with 1% content	88
Figure 4.24 Image of Fiber 6 under microscope	90
Figure 4.25 Image of Fiber 3 under microscope	90
Figure 4.26 Surface textures of Fiber 4 and Fiber 2 under microscope, respectively....	91
Figure 4.27 Closer view of spaces on surface of Fiber 1 under microscope.....	92
Figure 4.28 Comparison of the stress-penetration curves of Fiber 1, 2, 3, 4, 5 and 6 (1%) with combining Geotextile 1 reinforced pavements	94
Figure 4.29 Comparison of the stress-penetration curves of fiber and geotextile reinforcement combinations (a) Fiber 1, (b) Fiber 2, (c) Fiber 3, (d) Fiber 4, (e) Fiber 5, (f) Fiber 6	98

LIST OF TABLES

Table 2.1 Studies based on the effects of using fiber reinforcements in soil.....	21
Table 3.1 Dry Unit Weight Results.....	34
Table 3.2 Detailed Soil Properties	37
Table 3.3 Material Properties of Geotextiles	38
Table 3.4 Properties of Geogrids	42
Table 3.5 Properties of fibers	43
Table 3.6 Fixed parameters and values that were assumed for the cost analysis.....	54
Table 3.7 Fixed parameters and values that were assumed for the cost analysis (subbase)	55
Table 3.8 Fixed parameters and values that were assumed for the cost analysis (base)	56
Table 4.1 Maximum stress values for unreinforced sand at different penetration levels (kPa)	58
Table 4.2 Maximum stress values for Geotextile 1 at different penetration levels (kPa)	59
Table 4.3 Bearing capacities of reinforced sand with Geotextile 1	59
Table 4.4 Maximum stress values for Geotextile 1 at different penetration levels (kPa)	61
Table 4.5 Bearing capacities of reinforced sand with different Geotextile 1 combinations.	62
Table 4.6 Maximum stress values for Geotextile 2 at different penetration levels (kPa)	63
Table 4.7 Bearing capacities of reinforced sand with Geotextile 2	64
Table 4.8 Maximum stress values for Geotextile 3 at different penetration levels (kPa)	65
Table 4.9 Bearing capacities of reinforced sand with Geotextile 3	66
Table 4.10 Maximum stress and CBR comparison of Geotextile 1, 2 and 3 at h/4 depth	67
Table 4.11 Maximum stress values for Geotextile 4, 5 and 6 at different penetration levels (kPa)	70
Table 4.12 Bearing capacities of reinforced sand with Geotextile 4, 5 and 6.....	70

Table 4.13 Maximum stress values for Geotextile 7, 8, 9, 10 and 11 at different penetration levels (kPa)	72
Table 4.14 Bearing capacities of reinforced sand with Geotextile 7, 8, 9, 10 and 11	73
Table 4.15 Maximum stress values for Geotextile 12, 13 and 14 at different penetration levels (kPa)	76
Table 4.16 Bearing capacities of reinforced sand with Geotextile 12, 13, and 14	76
Table 4.17 CBR results of geotextile reinforced models.....	79
Table 4.18 Maximum stress values for Geogrid 1, 2 and 3 at different penetration levels (kPa).....	81
Table 4.19 Bearing capacities of reinforced sand with Geogrid 1, 2, and 3.....	81
Table 4.20 Maximum stress values for laid fibers at different penetration levels (kPa).....	85
Table 4.21 CBR results of fiber reinforced models.....	85
Table 4.22 Bearing capacities of reinforced sand with Fiber 1, 2, 3, 4, 5, and 6	86
Table 4.23 Maximum stress values for fibers at different penetration levels (kPa)	89
Table 4.24 CBR results of fiber reinforced models.....	89
Table 4.25 Bearing capacities of reinforced sand with %1 Fiber 1, 2, 3, 4, 5, and 6.....	93
Table 4.26 Maximum stress values for Geotextile 1 and fiber combinations at different penetration levels (kPa)	95
Table 4.27 CBR results of Geotextile 1 and fiber reinforced models	95
Table 4.28 Bearing capacities of reinforced sand with Geotextile 1 and Fiber 1, 2, 3, 4, 5, 6 combinations	96
Table 4.29 CBR, M_R and SN results for unreinforced and reinforced pavement models	99
Table 4.30 Calculated layer thickness values for subbase according to SN results (D_3)	101
Table 4.31 Cost of subbase soil for unreinforced and reinforced pavements for 1 km	102
Table 4.32 Costs of geosynthetics	103
Table 4.33 Cost of fibers	104
Table 4.34 Reinforcement cost of fiber and geotextile combination	104
Table 4.35 Total cost values of reinforced pavements	105
Table 4.36 Calculated layer thickness values for base according to SN results (D_2)....	107
Table 4.37 Cost of base soil for unreinforced and reinforced pavements for 1 km	107
Table 4.38 Total cost values of unreinforced and reinforced base pavements.....	108

SYMBOLS AND ABBREVIATIONS

Symbols

C_c	Coefficient of Curvature
C_u	Uniformity Coefficient
D_r	Relative Density
e	Void Ratio
e_{Max}	Maximum Void Ratio
e_{Min}	Minimum Void Ratio
h	Height
kN	Kilonewton
kPa	Kilopascal
mm	Millimeter
M_R	Modulus of Resilience
\emptyset	Friction Angle
psi	Pounds per Square Inch
q	Stress
S_0	Overall Standard Deviation of Traffic
SN	Structural Number
W_{18}	Number of 18-kip Equivalent Single Axle Load (ESALs)
Z_R	Standard Normal Deviate
ΔPSI	Allowable Serviceability Loss
ρ_d	Dry Unit Weight
$\rho_{k_{max}}$	Densest State Soil Density
$\rho_{k_{min}}$	Loosest State Soil Density
ρ_s	Density of Soil

ρ_w Density of Water

Abbreviations

AASHTO American Association of State Highway and Transportation Officials

ASTM American Society for Testing and Materials

BR Bearing Ratio

CBR California Bearing Ratio

FHWA The Federal Highway Administration

USCS Unified Soil Classification System

1. INTRODUCTION

Layer designs of roads is one of the problems for transportation engineering. Especially managing the design process correctly is very essential in terms of construction cost. Since highways are larger than other structures in terms of length, choosing cost-effective materials which provide required performance becomes even more critical. Therefore, choosing suitable materials and methods are significant for both economy and applicability for road construction.

One of the most common method to obtain the desired performance and bearing capacity from pavement is to increase thickness of the pavement layers. However, this can cause a significant increment according to cost. Besides, different expenses can also occur in long term due to other reasons such as settlement and decrease in the service life of the pavement. Because of this, using low cost reinforcement materials is one of the major and critical topics.

In this study, it was planned to examine the effects of different reinforcements on the bearing capacity of highway pavements. Thus, California Bearing Ratio tests were done and effects of different types of reinforcements on pavements were investigated. Unreinforced and reinforced tests were conducted, and the behaviors of different reinforcements were compared. Effects of different quantities and placement methods for reinforcements were also investigated. Laboratory experiments were performed with geosynthetic reinforcements (geotextiles and geogrids) and polypropylene fiber types. Then, geotextile and fiber reinforcements were combined in pavement and their effects on CBR values and stress-penetration behavior were studied. Additionally, microscopy analyses were done for all reinforcements to understand the relation between their behaviors and physical properties. Differences on bearing ratios under heavy traffic loads and improving behaviors were discussed for all experiments.

Afterwards, cost estimation for each model was performed. A sample road was designed with the guide of AASHTO's flexible pavement design formula. Reduction on the thickness values of reinforced pavements were examined, and total cost of pavements were compared to unreinforced condition.

The main contribution of this study to the literature is that the effects of more than twenty reinforcements on pavement soil were focused in laboratory CBR tests. It was expected to achieve an idea to design cost-effective pavement models with providing higher performances by reducing thickness values with the benefits of reinforcements for highways. So, preliminary research was obtained about which type of material and placement method would be more cost efficient for road design according to their bearing capacities and performances in long term conditions. Best California Bearing Ratio results were obtained when single layer of reinforcement was applied in soil. Also, it was observed that effectiveness of reinforcements decreases as the placement distance from top surface increases. Highest performance improvements were observed from the geotextile reinforced models and application of geotextiles for thickness reduction were found cost beneficial. It can be thought that this project will have important contributions to science and real civil engineering problems in fields.

2. LITERATURE REVIEW

2.1. General Information About Pavement Design

Transportation generally includes highways, airlines, seaways, and railways. Improving behaviors of highways to achieve better performance is one of the topics for many researchers. The American Association of State Highway and Transportation Officials (AASHTO), which is one of the most known organizations by the road authorities, is a standard setting body that publishes specifications, test protocols, and guidelines that are used in highway design and construction. In 1993, AASHTO published a guide for design of pavement structures and mentioned that, California Bearing Ratio (CBR) and modulus of resilience (M_R) values have important influences on the design of the flexible road pavement.

CBR test was developed in 1930s by California Division of Highways and main purpose of CBR test is to evaluate the strength properties of subgrade and base coarse materials for pavements. The stress-penetration curve results of CBR tests are used to determine the thickness of pavement and its component layers. For the flexible pavement design, CBR is typically foremost used method and related with the modulus of resilience of pavement.

AASHTO (1993) mentioned that, resilient modulus (M_R) is another important parameter for road design. In 1950s, researchers began using repeated load triaxial tests in the laboratory to evaluate the stiffness and other behavior of pavement materials. These tests were conducted under conditions which simulated real traffic loadings in the field. Seed et al. (1962), and Seed & McNeill (1956) are the researchers who firstly studied deformation characteristics and M_R of compacted subgrades. These researchers concluded with the idea of behavior of soils under traffic loading should be obtained from repeated load tests whenever possible. This outcome was substantiated by field data obtained by the California Department of Highways as Federal Highway Administration (FHWA) mentioned. In addition, FHWA highlighted that, there is a relation between bearing capacity of the subgrade and modulus of resilience. Lot of tests and studies were done in literature to correlate the relation between resilient modulus and CBR. Different M_R formulas were created and improved by different researchers up to now.

According to the research of Heukelom et al. (1962), Transportation and Road Research Laboratory (TRRL) suggested Equation 2.1 for the correlation of modulus of resilience and California Bearing Ratio.

$$M_R (\text{psi}) = 2555 \times (\text{CBR})^{0.64} \quad (2.1)$$

Afterwards, Green & Hall (1975) developed an Equation 2.2 which the U.S. Army Corps of Engineers recommended for resilient modulus evaluation.

$$M_R (\text{psi}) = 5409 \times (\text{CBR})^{0.71} \quad (2.2)$$

The AASHTO design guide (1993) suggests that the resilient modulus of fined grained soil which was developed by Heukelom & Klomp (1962) and represented in Equation 2.3. However, it is noted that coefficient of CBR that is used in this approach can have the range between 750 to 3000 (Powell et al., 1984).

$$M_R (\text{psi}) = 1500 \times \text{CBR} \quad (2.3)$$

According to the study of Nazzal (2003), South African Council on Scientific and Industrial Research (CSIR) suggests a relation which is given in Equation 2.4.

$$M_R (\text{psi}) = 3000 \times (\text{CBR})^{0.65} \quad (2.4)$$

Although there are many approaches for CBR and M_R relation, each research has different specific limitations. Researchers reported that, some of the relations should be used only for the specific cases. For example, formula that is suggested by Heukelom & Klomp (1962) can be applicable for the subgrades which have California Bearing Ratios values less than 10. And some of them should not be used if the CBR samples are submerged in curing pool to achieve soaked CBR.

Moreover, Dione et al. (2014) highlighted that none of these formulas can exactly give the resilient modulus of the subgrade only with mathematical approaches. Correlations between M_R and CBR should be used carefully because they tend to “over-predict” or “underpredict” the modulus of resilience. The best method to determine the resilient

modulus is to use repeated load triaxial apparatus to consider the real behavior of unbound granular materials. So, the most efficient method is to obtain M_R with conducting series of tests for each soil.

In pavement design process, it was mentioned that CBR value directly affects M_R , which determines the structural number (SN) of pavement. Structural number is used to estimate the required thickness of each pavement layer which is inversely proportional with resilient modulus. Increase in the CBR value, increases M_R . Hence, SN decreases and thickness that is required for pavement layer decreases. To simplify, stronger pavements can provide the required performance with less thickness values.

When roads that are made with traditional methods are investigated, it can be observed that most of the production cost comes from the aggregate base. It is very essential that a pavement layer must be designed with correct thickness and quality to provide efficient bearing capacity and longer service life. It is also known that, the bearing capacity of the road increases as the thickness of pavement increases. In design process, increasing layer thickness can be a solution to achieve required bearing capacity but it causes higher costs in pavement construction process. Instead of increasing the pavement thickness, using reinforcements to improve the behavior of the pavement can be a more cost-effective solution. Especially for the roads that heavy traffic loads are applied on; it is more important to create pavement layers with higher bearing capacities in an economical way. Reinforcements are quite a common solution for this topic. Strength of pavement layers (specifically base and subbase), can be increased by using reinforcements in design and thickness of pavements can be reduced.

2.2. General Information About Reinforcements

Reinforcement concept has been used in different fields of civil engineering such as highways, airports, railways, foundations, pavements and retaining walls for a long time. Reinforcements can increase bearing capacity, service life, durability and provide isolation. Designing roads with higher performance and longer service life with the contribution of reinforcements are studied by many researchers.

There are different types of reinforcements used in civil engineering. Geosynthetics and fibers are commonly preferred reinforcements and have many benefits to pavement in long term. The comparison of the plate-shaped synthetic materials and fibers, which is known to be both cost efficient and applicable, needs to be examined for both literature and applicators. Because of that, this research was focused on geosynthetic and fiber reinforcement types to understand their effects on CBR values and pavement design. General background information and previous studies about these reinforcements are discussed in following section.

2.2.1 Geosynthetic Reinforcements

One of the most widely used materials in soil engineering are geosynthetics. Geosynthetics are polymeric structures and can be made of polypropylene, polyester, and polyethylene. Geosynthetics can be in different forms. Most known types of geosynthetics are geotextiles, geogrids, geomembranes, geocells and geonets.

Most important benefit of geosynthetics is to provide solutions for geotechnical problems. (Ziegler, 2017). These materials have many uses such as isolation, protection, filtration, drainage, and separation which are highly effective in road design as well. Geosynthetics can allow stabilization in foundations, also. Thanks to its separation function, geosynthetics can reduce the stress values that occur on the base course of the roads. Furthermore, geosynthetics provide the uniformity of the pavement with reducing the settlements and another reason to use geosynthetics in design for stabilization of subbase of a pavement. Figure 2.1 shows a geosynthetic reinforcement application on road embankment.



Figure 2.1 A road embankment reinforced with geosynthetic.

(<https://images.app.goo.gl/VQRPY816XRTYum5KA>)

Besides providing technical advantages, geosynthetics are also cost beneficial. Geosynthetics can reduce the cost of filling which is especially important for the economic aspects. Geosynthetics can decrease the amount of aggregates that are necessary (Yılmaz & Eskişar, 2003). And roads can be constructed with less quality aggregates thanks to the improvement of geosynthetics. They can extend the service life of the roads and decrease the maintenance costs to minimum which is important as well. In addition, geosynthetics are easily accessible and environmentally sensitive materials that can also shorten construction time (Yılmaz & Eskişar, 2007).

For the scope of this thesis, geotextiles and geogrids were focused as geosynthetic reinforcements. Background information about geotextile and geogrid reinforcements are given as follow:

2.2.1.1. Geotextiles

Geotextiles are textile products, which are defined as permeable geosynthetics. Polypropylene, polyester, polyamide (nylon) and polyethylene raw materials are widely used in the production of geotextiles. In literature, some researchers study about creating natural geotextiles as well, which can be made of coir and jute. According to their production technique geotextiles are divided into two groups, which are woven

geotextiles and non-woven geotextiles. Woven geotextiles have high tensile strength and can be used for strength improvement. In contrast, tensile strength of non-woven geotextiles is lower and because of that, they are used for features such as separation and filtration. A geotextile application in soil is represented in Figure 2.2.



Figure 2.2 Geotextile reinforcement application.

(<https://images.app.goo.gl/aNFuWWG7y3tUm8cs7>)

In the literature studies, different geotextile types were investigated for roads to achieve cost-effective solutions. Meshram et al. (2013) suggested using natural materials like coir geotextile as an option to improve the poor subgrade soil. The laboratory and field tests were conducted and reported that, coir geotextile in road construction can be a biodegradable, environment friendly and cost-effective solution. However, not all road authorities may support the use of organic materials in road design.

Sharma et al. (2013) studied the change in CBR values of cohesive soil which was reinforced with jute geotextile. Different depths for geotextile placement in soil were tested as 1, 2, 3, and 4 centimeters from top surface. Highest CBR value obtained from the geotextile at 1 cm depth. Study highlighted that, as the depth of geotextiles from top increased, percentage increase in CBR decreased. On the other hand, application of geotextile reinforcement increased CBR value of unreinforced soil by 130.74% and could

reduce the layer thickness. However, it is concluded that burying jute geotextiles in pavement can cause strength loss in time due to biodegrading of fibers.

Yashas & Muralidhar (2015) investigated the effect of geotextured jute fiber mat on CBR values for flexible pavement design as well. Natural soil samples were reinforced with one, two- and three-layered reinforcements and thickness of pavement layers were calculated by considering the traffic and CBR values. Models included surface, base, and subbase layers and reduction in the thicknesses were compared. It is shown that, CBR value of natural soil increased by 38.31% when single layer of reinforcement applied. Two layered model increased the maximum dry density by 4.06% and CBR value 144.93%. However, obtained CBR values were insufficient to reach minimum design requirements. In three-layered model, percentage increase for these values were 6.26% and 234.35% which satisfied minimum CBR requirements. Additionally, another model was prepared with including 50% of gravel content and CBR value was obtained as 1.4%. When three layers of reinforcement applied with %50 gravel model, soaked CBR value was calculated as 4.3%, which was found applicable for pavement design. Though, thickness of pavement did not change at the end of the analytical process because stress and strain at first and second interface calculated were not in permissible limit and exceeded the stress and deformation criteria.

Azar & Dabiri (2015) conducted laboratory tests to evaluate the effect of geotextiles on the bearing capacity of the gravel. Tests were performed in three relative densities which were 90, 95, and 100%. Geotextiles were examined in two positions. Firstly, one geotextile was placed in the middle section of the sample. Then, two geotextile layers were placed alternatively. Laboratory studies showed that, one geotextile layer improved the bearing capacity. In contrast, two geotextile layers, which were alternatively put in the samples caused decrease in bearing capacity and resistance of the soil. Research recommended that, further studies can be conducted on the effects of the number of geotextile layers and their arrangement in different soil compounds and specimens.

Masoumi et al. (2017) studied geotextile properties in soil to evaluate changes in the bearing capacity of highway roadbed with conducting laboratory experiments. Behavior of geotextile reinforced CBR test samples are examined in two type of soils which were clay and sand. Three types of geotextiles with 150, 200, 300 g/m² weights were placed at

5, 10, 20, 30, 50, 100 mm depths. These geotextiles were tested with two methods, one-layered and two-layered. In both clay and sand samples, bearing characteristics increased approximately 3 and 2.6 times greater than unreinforced models when one layer of geotextile was used. Though, two-layered geotextile caused a change in soil behavior because of the discontinuity of aggregates and performance affected. According to the CBR test results, highest values observed from 150 and 200 g/m² geotextiles in clayey soil which indicated better responses under loading conditions. In two-layered tests, highest CBR result was observed from 150 g/m² geotextile application. To summarize, study reported that, as the number or weights of geotextile in samples increase, the natural composition of the soil changed, and the results can be unreliable. Also, it was observed that, after certain depth, geotextile material had no remarkable effect on performance of soil.

Vikram (2018) used geotextile reinforcements in granular soil and performed CBR tests to examine their behavior. Different grading soil samples are selected for the study and geotextiles were placed at certain depths. The effects of geotextiles on the bearing capacity were examined by placing one and two layers in granular soils and performance of geotextiles discussed. Results showed that, geotextile reinforcements improved the CBR values and the strength of soils. Since geotextiles increased load bearing capacity of soils, it is mentioned that, geotextile reinforced unpaved roads will perform better than unreinforced roads. However, models with two geotextiles decreased the CBR value of soil. Study highlighted that, using multiple geotextiles can decrease the interlocking between grains of soil and this can affect CBR value. Additionally, it is concluded that improvement of soil strength with geotextiles depends on the soil gradation and effects are more significant for finer soils.

Goodarzi & Shahnazari (2019) studied about strength enhancement of geotextile reinforcement in carbonate sand. Study showed that, the interlocking between aggregates can be increased by reinforcing sand with geotextile. Additionally, it is noted that post-peak strength loss can be reduced and axial strain at failure and maximum strength can be increased by geotextiles.

Sayida et al. (2019) studied the effects of geotextiles on subgrade with field California Bearing Ratio tests and laboratory studies. These tests were performed for rural roads

which had reinforced and unreinforced sections. It was observed that, settlement reduction on the reinforced model was more remarkable compared to the unreinforced section. As the mass per unit area of geotextile increased, percentage reduction in settlement increased. The highest percentage reduction in settlement was observed from heaviest woven geotextile and lightest geotextile showed lowest reduction. Moreover, the study showed that, geotextile reinforcement increased CBR (in-situ) between 21-63% than unreinforced scenario. Researchers concluded that, use of geotextile reinforcement can provide about 68% saving in initial cost and can reduce maintenance cost as well. Study concluded that, geotextile is an effective reinforcing material on subgrades with low CBR values and can be used in rural roads to increase the long-term performance.

Çelik (2020) studied the effects of nonwoven geotextiles on sand foundation. Model footing that was used in load tank was 12x12 cm square footing. Geotextiles were placed at three different depths which were 2, 5 and 10 cm from footing. Additionally, two geotextiles were placed together at same depth at as 2-2, 5-5 and 10-10 cm from surface and load applied. Then, same testing method was repeated with three geotextiles placed on top of each other at 2, 5 and 10 cm depths. It is shown that, in all testing methods for all samples, geotextiles increased the bearing capacity more when the geotextile layer used in the soil was placed closer to the footing. In other words, performance of geotextiles decreased as the layer depth increased. Since the geotextiles used in the experiments are non-woven type, it is suggested that, what kind of effect the woven geotextiles will have on bearing capacity can be investigated. In addition, how different type of reinforcements (geogrid, geocell, geotextiles or fibers) will influence the amount of settlement or bearing capacity of same soil sample can be examined.

2.2.1.2. Geogrids

Geogrids are high strength geosynthetic reinforcements which are made of various polymers. Geogrid reinforcements are used in soil to handle the stress that occurs in the tensile areas. Road constructions, stabilization of soils, and improvement of the foundations are the main fields for geogrid applications. Geogrids can be classified into four categories due to their working principles which are uniaxial, biaxial, quaxial and high-density polyethylene geogrids. An example for geogrid application in soil material is given in Figure 2.3.



Figure 2.3 Geogrid application. (<https://images.app.goo.gl/9XVWbHuydHiyvUs18>)

Geogrid reinforcements have been the subject of many studies and Giroud & Han (2004), are some of the researchers who specialized on geogrid reinforced road design. Studies about reinforcing the highways have become more popular and it is proven that reinforcements strengthen the bearing capacity of the road. Leng & Gabr (2006) created a model to examine the deformation-resistance behavior of unpaved roads. It is mentioned that, geogrid reinforcements can improve the performance when they are placed between subgrade and aggregate base course. Research reported that, using geogrid provided reduction in stresses and plastic deformation. The proposed model was supported with data obtained from field study. Computed base course thickness values and test results matched efficiently. However, researchers recommended that, further studies required to verify the method with field testing before it can be used as a design tool.

Zornberg (2012) investigated the performance of geosynthetic and lime reinforced roads with considering traffic loads and environmental conditions. Studied roads involved different sections which were unreinforced (for control), lime-treated subbase, geosynthetic-reinforced base with three types, and combinations of lime-treated subbase with geosynthetic-reinforced base systems. It was observed that, geogrid reinforced sections prevented longitudinal crack developments which were developed by seasonal shrinkage and swelling. In addition, geogrid reinforcements enhanced the performance and relocated cracks from the paved area to out of the paved surface. Despite, performance improvement on the sections that were lime-treated were less than geogrid reinforced sections, performance of lime-treated sections was found better than

unreinforced sections. Additionally, it is highlighted that, performance improvement with combining geosynthetic reinforcement and lime treatment were not found effective as using geosynthetic reinforcement only. Study concluded that, geosynthetic reinforcement materials extend the service life of roads and can reduce the traffic loads which are transferred from tires.

Lavasan & Ghazavi (2012) used geogrids in sand and noted that 25-40% increase in the ultimate bearing capacity of the interfering footing. It is mentioned that, increasing the number of geogrid layers under footings reversed the tilting direction of footings which were closely spaced and under vertical centric loads. Besides, geogrid reinforcements decreased the amount of settlements.

Nazia & Deepthy (2016) investigated the compaction behavior of compressive soil with using jute reinforcement in the form of fibers and geogrids. Soaked and unsoaked CBR tests were performed in study for bitumen coated and uncoated soil. It was observed that unsoaked CBR values increased by 275% and 289% for uncoated and coated geogrid reinforced soils, respectively. And for soaked CBR tests, bearing ratios increased as 231% and 289% for uncoated and coated geogrid reinforced soils, respectively. Study concluded that, strength ratios for all tests were increased significantly by using geogrid reinforcement in soil.

Tavakoli Mehrjardi & Khazaei (2017) conducted repeated plate load tests to examine the scale effect on geogrid-reinforced soil. Four soils with different gradations, two geogrids with different aperture sizes and three loading plates with different sizes were studied as variables. Loadings and surface settlements were examined in tests. It is reported that, bearing capacity of geogrid reinforced models can increase up to 635% if geogrid is applied with correct grain size. Research shown that ratio between the optimum aperture size of geogrids and medium grain size of soil should be about 4 times. Further, study recommended that, geogrid with the aperture size 0.2 times of footing width should be selected for best results.

Jayalath et al. (2018) studied on two identical pavement models. In order to examine the effects of geogrid as subgrade reinforcement, models were prepared in unreinforced and composite-geogrid reinforced conditions. Test results showed that, geogrid

reinforcements can reduce the rutting depth on granular pavement remarkably. Moreover, 25-35% of vertical stress which applied on subgrade can be reduced with using geogrid at the interface of the base and subgrade.

Gökova (2019) searched the effects of geogrid on performance of highway pavement which was subgrade material with low bearing capacity. California Bearing Ratio tests were conducted for geogrid reinforced soil and reported that geogrids decreased rutting. Additionally, it is mentioned that, using geogrids in soil can increase service life of pavement.

2.2.2. Fiber Reinforcements

Fibers can be categorized into two, which are natural fibers and synthetic fibers. Both fiber types have often been the subject of many researchers. In general, coconut, straw, palm tree, jute, linen, cane, and bamboo tree fibers are studied as natural fibers. And for synthetic fibers, which are man-made; polypropylene, polyester, polyethylene, nylon, steel, and polyvinyl alcohol are studied for examination (Hejazi et al., 2012). Fibers are usually used in structural industry, geotechnical solutions, design of airport runways, concrete applications, and pavement designs as reinforcement.

Over many years, researchers made lot of investigations in laboratory and created models with numerical analyses to understand the effects of reinforcement materials. It is identified that structures that were built with natural or synthetic fibers, are improved (El-Naggar, 1997). For instance, Santoni et al. (2001) reported that, foundations which were reinforced with fibers showed higher performance in terms of shear strength in compression tests. Fibers that are applied to improve soil may also be effective to strengthen highway pavements. Thus, it is thought that fibers may allow engineers to reduce layer thicknesses and choose thinner layers for structure. Detailed information and background about both natural and synthetic fiber types are given as follow:

2.2.2.1. Natural Fibers

Natural fibers are the reinforcements that can be found in nature. Being biodegradable, cost beneficial, renewable, and easily available in nature are the main advantages of

natural fibers. Since ancient times, natural fibers have been used as reinforcement (Yetimoğlu & Salbas, 2003). For example, ancient civilizations used straw to strengthen the building blocks (The Great Wall of China, Babylon, etc.). Figure 2.4 represents an example for straw fiber.



Figure 2.4 Straw fibers. (<https://images.app.goo.gl/FyTgiWTKwCjnGKH79>)

Nowadays, natural fibers are still the subject of research. Hossain et al. (2015) studied the effects of jute fibers and geotextile reinforcement as a tensional material on granular soil. At first, California Bearing Ratio (CBR) tests were conducted to examine the load-penetration behavior of geotextile reinforced and unreinforced soil. Geotextiles were tested as one, two and three layers at certain depths under soaked condition. Relation between the number of geotextile layer and increase in bearing capacity examined. Then, behavior of fiber reinforcements was investigated by mixing in soil at 0.5%, 1.0%, 1.5% and 2.0% by weight of the soil. Lastly, granular soil was reinforced with the combination of geotextile and jute fiber. Geotextiles were placed at top and middle layer of the samples and jute fibers were added by 0.5% and 1% weight of soil. It is highlighted that, highest amount of change in CBR values were observed when jute fibers were mixed by 0.5% and 1.0% content and sample with geotextile at top position provided better result than middle or bottom placed samples. In addition, this study shown that combining single geotextile with jute fiber with 0.5% and 1.0% content can be as effective as two and three geotextile layered samples.

Dhand et al. (2015) studied basalt fibers which are ecofriendly, lightweight natural fibers. Study noted that, cost-effective basalt fibers can provide exceptional properties over glass

fibers such as better mechano-physio-chemical advantages. Researchers showed that, costs in industrial applications may be reduced by using fiber reinforcements. In addition, fibers were investigated in different fields and it is noted that the shapes of the reinforcements have influences on performance as well.

Experimental tests are conducted to analyze the effects of fibers on CBR value of soil for pavement evaluation. Pandit et al. (2016) studied the strength improvement of flexible pavement (subgrade) with conducting CBR tests. Soil samples were reinforced with coir and jute fibers which had different proportions and lengths. It was observed that, CBR values increased with the increase in fiber proportions up to significant point and then, increasing fiber proportions decreased CBR values. Maximum CBR value was obtained from 0.7% fiber content and optimal fiber length was found as 15 mm. Thickness of soil subgrade was compared for reinforced and unreinforced conditions as well. Since both fiber types increased the CBR values of soil, it is mentioned that the thickness of the flexible pavement can be decreased with fiber reinforcements. Therefore, study highlighted that, using fibers in soil may reduce the pavement cost.

Wei et al. (2018) investigated the mechanical properties of soil with adding wheat straw, rice straw, jute, and polypropylene fibers. Unconfined compressive tests were conducted to define optimum length and optimum content for reinforcing soil. Research concluded that, 0.2-0.25% were the optimum fiber contents and the optimal fiber length was around 30-40% of the sample diameter. Study showed that, materials like wheat straw, rice straw and jute increased cohesion and friction angle of the soil. All fiber types that were used in this research improved the strength of soil and lime-soil. Kumar & Mir (2018) are the researchers who also observed increase in the California Bearing Ratio values and unconfined compressive strengths by mixing jute fibers in the soil. Tough, polypropylene fibers provided best results in laboratory tests.

Tran et al. (2018) applied corn silk fibers into cemented soil and examined their behavior by conducting compaction, compression, and splitting tension tests. Fibers were applied as 0.25%, 0.5%, and 1% by weight of dry soil. It was found that, using corn silk with 0.25-0.5% of content improved the compressive and split tensile strength of the soil. A corn silk fiber example is given in Figure 2.5.



Figure 2.5 Corn silk fibers. (<https://images.app.goo.gl/xjgTSZgETyDvTT3s7>)

So, using natural fibers have many advantages for civil engineers. However, some road authorities suggest using synthetic fiber reinforcements for pavement improvement which are better for construction specifications and provide longer service life.

2.2.2.2. Synthetic Fibers

Synthetic reinforcements are the materials which are manmade products. Synthetic reinforcements are fabricated and as popular as natural fibers in civil engineering. Most known synthetic fiber reinforcements are produced of raw materials like glass, polypropylene, polyethylene, polyester, polyvinyl alcohol, carbon, and steel. Examples for glass, polypropylene, and steel fibers are represented in Figure 2.6 to Figure 2.8. Synthetic fibers can generally be seen in reinforcing columns, beams, and foundation designs in structural engineering. These fiber types are used in geotechnical and transportation engineering as well.



Figure 2.6 Glass fibers. (<https://images.app.goo.gl/TQJot2x6kTWJhW5J7>)

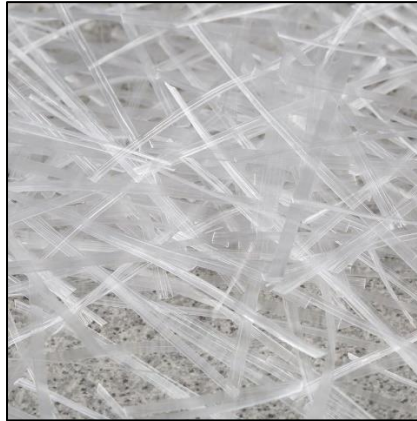


Figure 2.7 Polypropylene fibers. (https://www.yapikatalogu.com/en/concrete-and-concrete-admixtures/concrete-reinforcement-materials/atlas-1-yapi-fibermesh-650s-macro-synthetic-fiber-reinforcement_25144)



Figure 2.8 Steel fibers. (<https://images.app.goo.gl/Xdtx7tCyscaAyCxaA>)

For example, Yetimoğlu et al. (2005) performed CBR (California Bearing Ratio) tests to understand the behavior of randomly distributed fibers with soil material. It is highlighted that, benefits of fiber reinforcements increased with increase in content. Thanks to reinforcements, the increase in the bearing capacity was observed. The effect of fiber content and the importance of the change in brittle behavior had been mentioned in that research as well.

Some researchers combined synthetic fibers with other materials and saw it can be beneficial for some behaviors of soil. For instance, Yılmaz (2015) noted that combining multifilament polypropylene with 1% of mix content and fly ash with 30% of mix content together increased ultimate compressive strength of soil by 218%.

Besides, researchers started to investigate the effects of using recycled materials as synthetic fiber reinforcements. For example, Baricevic et al. (2018) studied about recycled tire polymer fibers and reported that, recycled fibers enhanced early age behavior of concrete. It is concluded that, recycled tire polymer fibers supported concrete when it is exposed to the aggressive environments. In addition, Leone et al. (2018) obtained short steel fibers from used tires at the end of their life and shown that it is effective in both terms for toughness and shear behavior of concrete.

Studies showed fiber reinforcements can improve the behaviors of soil under freeze thaw cycles as well. Kravchenko et al. (2018) tested polypropylene and basalt fibers by 0.25%, 0.5%, 0.75% contents and compared their results with unreinforced condition. It is known that strength and resilient modulus of soil decreases as the number of cycles increases. Both before and after freezing thawing, resilient modulus of fiber reinforced samples were obtained higher than unreinforced samples. Additionally, even after 15 freeze-thaw cycles, polypropylene fibers and basalt fiber increased compressive strength of soil by %70 and %41.2 when applied by 0.75% content. Moreover, the strength of soil increased by 70% when polypropylene fibers used as 0.75% of content and it is highlighted that, best result was obtained from polypropylene fiber reinforced soil.

Cui et al. (2018) experimented carbon fibers and nano silica under direct shear tests and conducted microscopy analysis. Results showed that, shear strength of reinforced samples increased. Carbon fibers effectively improved internal friction angle and cohesion of soil as well. Additionally, combining carbon fibers with nano silica improved the shear stiffness and shear strength of soil increased by 128.3%. As the proportion of the carbon fibers increased, increase in the shear strength parameters were observed. However, using fibers more than 2% decreased the cohesion increment. Study noted that, the reason of this decrease was the uneven distribution of high amount of carbon fibers in soil. Optimum carbon fiber content was found as 2% to achieve the maximum value of shear strength.

Abbaspour et. al (2019) mentioned that, engineering researchers have studied end of life tires as soil reinforcement. Treatment of end of life tires generates subproducts called waste tire textile fibers and this material is used to reinforce soil for the purpose of their research. Fibers were mixed by 0.5%, 1%, 2%, 3%, and 4% proportions on clayey and

sandy soils and laboratory tests conducted including California Bearing Ratio. It was observed that, fibers increased the strength of soil and ascended ductility parameters. In clayey soil, fibers decreased CBR values when applied with low content. On the other hand, using fibers in sandy soil increased CBR values up to 270%. When engineering characteristics are examined, it is important that maximum dosage of fibers should be around 1% for road design. Detailed literature study about fiber reinforcements are given in Table 2.1.

Table 2.1 Studies based on the effects of using fiber reinforcements in soil.

Author	Soil Type	Reinforcement Material	Fiber Diameter (mm)	Fiber Length (mm)	Tensile Strength of Fibers (MPa)	MOE (GPa)	Fiber Content (%)	Test Type	Findings
Kravchenko et al. (2018)	Clay (0.0016 - 0.06 mm)	Polypropylene	0.012-0.013	12	600	35	0.25	Tri-axial Compression	Highest results were observed when 0.75% content applied for both reinforcements. Polypropylene fibers and basalt increased strength of soil by 70% and 41.2%, respectively.
	Clay (0.0016 - 0.06 mm)	Polypropylene	0.012-0.013	12	600	35	0.50	Tri-axial Compression	
	Clay (0.0016 - 0.06 mm)	Polypropylene	0.012-0.013	12	600	35	0.75	Tri-axial Compression	
	Clay (0.0016 - 0.06 mm)	Basalt	0.012-0.014	12	3500	75	0.25	Tri-axial Compression	
	Clay (0.0016 - 0.06 mm)	Basalt	0.012-0.014	12	3500	75	0.50	Tri-axial Compression	
	Clay (0.0016 - 0.06 mm)	Basalt	0.012-0.014	12	3500	75	0.75	Tri-axial Compression	
Li et al. (2018)	Silty clay	Polypropylene	0.031	7	330-370	3.5	0.1	Direct Tensile	Best result was observed when 0.25% fiber content was applied. Fibers increased soil strength by 152.8%.
	Silty clay	Polypropylene	0.031	7	330-370	3.5	0.15	Direct Tensile	
	Silty clay	Polypropylene	0.031	7	330-370	3.5	0.25	Direct Tensile	
	Silty clay	Polypropylene	0.031	7	330-370	3.5	0.3	Direct Tensile	

Abbaspour et al. (2019)	Clay/Sand	Waste tire textile	0-0.5	0-20	-	-	0.5, 1, 2, 3, 4	Direct Shear, Compaction, UCS, STS, CBR	For sand, strength and ductility parameter increased. For clay, UCS, and CBR decreased. However, ductility and tensile strength increased. The reason could be the increase in the separation between aggregates due to fibers.
	Clay/Sand	Waste tire textile	0.5-0.8	20-40	-	-	0.5, 1, 2, 3, 4	Direct Shear, Compaction, UCS, STS, CBR	
	Clay/Sand	Waste tire textile	0.8<	40<	-	-	0.5, 1, 2, 3, 4	Direct Shear, Compaction, UCS, STS, CBR	
Yılmaz (2015)	Clay (80.2% passing No:200 sieve)	Fibrillated Polypropylene	-	6, 19	400	2.6	0.5	UCS, Triaxial	UCS of clay decreased when fibers added without fly ash. When 19 mm fibers added by 1% and mixed with 30% fly ash, UCS increased 218%.
	Clay (80.2% passing No:200 sieve)	Fibrillated Polypropylene	-	6, 19	400	2.6	1	UCS, Triaxial	
	Clay (80.2% passing No:200 sieve)	Multifilament Polypropylene	-	6, 19	700	3.5	0.5	UCS, Triaxial	
	Clay (80.2% passing No:200 sieve)	Multifilament Polypropylene	-	6, 19	700	3.5	1	UCS, Triaxial	

Ahmad et al. (2010)	Silty Sand (D50: 0.68 mm)	Oil Palm Empty Fruit Bunch	0.40	15, 30, 45	283	-	0.25, 0.5	Triaxial Compression	Shear strength increased as fiber proportions increased. Results of 30, 45 mm fiber reinforced soils were almost same. Increase in cohesion and friction angle was observed.
	Silty Sand (D50: 0.68 mm)	Coated Oil Palm Empty Fruit Bunch	0.51	15, 30, 45	306	-	0.25, 0.5	Triaxial Compression	
Cui et al. (2018)	Silty soil (1-0.001 mm)	Carbon Fiber	0.007	3	4900	230	2	Direct Shear	Using 2% carbon fiber and 3% nano silica increased shear strength by 128.3%. Increase in cohesion and friction angle was observed.
	Silty soil (1-0.001 mm)	Nano Silica	-	-	-	-	3	Direct Shear	
Ateş (2016)	Sand (1-0.01 mm)	Glass Fiber	0.4	4	1000-1700	72	1, 2, 3, 4	UCS	Highest strength was observed when 3% fibers were applied. After that, as the fiber content increased strength of soil decreased.

Wei et al. (2018)	2.2% Sand, 62.6% Silt, 35.2% Clay	Wheat Straw	3-5	6, 12, 19, 25, 31	3.6	-	0.1, 0.15, 0.2, 0.25, 0.3	Triaxial Compression, UCS	Reinforcements increased cohesion and friction angle of soil. Optimum results were observed for 0.2% and 0.25% fiber contents.
	2.2% Sand, 62.6% Silt, 35.2% Clay	Rice Straw	4-6	6, 12, 19, 25, 31	5.4	-	0.1, 0.15, 0.2, 0.25, 0.3	Triaxial Compression, UCS	
	2.2% Sand, 62.6% Silt, 35.2% Clay	Jute	-	6, 12, 19, 25, 31	263	-	0.1, 0.15, 0.2, 0.25, 0.3	Triaxial Compression, UCS	
	2.2% Sand, 62.6% Silt, 35.2% Clay	Polypropylene	0.018-0.048	6, 12, 19, 25, 31	358	-	0.1, 0.15, 0.2, 0.25, 0.3	Triaxial Compression, UCS	
Tran et al. (2018)	0.002-0.250 mm	Corn Silk	0.3	10	8.3	-	0.25	Compaction, Compression, Splitting Tension	Study recommended using corn silk fibers between 0.25-0.5% content. Compressive and split tensile strength of soil increased.
	0.002-0.250 mm	Corn Silk	0.3	10	8.3	-	0.5	Compaction, Compression, Splitting Tension	
	0.002-0.250 mm	Corn Silk	0.3	10	8.3	-	1	Compaction, Compression, Splitting Tension	

Hejazi et al. (2012)	Sand, Silty Sand, Black cotton, Clayey Soil	Polypropylene	0.023-0.150	6,12,18,24,35,50	120-450	3-3.5	0-3	UCS	Strength, ductility, and freeze-thaw resistance of soil enhanced. Swelling and shrinkage reduced. Fracture energy, the CBR value, the toughness and the secant modulus of the soil were increased by fibers. As the fiber length and/or content increased, UCS increased. UCS of 1% glass fiber reinforced cemented sand was 1.5 times of unreinforced sand. Peak strength of silty sand increased with the addition of fibers.
	Clayey Soil	Polyethylene	0.4-0.8	12, 25, 50	100-620	0.14-1	0-4	UCS	
	Fine Sand, Clayey Soil	Polyester	0.030-0.040	3, 6, 12, 20, 64	400-600	10-30	0-1	UCS	
	Sand, Silty Sand	Glass Fiber	0.003-0.019	25	1500-5000	53-95	0-1	UCS	
	Cemented River Sand	Polyvinyl Alcohol	0.1	12	1078	25	1	UCS	
Sharma et al. (2015)	Sandy Clay	Pinus Roxburghii	0.48	11.15	324	-	0.5, 1, 1.5, 2	UCS, Standard Proctor	Pinus Roxburghii fibers increased strength by 73-137%. For fibers of Grewia Optivia, soil strength increased by 94-200%.
	Sandy Clay	Grewia Optivia	0.03	15.35	730	-	0.5, 1, 2	UCS, Standard Proctor	

Erken & Torabi (2011)	Sand (D60: 0.35 mm), (D30: 0.27 mm), (D10: 0.22 mm)	Forta Mighty-Mono (PP)	-	19	570-660	-	0.1	Modified Proctor, Triaxial	No change was observed when fibers applied by 0.1%. Positive effects were observed for shear strength and liquefaction when fibers used by 0.5% and 1% proportions.
	Sand (D60: 0.35 mm), (D30: 0.27 mm), (D10: 0.22 mm)	Forta Mighty-Mono (PP)	-	19	570-660	-	0.5	Modified Proctor, Triaxial	
	Sand (D60: 0.35 mm), (D30: 0.27 mm), (D10: 0.22 mm)	Forta Mighty-Mono (PP)	-	19	570-660	-	1	Modified Proctor, Triaxial	
Anggraini et al. (2015)	5-20% Sand, 20-35% Silt, 35-70% Clay	Coir Fiber + Lime	0.2-0.3	5-15	76-102	-	-	Indirect Tensile Strength, UCS	Highest results for indirect tensile strength and unconfined compressive strength were observed for addition of 1% fiber content.
	5-20% Sand, 20-35% Silt, 35-70% Clay	Coir Fiber + Lime	0.2-0.3	5-15	76-102	-	0.5 & 5	Indirect Tensile Strength, UCS	
	5-20% Sand, 20-35% Silt, 35-70% Clay	Coir Fiber + Lime	0.2-0.3	5-15	76-102	-	1 & 5	Indirect Tensile Strength, UCS	
	5-20% Sand, 20-35% Silt, 35-70% Clay	Coir Fiber + Lime	0.2-0.3	5-15	76-102	-	1.5 & 5	Indirect Tensile Strength, UCS	
	5-20% Sand, 20-35% Silt, 35-70% Clay	Coir Fiber + Lime	0.2-0.3	5-15	76-102	-	2 & 5	Indirect Tensile Strength, UCS	

Moghal et al. (2018)	87.3% (finer than 200 micrometer)	Fibermesh + Lime	-	6	-	-	0.2	CBR	Fibers increased CBR value by 20%. Fiber which had 12 mm length, increased CBR values more than 6 mm fibers. Irrespective of the fiber types, it was observed that using higher amount of fibers increased CBR values of soil more effectively.
	87.3% (finer than 200 micrometer)	Fibermesh + Lime	-	6	-	-	0.4	CBR	
	87.3% (finer than 200 micrometer)	Fibermesh + Lime	-	6	-	-	0.6	CBR	
	87.3% (finer than 200 micrometer)	Fibermesh + Lime	-	12	-	-	0.2	CBR	
	87.3% (finer than 200 micrometer)	Fibermesh + Lime	-	12	-	-	0.4	CBR	
	87.3% (finer than 200 micrometer)	Fibermesh + Lime	-	12	-	-	0.6	CBR	
	87.3% (finer than 200 micrometer)	Fibercast + Lime	-	6	-	-	0.2	CBR	
	87.3% (finer than 200 micrometer)	Fibercast + Lime	-	6	-	-	0.4	CBR	
	87.3% (finer than 200 micrometer)	Fibercast + Lime	-	6	-	-	0.6	CBR	
	87.3% (finer than 200 micrometer)	Fibercast + Lime	-	12	-	-	0.2	CBR	
	87.3% (finer than 200 micrometer)	Fibercast + Lime	-	12	-	-	0.4	CBR	
	87.3% (finer than 200 micrometer)	Fibercast + Lime	-	12	-	-	0.6	CBR	

Raju et al. (2018)	% 59 Sand, %39.8 Silt Clay, %1.2 Gravel	Polyvinyl Alcohol (PVA)	2.2 (dtex) dtex: Grams per 10 kilometers of fiber	6	13 (cN/dtex)	280 (cN/dtex)	0	CBR, UCS, Split Tensile, Cyclic Triaxial	CBR value of 1.5% fiber reinforced soil was found 50 times of untreated soil. UCS value increased with the addition of 1.5% fiber in soil. The average split tensile strength almost increased by 250% with the addition of 1.5% fiber. Study highlighted that, the tensile load acting on the soil can be carried by the PVA fiber reinforcements.
	% 59 Sand, %39.8 Silt Clay, %1.2 Gravel	Polyvinyl Alcohol (PVA)	2.2 (dtex) dtex: Grams per 10 kilometers of fiber	6	13 (cN/dtex)	280 (cN/dtex)	0.5	CBR, UCS, Split Tensile, Cyclic Triaxial	
	% 59 Sand, %39.8 Silt Clay, %1.2 Gravel	Polyvinyl Alcohol (PVA)	2.2 (dtex) dtex: Grams per 10 kilometers of fiber	6	13 (cN/dtex)	280 (cN/dtex)	1.0	CBR, UCS, Split Tensile, Cyclic Triaxial	
	% 59 Sand, %39.8 Silt Clay, %1.2 Gravel	Polyvinyl Alcohol (PVA)	2.2 (dtex) dtex: Grams per 10 kilometers of fiber	6	13 (cN/dtex)	280 (cN/dtex)	1.5	CBR, UCS, Split Tensile, Cyclic Triaxial	
Hazırbaba (2017)	Sand (D50: 0.42 mm)	Geofiber Polypropylene	-	51	206.843	-	0.2	CBR, Modified Proctor	Fibers improved residual shear stress of soil when compared with unreinforced sand.
	Sand (D50: 0.42 mm)	Geofiber Polypropylene	-	51	206.843	-	0.5	CBR, Modified Proctor	
	Sand (D50: 0.42 mm)	Geofiber Polypropylene	-	51	206.843	-	0.8	CBR, Modified Proctor	

3. MATERIALS & METHODS

3.1. Materials

In this section, material properties of soil and reinforcements are given in details. Then, test methods used for the study can be seen. In the study, one soil type was used, and three types of reinforcements were chosen such as geotextiles, geogrids, and fibers.

3.1.1. Soil

Choosing the correct soil type is important for construction purposes, especially in highway engineering. Pavements generally includes base, subbase, subgrade, and there are standards that engineers use when it comes to build better quality roads. Each layer has its own requirements and this study was focused on subbase and base layers of the road. Therefore, analysis of soil is important. For this research, testing soil was chosen from a quarry in Ankara, Turkey and it can be observed from Figure 3.1. Tests to determine the behaviors of soil used are given as below:



Figure 3.1 The quarry testing pavement soil obtained.

3.1.1.1. Sieve Analysis

Collected soil for sieve analysis was weighed in the laboratory. Then, soil was dried in an oven for 24 hours with 110 °C to lose its water content. After that, sieve analysis was conducted. Proper sieves were prepared for this test and this procedure was followed according to AASHTO T88-19 (2019) standard. Figure 3.2 shows the sieves that were used in this test. Analysis results are shown in Figure 3.3.



Figure 3.2 Conducting the sieve analysis.

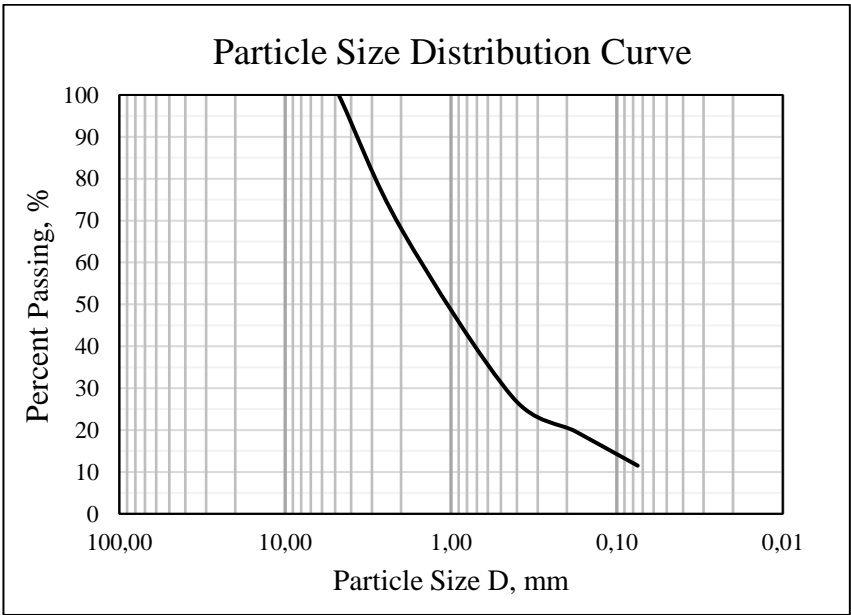


Figure 3.3 Grain size distribution of soil.

AASHTO Soil Classification System AASHTO M 145-91 (2017) was used to classify this soil. According to the results of the passing sieves, this soil sample was classified as A-1-b in terms of AASHTO standards. This code means, the soil was consisting of stone fragments which were well graded. In addition to this, soil was examined with the Unified Soil Classification System (USCS) and it was classified as SW (Well-Graded Sand) according to ASTM D2487-06 (2006).

With using this analysis, soil passing through 10% (D10), 30% (D30) and 60% (D60) of sieve sizes were found. Plotting these values to the following equations computed the coefficient of uniformity (3.1) and coefficient of curvature (3.2). Since D10, D30, D60 were equal to 0.07, 0.51, 1.68 respectively, Cu and Cc were found as 24 and 2.2.

$$C_u = \frac{D_{60}}{D_{10}} \quad (3.1)$$

$$C_c = \frac{D_{30}^2}{D_{10} \times D_{60}} \quad (3.2)$$

where;

D10 = 10% of the particles are finer than this size

D30 = 30% of the particles are finer than this size

D60 = 60% of the particles are finer than this size

3.1.1.2. Friction Angle

Another important property of soil was the angle of friction between particles. Standard test method for measuring the angle of repose was used and ASTM C1444-00 (2005) standard was followed. Repose of free-flowing method was used by many researchers like Infante et al. (2016). Angle was calculated with the following Equation 3.3 to ensure from the results as well.

$$\phi = \tan^{-1} \left(\frac{\text{Free Fall Height}}{\text{Radius of Soil Circle}} \right) \quad (3.3)$$

Friction angle was found approximately 35 degrees in both approaches which is shown in Figure 3.4. However, this angle did not represent the compacted internal friction angle of soil because it was examined at loosest state, just to define the material.



Figure 3.4 Friction angle of the testing soil.

3.1.1.3. Optimum Moisture Content (Modified Proctor Test)

Compaction of the pavement must be performed properly. Otherwise, problems like settlement can cause extra maintenance costs or even failure of the structure can be observed. Soil must be prepared up to its optimum water content to get the maximum compaction capacity. Modified Proctor test was conducted to determine optimum moisture content of the soil. Following modified test procedure was followed according to AASHTO T180-19 (2019) standard.

In order to conduct modified Proctor test, following testing apparatus were used: Cylindrical metal mold (with 5469 grams of weight and 2119 cm³ of volume), sensitive balance, modified compaction rammer (4.5 kg), trays, steel straightedge, and drying oven. 6 samples with 8 kg soil were prepared for this exercise to get the dry unit weights. Each sample was prepared with adding 100 ml more water on every trial (100 ml, 200 ml, 300 ml..). After that, wet samples were put into Proctor mold which had 5469 grams of mass and 2119 cm³ volume and separated with 4 equal layers for the purpose of this research. 4.5 kg rammer was used for compaction and 70 blows were applied with a free fall from a height of 450 mm for each layer. In traditional method, modified Proctor is done by 56

blows per 5 layers. In order to optimize the same compaction energy for 4 layers, 70 blows were applied with 4.5 kg rammer. Afterwards, the top of the mold was removed. Sample preparation for modified Proctor test is shown in Figure 3.5.



Figure 3.5 Modified Proctor test sample.

Mass of molds and soil together were weighed, and soil samples were taken and put into trays to define water content for each trial. Weight of the trays which contained the bulk samples were calculated and put in oven for 24 hours to obtain dry weights. Then, oven dried samples were collected. Dry weight and amount of water on each sample was determined. After this process, water contents were found by the Equation 3.4.

$$\text{Water Content} = \frac{\text{Weight (Bulk Sample - Dry Sample)}}{\text{Weight (Dry Sample)}} \times 100 \quad (3.4)$$

Water content of samples were found as 3.0, 4.2, 5.5, 6.4, 7.5 and 8.9 percent. Since the water contents were determined, bulk unit weights were needed to find dry unit weights. Weight of bulk samples were divided by their volumes to obtain bulk unit weights. Formulas are represented in Equation 3.5 and 3.6 shows this process in detail.

$$\text{Bulk Unit Weight } (\rho) = \frac{\text{Weight of Bulk Sample}}{\text{Volume of Bulk Sample}} \quad (3.5)$$

$$\text{Bulk Unit Weight } (\rho) = \frac{\text{Weight (Bulk Sample + Mold)} - \text{Weight (Mold)}}{\text{Volume (Mold)}} \quad (3.6)$$

Bulk unit weights of samples were found as 2.132, 2.182, 2.270, 2.297, 2.319 and 2.319 g/cm³. So, moisture contents and the bulk unit weights of samples were determined, and dry unit weights could be calculated. Relation between the bulk unit weight, moisture content and dry unit weight is given by the following Equation 3.7. Results that were found from modified Proctor tests were shown in Table 3.1.

$$\text{Dry Unit Weight } (\rho_d) = \frac{\text{Bulk Unit weight}}{1 + \text{Water Content}} \quad (3.7)$$

Table 3.1 Dry Unit Weight Results

Mold No.	1	2	3	4	5	6
Bulk unit weight, g/cm ³	2.132	2.182	2.270	2.297	2.319	2.319
Moisture Content, %	3.0	4.2	5.5	6.4	7.5	8.9
Dry unit weight, g/cm ³	2.070	2.094	2.151	2.159	2.157	2.130

Moisture content that refers to maximum dry unit weight which was 2.159 g/cm³. It was decided to define the optimum water content for tested soil as 6.5% for most efficient compaction on California Bearing Ratio tests which is shown in Figure 3.6.

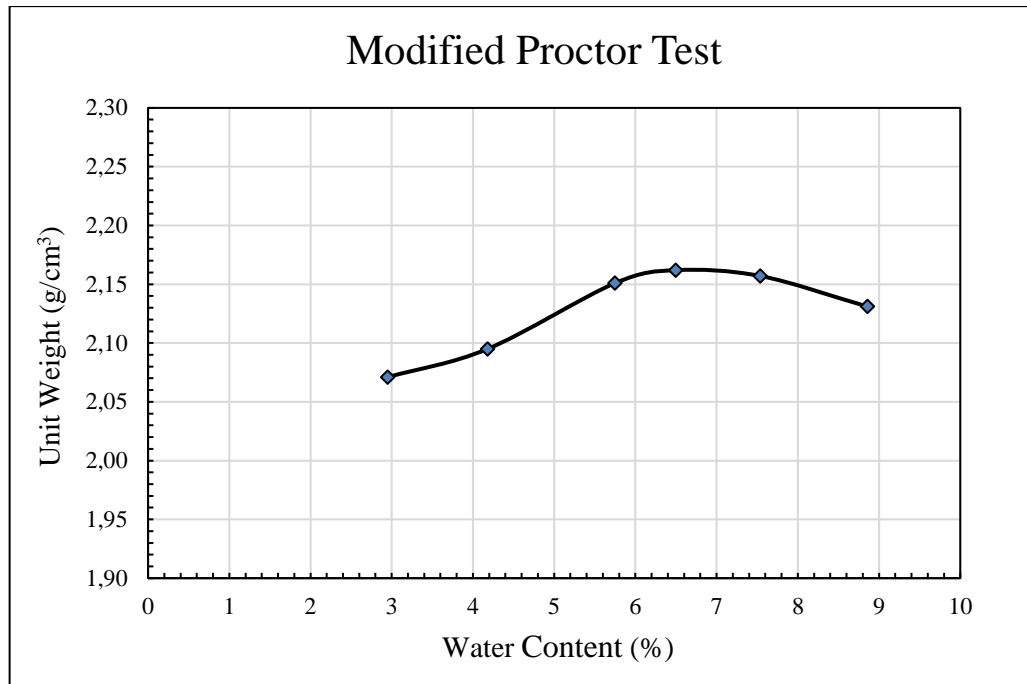


Figure 3.6 Modified Proctor Test Results (Dry Unit Weight vs. Water Content).

3.1.1.4. Relative Density

Relative density (D_r) is a critical value for soil, which defines the ratio of the density of a material to another reference material. Generally, density of water is used for this approach. If the voids between the particles that soil consists of are a lot, soil is classified as loose and can be compressive under loading. In contrast, soils with less voids between particles called dense soils which have higher internal friction angle and settlements occur less. e (void ratio of soil), e_{Max} (maximum void ratio of soil at loosest state), e_{Min} (minimum void ratio of soil at densest state) should be known to calculate D_r value of a soil. Following relations 3.8 and 3.9 were used to calculate e_{Max} and e_{Min} .

$$e_{Min} = (\rho_s / \rho_{k_{min}}) - 1 \quad (3.8)$$

$$e_{Max} = (\rho_s / \rho_{k_{max}}) - 1 \quad (3.9)$$

where;

ρ_s = Soil particle density

$\rho_{k_{min}}$ = Loosest state soil density

$\rho_{k_{max}}$ = Densest state soil density

Density of soil (ρ_s) is equal to specific gravity of soil times water density ($G_s\rho_w$). Therefore, density of soil was calculated with the ratio of mass of soil over mass of water which has equal volume with soil (Equation 3.10). ASTM D854-14 (2014) procedure was followed to find the specific gravity of soil. Averages of tests were taken and ρ_s was found as 2.68.

$$\rho_s = G_s\rho_w = \frac{(W2 - W1)}{(W2 - W1) - (W3 - W4)} \quad (3.10)$$

where;

W1 = Mass of density bottle

W2 = Mass of the density bottle and oven dry soil

W3 = Mass of the density bottle and soil and water

W4 = Mass of density bottle and water

G_s = Specific gravity of soil

ρ_w = Density of water

To calculate $\rho_{k_{max}}$, soil was placed into the mold and compacted with hammer to reduce all voids in it. Weight of the compacted soil was divided into volume of the mold. For $\rho_{k_{min}}$, soil was placed into mold without any compaction (Uzuner, 2015). Weight of soil was calculated and divided into volume of the mold. $\rho_{k_{min}}$ and $\rho_{k_{max}}$ were found as 1.6 and 1.9, respectively. So, e_{Min} and e_{Max} were found 0.41. and 0.68. Since void ratios were determined, D_r was calculated with the relation between the relative density and voids (Equation 3.11). As a result, D_r of soil was found 70%.

$$D_r = \frac{e_{Max} - e}{e_{Max} - e_{Min}} \times 100 = \frac{\rho_{k_{max}}}{\rho_k} \left(\frac{\rho_k - \rho_{k_{min}}}{\rho_{k_{max}} - \rho_{k_{min}}} \right) \times 100 \quad (3.11)$$

Required soil properties were determined through laboratory experiments before testing with reinforcements. Detailed soil properties are formed in Table 3.2 to summarize the properties after all tests. Also, closer image of the soil particles was captured by using microscope which was in Figure 3.7. As can be seen in the image, testing soil consists of different sized particles. Particles are angular shaped and have rough surfaces.



Figure 3.7 Soil sample under microscope.

Table 3.2 Detailed Soil Properties

Property	Unit	Value
Specific Gravity	-	2.68
Maximum Dry Unit Weight	kN/m ³	21.16
Maximum Void Ratio (eMax)	-	0.68
Minimum Void Ratio (eMin)	-	0.41
D _R	-	70%
D ₁₀	mm	0.07
D ₃₀	mm	0.51
D ₅₀	mm	1.29
D ₆₀	mm	1.68
AASHTO Classification	-	A-1-b
USCS Classification	-	SW
Cohesion	kPa	0
Angle of Friction	°	35
Coefficient of Curvature	-	2.2
Coefficient of Uniformity	-	24
Optimum Moisture Content	-	6.5%

3.1.2. Reinforcements

Two types of geosynthetics, which were geotextiles and geogrids, and various fiber types were studied in this research. Detailed properties or reinforcements are given as below:

3.1.2.1. Geotextiles

14 different types of geotextiles were investigated in this research. Some of them were made of polypropylene and others were polyester. Weight, thickness, and tensile strength values of geotextiles which were obtained from the manufacturer, detailed in Table 3.3. Laboratory tests were conducted to understand the effect of the physical properties of geotextile reinforcements on bearing capacity of pavement.

Table 3.3 Material Properties of Geotextiles

Reinforcement	Material	Weight (g/m²)	Thickness (mm)	Tensile Strength (kN/m)
Geotextile 1	Polypropylene Geotextile	110	0.5	7.3
Geotextile 2	Polypropylene Geotextile	150	1	10.3
Geotextile 3	Polypropylene Geotextile	1000	5	60-70
Geotextile 4	Polyester Geotextile	538	4	8-9
Geotextile 5	Polyester Geotextile	450	3	7-8
Geotextile 6	Polyester Geotextile	330	2	3-4
Geotextile 7	Polyester Geotextile	300	2.2	3-4
Geotextile 8	Polyester Geotextile	500	4	5-7
Geotextile 9	Polyester Geotextile	100	1.1	0.5-1
Geotextile 10	Polyester Geotextile	200	1.5	1.5-2
Geotextile 11	Polyester Geotextile	350	2.6	3-4
Geotextile 12	Polypropylene Geotextile	155	1	9.5
Geotextile 13	Polypropylene Geotextile	180	2	12
Geotextile 14	Polypropylene Geotextile	200	3	13.5

Since some of the geotextile reinforcements were produced of same material, similar ones were grouped, and features were compared in CBR tests. For example, Geotextile 1, 2, and 3 were made of polypropylene. Their physical features like thickness, weight per meter square, tensile strength and texture distinguishes them from each other. Figure 3.8 represents the surface textures of Geotextile 1, 2 and 3. Another group of geotextiles that were grouped and examined together was Geotextile 4, 5 and 6. These geotextiles were made of polyester and have different technical features. Surface textures of Geotextile 4, 5 and 6 are given in Figure 3.9. Then, Geotextile 7, 8, 9, 10 and 11 was defined as another group that made of identical raw material. This group of geotextiles was also polyester like previous group, however, Geotextile 7, 8, 9, 10, and 11 were made of recycled materials and each had different physical properties. This group of geotextiles are represented in Figure 3.10 and 3.11. Final geotextile group that were made of polypropylene was Geotextile 12, 13, 14. Geotextile 12, 13 and 14 are shown in Figure 3.12.

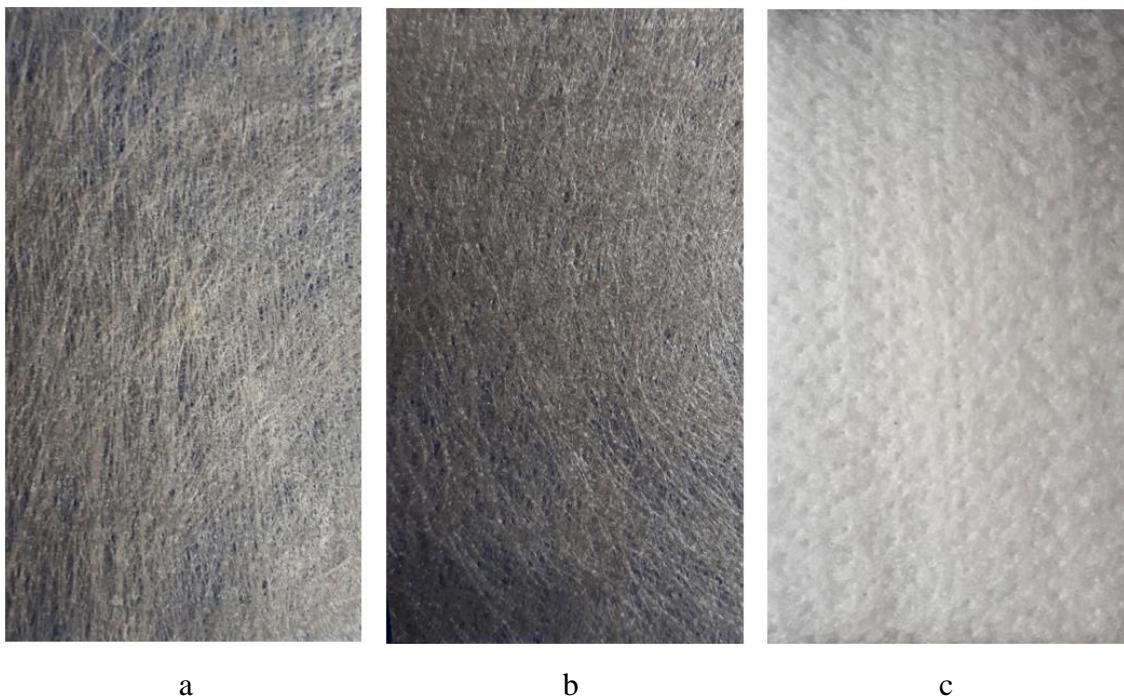
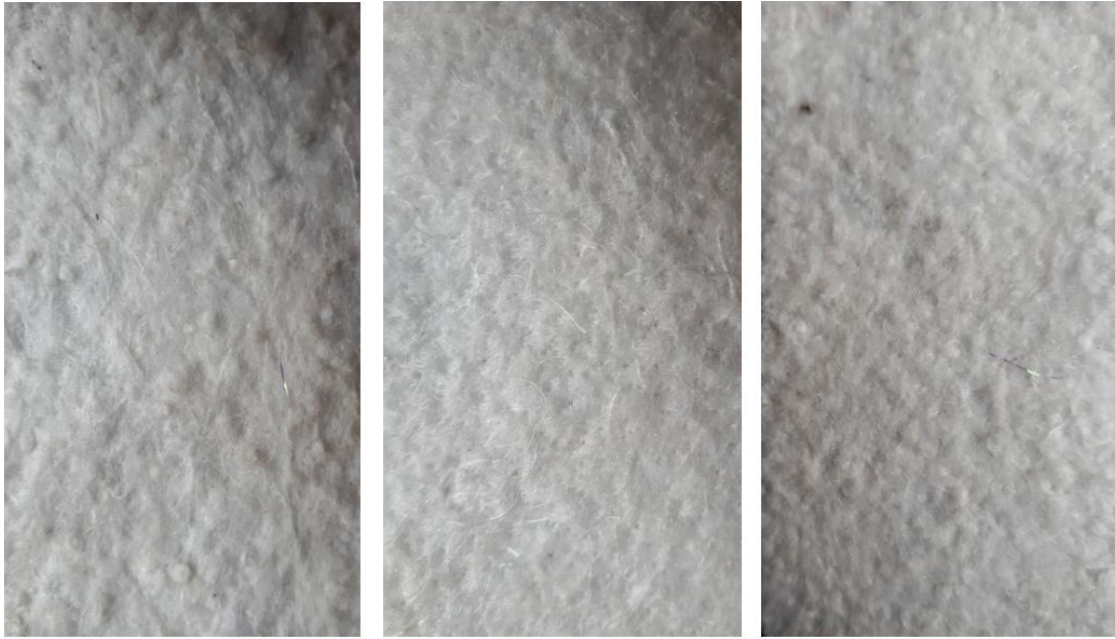


Figure 3.8 Surface textures of geotextiles; (a) Geotextile 1, (b) Geotextile 2, (c) Geotextile 3.



a

b

c

Figure 3.9 Surface textures of geotextiles; (a) Geotextile 4, (b) Geotextile 5, (c) Geotextile 6.



a

b

c

Figure 3.10 Surface textures of geotextiles; (a) Geotextile 7, (b) Geotextile 8, (c) Geotextile 9.



a

b

Figure 3.11 Surface textures of geotextiles; (a) Geotextile 10, (b) Geotextile 11.



a

b

c

Figure 3.12 Surface textures of geotextiles; (a) Geotextile 12, (b) Geotextile 13, (c) Geotextile 14.

3.1.2.2. Geogrids

Geogrids are commonly using for transportation engineering problems nowadays. The gaps between the stripes allow soil material to pass through and this behavior causes cohesion. Besides, there are other usage fields of geogrids which are placement under the aggregates on unpaved roads, repair of the landslide due to failure of slopes and as asphalt reinforcement on pavements (Yılmaz & Eskişar, 2007).

For this research three types of two-way geogrids were used which are given in Figure 3.13. In general, two-way (biaxial) geogrids increase the bearing capacity of the soil and extend the service life. Moreover, two-way geogrids restrain the pavement from cracking and reduce patching cost. Detailed properties of geogrids can be noticed in Table 3.4.

Table 3.4 Properties of Geogrids

Reinforcement	Material	Tensile Strength	Aperture Size	Weight
		(kN/m)	(mm)	(g/m ²)
Geogrid 1	Polyester	30	30x30	270
Geogrid 2	Polyester	40	25x30	370
Geogrid 3	Polyester	80	20x25	360

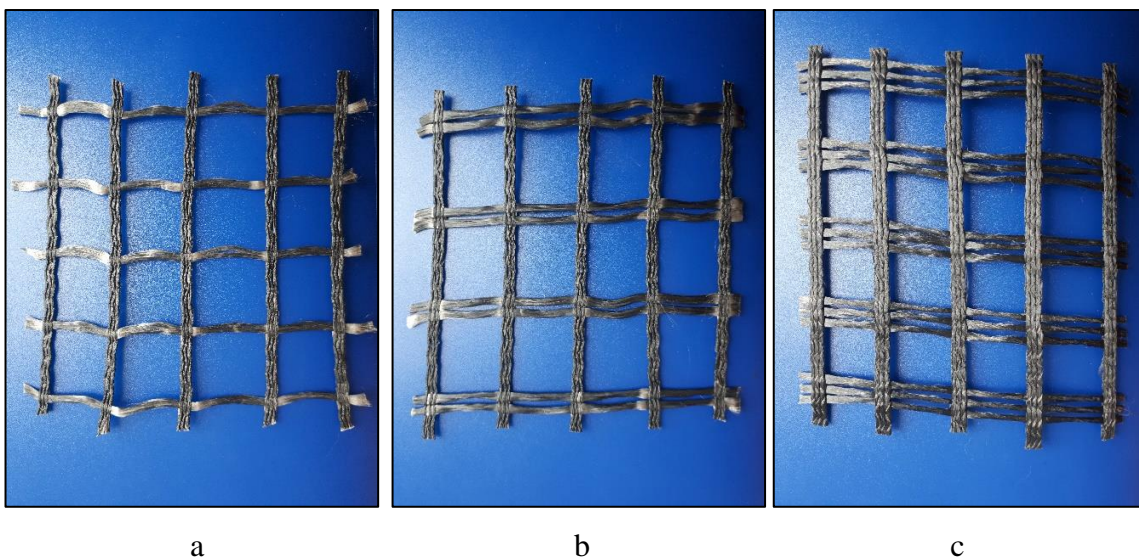


Figure 3.13 Images of geogrids; (a) Geogrid 1, (b) Geogrid 2, (c) Geogrid 3.

3.1.2.3. Fibers

As can be known that, natural fibers were the materials used as reinforcements in ancient times for stabilizing the roads. However, nowadays, engineers use different types of man-made synthetic fibers in constructions. Polyolefin and polypropylene fibers are the most known synthetic fibers. It is known that the most efficient mixing proportion for fibers is around 1% content of the mixture (Yılmaz, 2015). Therefore, in this study only this proportion was used as fiber content to reinforce soil.

For this research, 6 types of polypropylene fibers were used, and each fiber had different physical properties such as length, tensile strength, and quantity per amount. Properties of the fibers were taken from the manufacture firms. Detailed properties of each fiber type can be seen in Table 3.5. Images of the fibers are in Figure 3.14.

Table 3.5 Properties of fibers

Reinforcement	Material	Fiber Length, mm	Fiber Amount, per 50 g	Tensile Strength, MPa
Fiber 1	Polyolefin (%99 Polypropylene)	50-60	1.850	600
Fiber 2	Polyolefin (%99 Polypropylene)	54	3.000	600-700
Fiber 3	Copolymer (%99 Polypropylene)	54	>10,000	600-750
Fiber 4	Polyolefin (%99 Polypropylene)	48-54	>10,000	600-800
Fiber 5	Polypropylene	18	>10,000	350-500
Fiber 6	Polypropylene	18	>4,000,000	380-450

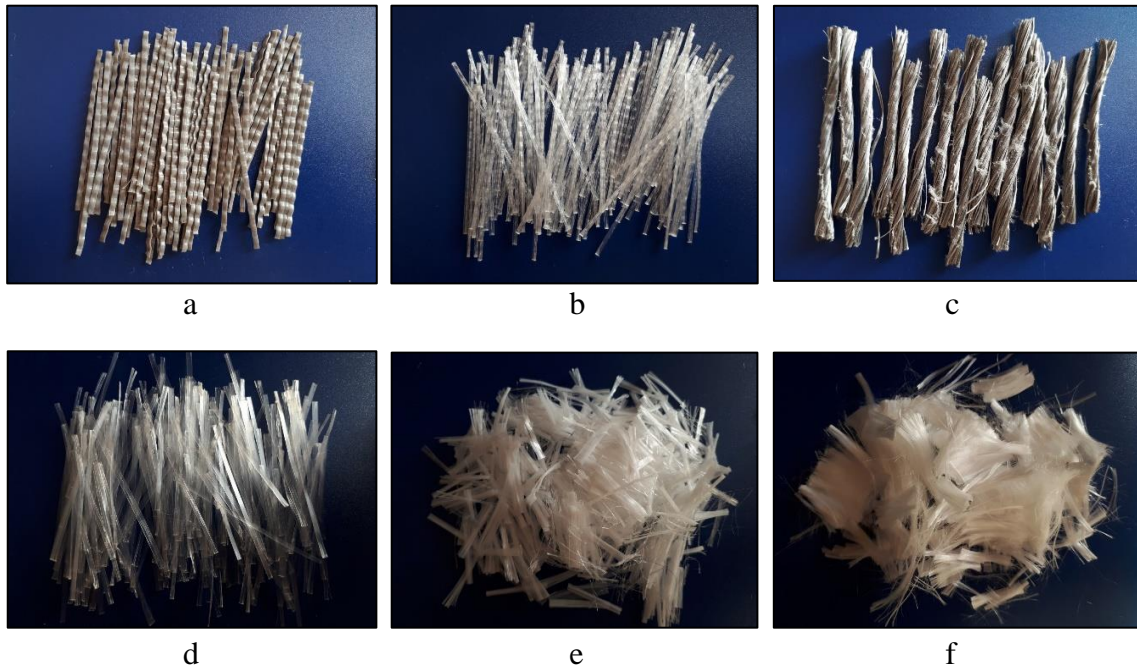


Figure 3.14 Fiber types used in the study; (a) Fiber 1, (b) Fiber 2, (c) Fiber 3, (d) Fiber 4, (e) Fiber 5, (f) Fiber 6.

3.2. Methods

California Bearing Ratio (CBR) tests were conducted to determine the effects of the reinforcements on pavement. In addition, reinforcements and soil were examined under microscope to understand the detailed structure of the materials. Details of the tests can be seen as below:

3.2.1. California Bearing Ratio Testing Program

California Bearing Ratio, which is commonly known as CBR, is an important parameter for civil engineering. CBR value of the pavement helps engineers to determine the bearing capacity of the pavement under stress. For each layer of the pavement, different CBR values expected to construct safer and longer service time roads. Following modified test procedure was conducted according to AASHTO T193-13 (2017) standards.

For California Bearing Ratio Test, following testing apparatus were used: Cylindrical metal mold, sensitive balance, modified compaction rammer (4.5 kg with), metal disk,

weights, trays, steel straightedge, CBR testing machine and drying oven. Optimum moisture content was found with using modified Proctor test is given on the previous section. Since optimum water content for maximum compaction was known, which was 6.5%, samples were prepared for the CBR tests. At first, molds were measured and values like molds heights and diameters were noted down to calculate the volumes of the molds. Secondly, weights were placed inside the molds. Soil was taken and mixed with 6.5% water. And little specimens from the samples were taken and put in the oven to double check the water content of the mixture. Soil that was going to put in the mold was divided into 4 equal layers for the purpose of this research and samples were compacted. Compactions were done with 70 blows for each layer (Figure 3.15). Next, top part of the mold was extracted to trim excess soil on the mold. Each sample was weighed on sensitive balance and soaked in the curing pool for 4 days (Figure 3.16).



Figure 3.15 Compacting soil samples with 4.5 kg rammer.



Figure 3.16 Compacted samples in the curing pool.

After that, molds were taken from the curing pool and put on the CBR testing machine. A dial was placed on each mold to observe the penetration values and calibrations were checked. Rate of penetration values on dials were tracked by timer and loadings at each 2.5 mm penetration were noted, which was going to be divided by standard load values in the following process. Finally, CBR test results were calculated with the Equation 3.12. For California Bearing Ratio calculations, 1370 kgf were taken as standard loads.

$$\text{CBR} = \frac{\text{CBR Test Load}}{\text{Standard Load}} \times 100 \quad (3.12)$$

Then, bearing capacities of all samples were determined and compared. For this approach, maximum stress value at specific penetration level for reinforced pavement was divided by maximum stress obtained from unreinforced model at same penetration level which was given in Equation 3.13. Increases, decreases and effects of reinforcements on bearing capacity of pavements were discussed.

$$\text{BR} = \frac{q}{q_0} \quad (3.13)$$

where;

q = Maximum stress obtained from reinforced pavement

q_0 = Maximum stress obtained from unreinforced pavement

In California Bearing Ratio tests, three different types of reinforcements were used in soil: geotextiles, geogrids and fibers. Additionally, different placements methods and combinations of multiple reinforcements were tested with California Bearing Ratio procedure to see the differences on the effects on the bearing capacity of the pavement.

As a first step of this research, the best location of a reinforcement in soil and the number of them were investigated. In order to find the best placement depth in soil, reinforcements were tested on three positions which were on top (c), middle (d) and bottom (b) of the mold. Top and bottom reinforcements were placed between soil layers with a significant distance from top and bottom surfaces. Since the soil was equally divided into four layers for compaction, the required distance for reinforcements was determined as quarter of mold's height which was between two compacted layers. Locations of the reinforcements at these points are detailed in Figure 3.17.

In addition, one-layered, two-layered, and three-layered pavement models were prepared and tested to determine the most efficient reinforcement amount in soil. Single reinforcement was placed at $h/4$ (c) depth in soil. Two reinforcements were placed at $h/4$ and $3h/4$ depths together (e), and three reinforcements were placed at $h/4$, $h/2$, and $3h/4$ (f) positions. The experiments deemed necessary were repeated to ensure the accuracy of the results.

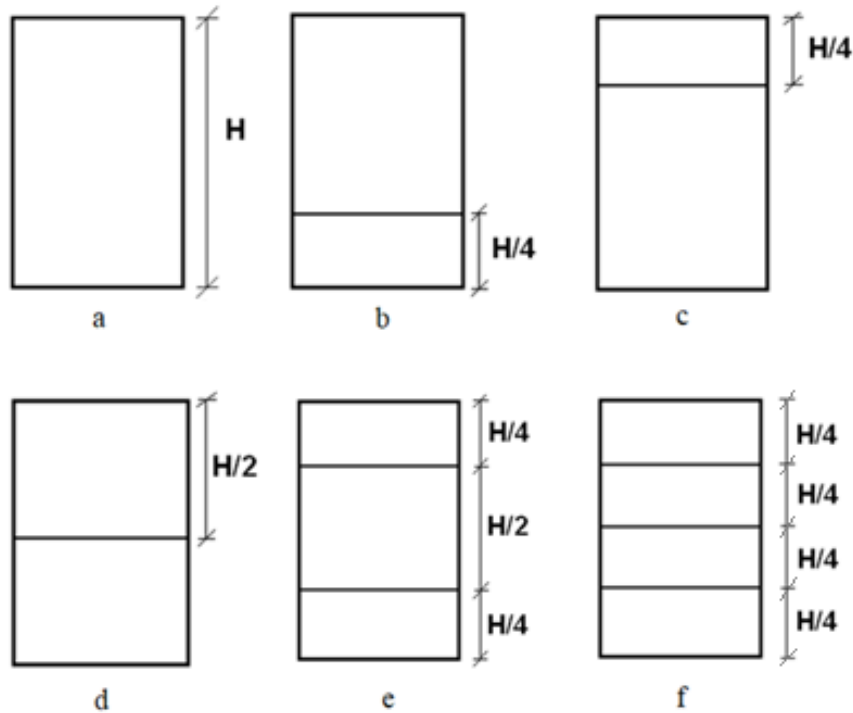


Figure 3.17 Different locations of reinforcements that were placed in molds; (a) unreinforced sample, (b) bottom reinforcement, (c) top reinforcement, (d) reinforcement, (e) two-layered reinforcement and (f) three-layered reinforcement.

3.2.1.1. Geotextile Reinforced Pavement Tests

In the first geotextile tests, Geotextile 1 was tested on 5 different positions which were on top, middle, bottom, top & bottom together and top & bottom and middle together. Next, compactions and curing done. Samples were tested on CBR and behaviors were investigated.

Afterwards, Geotextile 2 and 3 were examined. Since Geotextile 2 and 3 were also made of same material with Geotextile 1, they were tested on single (at $h/4$ depth) and three-layered conditions for detailed comparison with Geotextile 1. Then, CBR results were noted and behavior of pavements under loadings investigated. A sample preparing with geotextile reinforcement is shown in Figure 3.18.



Figure 3.18 A geotextile reinforcement placed between soil layers.

As a second step, different reinforcement types were compared in same conditions. So, Geotextile 1, 2 and 3 were compared on single (at $h/4$ depth) and three-layered positions. Afterwards, Geotextile 4, 5 and 6 were examined. These geotextiles were made of same material, which was polyester, but had different thicknesses and tensile strengths. Geotextile 4, 5 and 6 were placed at $h/4$ depth and CBR values and behaviors were examined. Another similar group of geotextiles were 7, 8, 9, 10 and 11 because they were all made of polyester. However, these geotextiles had various physical properties like thickness and tensile strength which was good for comparison. CBR values and behaviors under loadings of these geotextiles were examined. Finally, geotextile test series were conducted for another geotextile types, which were look alike and made of polypropylene, Geotextile 12, 13 and 14. CBR values and behaviors were investigated.

3.2.1.2. Geogrid Reinforced Pavement Tests

In this research, three types of geogrids were used as reinforcement to improve the bearing capacity of the pavement. In each test, one type of geogrid reinforcement was placed at $h/4$ depth and CBR values were obtained from the tests. Figure 3.19 shows geogrid placement between two soil layers.



Figure 3.19 A geogrid placed between compacted soil layers.

3.2.1.3. Fiber Reinforced Pavement Tests

Tests for fiber reinforced pavements were conducted by using two different method types. Fiber placement methods for this test series were modeled in Figure 3.20. First method was to use fibers by 1% amount of total mixture and put between soil layers like a geosynthetic material. Placement depth of all fiber reinforcements were chosen as $h/4$ (Figure 3.21). Next, compactions of the layers and curing were done and CBR values calculated. Second method was to mix fibers with whole mixture. Researchers reported that, fibers can be mixed in soil by hand. Besides, mechanical stirring methods may damage the fibers which causes decrease in their strength. Chang et al. (2014) mentioned that, their samples which were hand mixed showed better results than mechanical stirred samples in their tests. So, fibers and soil were mixed by hand which is represented in Figure 3.22. After compactions and curing, CBR values were examined. According to the research of Yılmaz (2015) fiber reinforced soil samples were prepared with using 1% content to achieve best results in CBR tests.

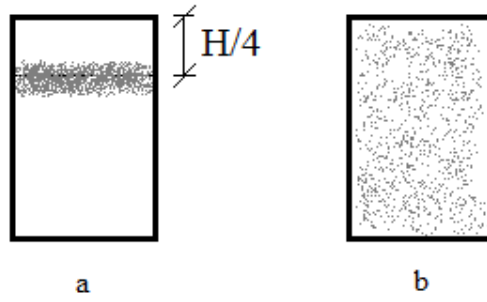


Figure 3.20 Fiber reinforcement placement; (a) 1% content by total mass at $h/4$ depth, (b) 1% content by total mass mixed in soil.



Figure 3.21 Synthetic fiber reinforcements that were placed between soil layers at $h/4$ depth.



Figure 3.22 Fiber reinforcements and soil after mixed by hand.

3.2.1.4. Geotextile and Fiber Combined Pavement Tests

It is reported that, using 0.5-1% fibers with a single geotextile can be effective as using multiple reinforcements in pavement (Hossain et al., 2015). For this test series, models created with combining single Geotextile 1 with all fiber types. Geotextiles were placed at h/4 depth in models and mixed with fibers by 1% proportion of total mass. Afterwards, CBR tests were conducted for combined reinforced samples. Behavior of the pavements under loadings were examined.

3.2.2. Microscopy Analysis

A representative soil sample, geotextiles, geogrids, and fiber reinforcements were examined under a microscope to understand the internal structures. Surfaces of the reinforcements were examined in detail. Images were obtained by S9i Leica microscope. Lens was chosen for the analysis was APO 1.6x/WD 50 mm. All microscopic images were obtained under same conditions, lighting, and distances. Since Fiber 5 and 6 were transparent, their images were taken in the black background for better comparison. Representative soil was examined in black background to see smaller granular particles clearly as well. Materials were investigated in this study were sixteen times magnified under microscope. Images of the materials were acquired from the software called as LAS Core on computer and observations discussed.

3.2.3. Cost Analysis

Layer thickness is one of the most important parameters in cost calculation, that reinforcements influence. A sample unpaved road was designed, and the total cost of the unreinforced and reinforced pavements were analyzed to understand the economical solution. The effect of reinforcements on pavement thickness were separately examined for both subbase and base layers. Design parameters of the road were assumed and fixed at the beginning only to focus on the effects of reinforcements on the pavement thickness. Length of the road was assumed as 1 kilometer with 3 meters lane width for this exercise. Subbase and base thickness values were determined for unreinforced and reinforced scenarios with AASHTO's Guide for Design of Pavement Structures (1993). Recommended flexible pavement design formula is given in Equation 3.14.

$$\log_{10}(W_{18}) = Z_{R_{S_0}} + 9.36 \log_{10}(SN+1) - 0.20 + \frac{\log_{10}\left(\frac{\Delta PSI}{(4.2 - 1.5)}\right)}{0.40 + \left(\frac{1094}{(SN + 1)^{5.19}}\right)} + 2.32 \log_{10}(M_R) - 8.07$$

(3.14)

where;

W_{18} = Number of 18-kip equivalent single axle load (ESALs)

Z_R = Standard normal deviate (function the design reliability level)

S_0 = Overall standard deviation of traffic (function the overall design uncertainty)

ΔPSI = Allowable serviceability loss at end of design life

M_R = Soil resilient modulus

SN = Structural number (required structural capacity)

Firstly, a sample flexible pavement designed to obtain the layer thickness for unreinforced condition. It was expected that, both geosynthetic and fiber reinforcements to reduce the thickness of subbase. SN value determines the required pavement thickness in this equation. So, all variables except SN, were fixed to understand the effects of reinforcements on thickness reduction. Variables were chosen in accordance with AASHTO's guide. AASHTO suggested 85-99.9% level of reliability for urban roads so it was taken as 95%. Roads under higher loadings should have more thickness values to provide the required bearing capacity. Therefore, W_{18} , axle load on this pavement was chosen highly to create a need for thicker and stronger pavement. Another parameter was present serviceability index (PSI). PSI is a value that determines serviceability of pavement, which is between 5 (excellent) and 0 (poor). Typically, PSI value for a flexible pavement is 4.2 immediately after construction. For pavements with terminal PSI value under 2.5, rehabilitation is recommended. Since ΔPSI stands for serviceability loss between terminal and initial conditions, it was taken 1.9 as an average. Following Table 3.6 shows the constants that were taken from AASHTO flexible road design tables for the assumed parameters.

Table 3.6 Fixed parameters and values that were assumed for the cost analysis

Reliability % (Interstate and other freeways, Urban)	95
Z_R (for reliability %95)	-1.645
S_0	0.350
W_{18}	14×10^6
ΔPSI	1.90

Structural number (SN) determines the thickness of pavement layer. As the SN increases, thickness of pavement increases. An important parameter for structural number (SN) calculations that this study especially focused on was the resilient modulus (M_R) of pavement because M_R is related with the CBR value of the road. Federal Highway Administration defines resilient modulus as a ratio of the cyclic stress to the recoverable (elastic) strain after many cycles of repeated loading. Since AASHTO's M_R formula is applicable only for the soils that have CBR less than 10, formula that Heukelom and Klomp (1962) suggested was chosen to create CBR and M_R correlation. Besides, this formula gives the least M_R result because of the coefficients, which was good for pavement design to be on the safer side. CBR and M_R relation is given in Equation 3.15.

$$M_R (\text{psi}) = 2555 \times (\text{CBR})^{0.64} \quad (3.15)$$

After finding the resilient modulus for all pavements, SN values were calculated by solving the flexible pavement equation. According to AASHTO, relation between SN and layer thicknesses was defined as the following Equation 3.16.

$$SN = a_1 D_1 + a_2 D_2 m_2 + a_3 D_3 m_3 \quad (3.16)$$

where;

SN = Structural Number

D_1, D_2 and D_3 = Structural layer thicknesses wearing surface, base, and subbase

a_1, a_2 and a_3 = Structural layer coefficients for wearing surface, base, and subbase

m_2, m_3 = Drainage coefficients for base and subbase

Layer and drainage coefficients and thickness values of wearing surface and base were fixed to focus on the changes on the subbase and base thickness and materials were assumed as Table 3.7. D_1 and D_2 were taken as minimum that is suggested from standards to focus on D_3 .

Table 3.7 Fixed parameters and values that were assumed for the cost analysis (subbase)

a_1 (Hot-mix asphaltic concrete - wearing surface)	0,44
a_2 (Crushed stone - base)	0,14
a_3 (Crushed stone - subbase)	0,11
m_2 (inches)	1,0
m_3 (inches)	1,0
D_1 (inches)	3,5
D_2 (inches)	6

After finding subbase thickness values (D_3), total costs of all models were estimated. Firstly, volume of soil that was required for unreinforced pavement was determined according to obtained thickness value. Then, cost of soil was noted due to the type of soil that was used in the CBR tests. Secondly, the amounts of required reinforcements were determined. Geosynthetic reinforcements that were required for the design pavement, were estimated in terms of surface area, and required fiber reinforcements were calculated as 1% of total soil mass. Unit prices of all reinforcements were obtained from manufacturer and total cost of reinforced pavements were determined by adding soil prices. Finally, the cost of unreinforced pavement was compared with the costs of reinforced pavements. Besides their costs, performances, and other advantages of using reinforcements for all models were discussed thereafter.

In addition, the same procedure was repeated to observe how the results would change if the reinforcements were used in base layer (D_2). SN values were calculated for first approach. Coefficients and thicknesses were fixed for wearing and subbase courses which are given in Table 3.8. Then, base thicknesses were examined after application of top five most effective reinforcements and results were discussed.

Table 3.8 Fixed parameters and values that were assumed for the cost analysis (base)

a ₁ (Hot-mix asphaltic concrete - wearing surface)	0,44
a ₂ (Crushed stone - base)	0,14
a ₃ (Crushed stone - subbase)	0,11
m ₂ (inches)	1,0
m ₃ (inches)	1,0
D ₁ (inches)	3,5
D ₃ (inches)	8

4. RESULTS AND DISCUSSION

This section consists of two parts. As a first section, it has results of California Bearing Ratio tests and microscopy analysis conducted with different reinforcement types. Both results were expressed together to understand the behavior of reinforcements for pavements. In the second section, pavement design was conducted for different conditions and cost analysis for these conditions were investigated.

4.1. Test Results

One of the aims of this study is investigating the effects of geosynthetics and fibers on the bearing capacity of pavement layer. Therefore, California Bearing Ratio tests were conducted in the laboratory. In the study, especially, the first experiments were repeated to ensure the results. After their accuracy had been proved, other tests were conducted and when a different behavior was seen the tests were repeated, also different reinforcements were used in the experiments. The first test series were performed to achieve an idea about the best location of reinforcement. Then some test series were conducted to understand the effects of amount of reinforcements on CBR in pavement. Performance of reinforced models and some combinations were examined. In the following section, firstly, detailed results of geotextile and geogrid reinforcements in soil are given. Secondly, fiber reinforced models and finally geotextile combined with fiber models were studied. CBR results, microscopy analysis and bearing ratios of all samples were discussed as below:

4.1.1. Unreinforced Test

Firstly, unreinforced road soil was tested in the laboratory and CBR value was found as 38.6. As can be seen from Figure 4.1, stress-penetration curve increased linearly. Additionally, stress values of unreinforced model for different penetration levels are shown in Table 4.1.

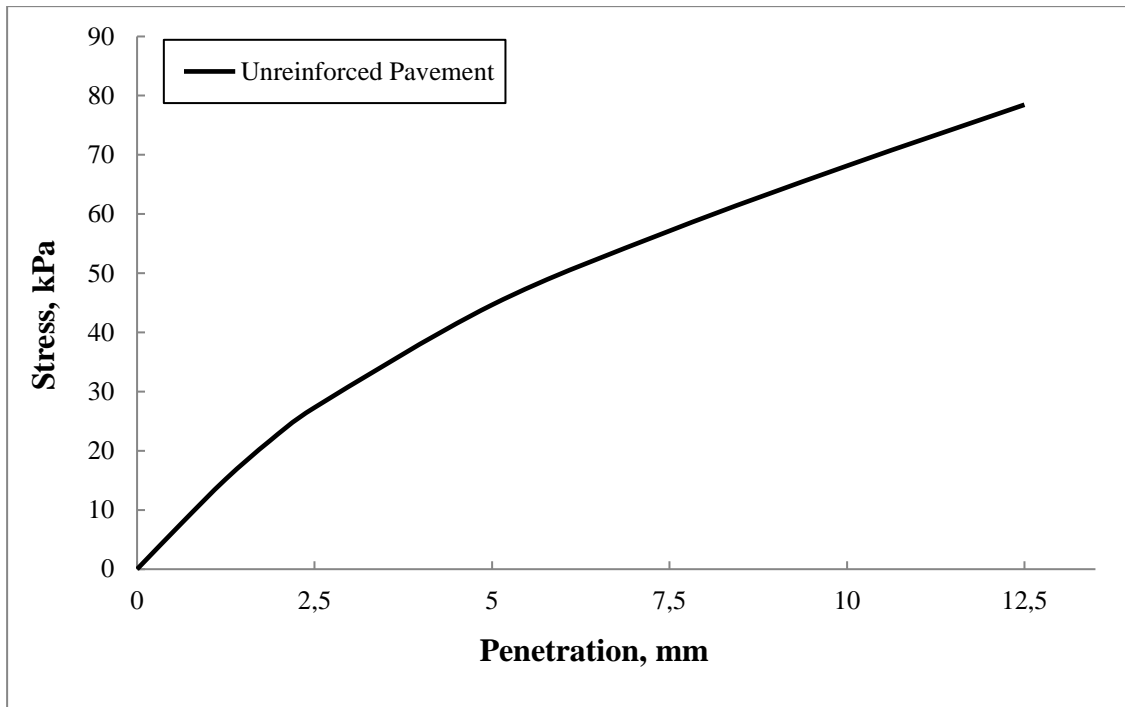


Figure 4.1 Stress-penetration graph of unreinforced pavement.

Table 4.1 Maximum stress values for unreinforced sand at different penetration levels (kPa)

Reinforcement Type	Penetration Levels (mm)		
	2.5	5	10
Unreinforced	27.31	44.65	68.14

4.1.2. Geotextile Reinforced Pavement Tests

First experimental series were conducted to determine the most efficient placement of the reinforcements. Chosen locations were top, bottom, and middle sections of the mold. Top and bottom reinforcements were placed at a distance from the mold's top and bottom surfaces with quarter height of the mold. Geotextile 1 reinforcement was used in these experiments and test results of each positioning can be observed in Figure 4.2. Maximum stress levels due to penetration levels are shown in Table 4.2 and bearing ratio of each placement were compared in Table 4.3.

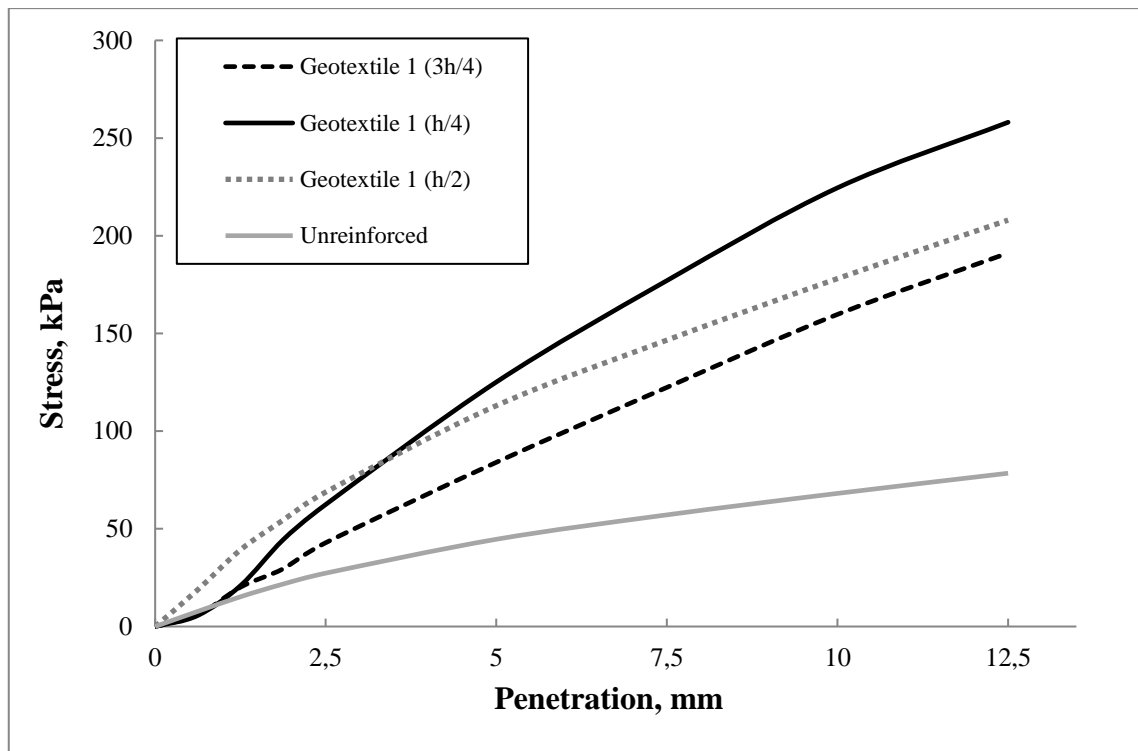


Figure 4.2 Comparison of the stress-penetration curves of Geotextile 1 on different placement conditions.

Table 4.2 Maximum stress values for Geotextile 1 at different penetration levels (kPa)

Reinforcement Placement Depths	Penetration Levels (mm)		
	2.5	5	10
3h/4	42.89	84.04	159.76
h/2	68.81	113.05	178.09
h/4	62.46	125.13	224.54

Table 4.3 Bearing capacities of reinforced sand with Geotextile 1

Penetration (mm)	Reinforcement Placement Depths		
	3h/4	h/4	h/2
2.5	1.57	2.29	2.52
5.0	1.88	2.80	2.53
10.0	2.34	3.30	2.61

When the results were compared it can be said that, placing reinforcement closer to the top of the testing mold was found the most effective location for one layered reinforced sample. Although the maximum stress at 2.5 mm and CBR was highest on h/2 depth placed specimen, h/4 placed specimen showed higher bearing capacity on total experimentation process. After 3.0 mm penetration, stress-penetration curve of h/4 placed geotextile passed other reinforced samples. At the end of the experiments, the bearing capacity of h/4 placed sample was almost 1.4 times higher than other samples. These results were compared with previous studies in the literature and similar outcome was observed about reinforcement positioning too. As the placement of the reinforcement goes deeper from top surface, effect of geotextiles on CBR value decreases (Sharma et al., 2013). Researchers repeated CBR tests with different sized molds and reported decrease on the CBR values again as the distances of geotextiles from top of the mold increased. Also, Masoumi et al. (2017) studied the effects of three types of geotextiles on sandy soils and highlighted that, by increasing the depth in all types of geotextiles, reduction on CBR values occurred. It was shown that the advantages of using geotextiles on CBR value decreased as the placement depth increased. Hossain et al. (2015) researched about the effects of placement of geotextile reinforcement in soil and reported that, using geotextile at top position is found more effective than middle or bottom positions. So, following tests were all conducted with adding reinforcements at h/4 depth from top surface to achieve the best CBR results.

Then single, two-layered and three-layered reinforced models were tested, and Figure 4.3 shows the comparison of the pavements under four different combinations: Unreinforced, single reinforcement (at h/4 depth), two reinforcements (at h/4 and 3h/4 depths) and three reinforcements (at h/4, h/2, 3h/4 depths) which is represented in Figure 3.17. Maximum stress values for Geotextile 1 at different penetration levels for single, two, and three-layered experiments are represented in Table 4.4.

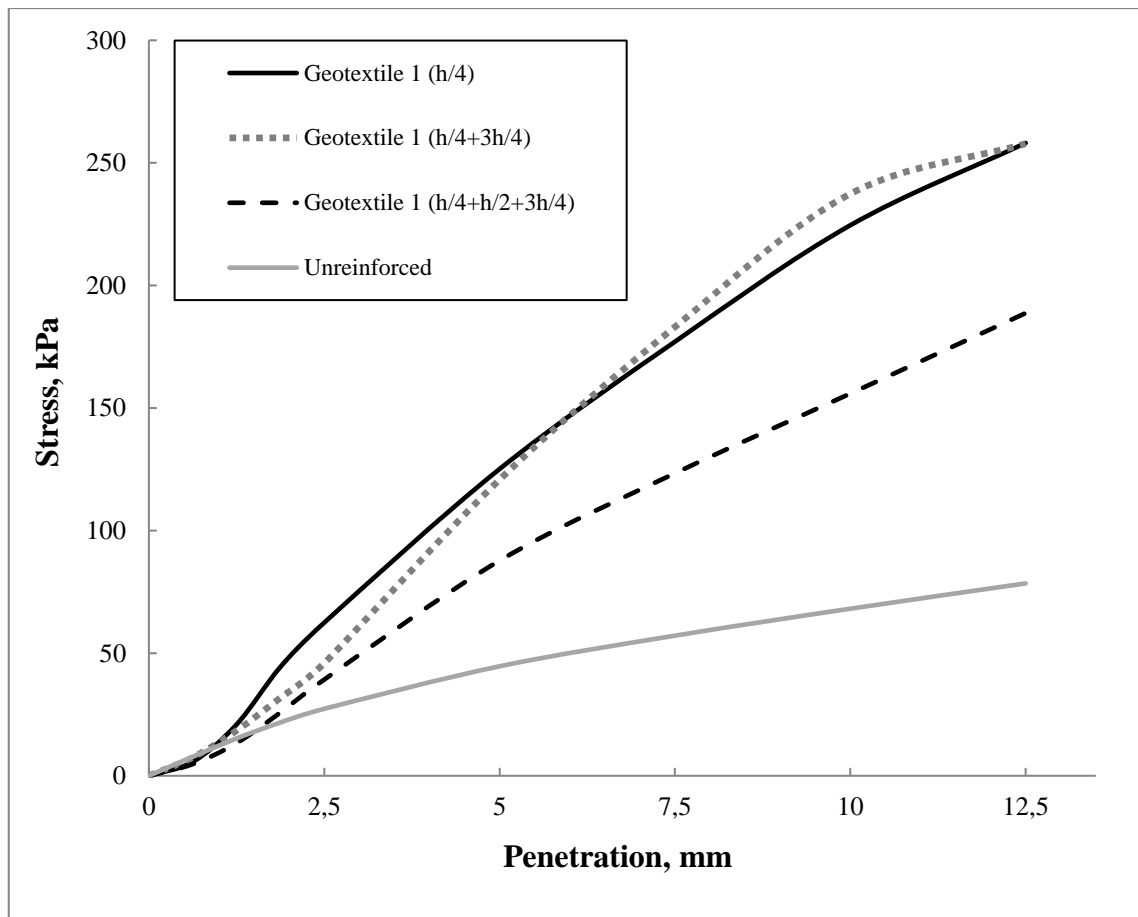


Figure 4.3 Comparison of the stress-penetration curves with different quantities of Geotextile 1 reinforced pavement.

Table 4.4 Maximum stress values for Geotextile 1 at different penetration levels (kPa)

Reinforcement Placement Depths	Penetration Levels (mm)		
	2.5	5	10
h/4	62.46	125.13	224.54
h/4 + 3h/4	45.94	120.79	237.35
h/4 + h/2 + 3h/4	39.23	87.76	155.90

As can be seen all geotextile reinforced models increased the bearing capacity on unreinforced model. Bearing capacities of Geotextile 1 reinforced pavements over unreinforced condition can be seen in Table 4.5.

Table 4.5 Bearing capacities of reinforced sand with different Geotextile 1 combinations

Penetration (mm)	Reinforcement Placement Depths		
	h/4	h/4 + 3h/4	h/4 + h/2 + 3h/4
2.5	2.29	1.68	1.44
5.0	2.80	2.71	1.97
10.0	3.30	3.48	2.29

As can be seen from the test results, using reinforcement affects the bearing capacity of the pavement. As the number of reinforcements added in the pavement increased, decrease in CBR values were observed. CBR value of single geotextile at h/4 depth placed model was higher than two-layered model. Only after 6 mm penetration, two-layered model slightly showed higher stress values than single reinforced pavement. Masoumi et al. (2017) studied two-layered geotextile models in sandy soil as well and reported that, two geotextile layers caused a change in the inherent behavior of soil due to discontinuity of aggregates. In addition to this, CBR result they obtained from one-layer model was higher than two-layered geotextile model as found in this study.

Another observation was the comparison between the performances of two-layered model and three-layered model. CBR result of two-layered model was higher than three-layered model. It was thought that, using multiple reinforced layers deteriorate the pavements natural structure which caused pavement layers to separate from each other and work independently. Naeini & Mirzakhani (2008) studied on the effects of geotextiles on granular materials and observed that, CBR value of three-layered model was lower than two-layered model too. However, they tested these scenarios in three different soil types and CBR values increased in other soil types. According to their research, the improvement of CBR with geotextile reinforcements depends on the soil grading. Soil with finer content has more affected from geotextiles and can show higher CBR results in multiple layered utilization. Because of that, multiple layered geotextile models were tested for Geotextile 2 and Geotextile 3 to understand and ensure the behavior of the soil that was used in this study.

Afterwards, Geotextile 2 was tested with as single reinforced and three-layered reinforced models. Although three-layered model increased unreinforced pavements CBR values, model with single reinforcement at $h/4$ depth showed approximately two times higher CBR values. Stress-penetration curves can be seen in Figure 4.4. Maximum stress values of Geotextile 2 reinforced tests are given in Table 4.6.

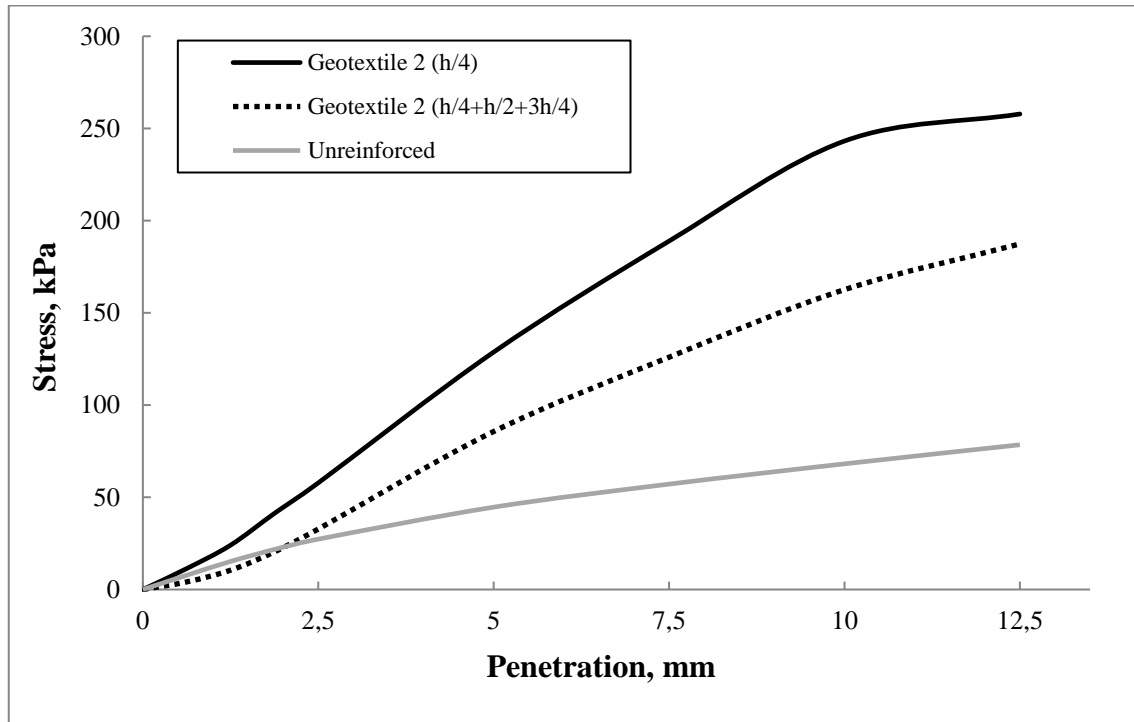


Figure 4.4 Comparison of the stress-penetration curves of Geotextile 2 reinforced pavements.

Table 4.6 Maximum stress values for Geotextile 2 at different penetration levels (kPa)

Reinforcement Placement Depths	Penetration Levels (mm)		
	2.5	5	10
h/4	57.81	128.74	243.18
h/4 + h/2 + 3h/4	32.78	85.69	162.60

Test with single reinforcement at $h/4$ depth concluded with higher CBR value than three-layered model tests just as Geotextile 1 series. Besides, bearing capacity of single Geotextile 2 over unreinforced pavement was 3.57 on 10 mm penetration which was higher than three-layered model's bearing capacity, 2.39. Detailed bearing capacity

results of both experiments are shown in Table 4.7. When reinforcements were compared from Figure 3.8 and Table 3.3, it can be seen that, Geotextile 1 and 2 were made of same materials but Geotextile 2 has more thickness. These experiments created the idea of the increase on the thickness of a geotextile could decrease the bearing capacity of the pavement too.

Table 4.7 Bearing capacities of reinforced sand with Geotextile 2

Penetration (mm)	Reinforcement Placement Depths	
	$h/4$	$h/4 + h/2 + 3h/4$
2.5	2.12	1.20
5.0	2.88	1.92
10.0	3.57	2.39

Then, tests for Geotextile 3 was conducted and as detailed in Figure 4.5. Using one Geotextile 3 at $h/4$ depth in pavement decreased the bearing capacity of the road. Therefore, it can be thought that the reason of this behavior could be the thickness of the Geotextile 3 reinforcement which is given in Table 3.3. The reinforcement could separate the soil layers which caused them to act independently from each other. Moreover, tests were also conducted with three-layered reinforced model which reinforcements were placed with equally distanced in the mold and results were found similar with combinations of Geotextile 1 and Geotextile 2. In all cases, three-layered reinforced models less the bearing capacity than one-layered models as can be observed in Figure 4.5. In literature, it is reported that the bearing capacity of the clay could increase with adding multiple reinforcements (Masoumi et al., 2017). In addition, soil grading has an influence on the improvement of soil strength and CBR with geotextile material. For soil with more fine percent, the effect becomes more significant (Vikram, 2018). However, pavement material that was used in this study is granular and stronger. The processing of granular material and geotextiles in water caused the swelling of the geotextiles, which separated soil layers and decreased CBR values.

On the other hand, at the beginning of the one-layered test, thickness of Geotextile 3 was so high that it reduced the interlocking of the structure and caused a change in the type of friction angle. After at 7.5 mm penetration, curve of sand with single Geotextile 3 reinforcement got higher than unreinforced condition. The reason of this behavior could be the reduction of the thickness of Geotextile 3 due to compressive loading at 7.5 mm penetration level. Stress-penetration values can be seen in Table 4.8.

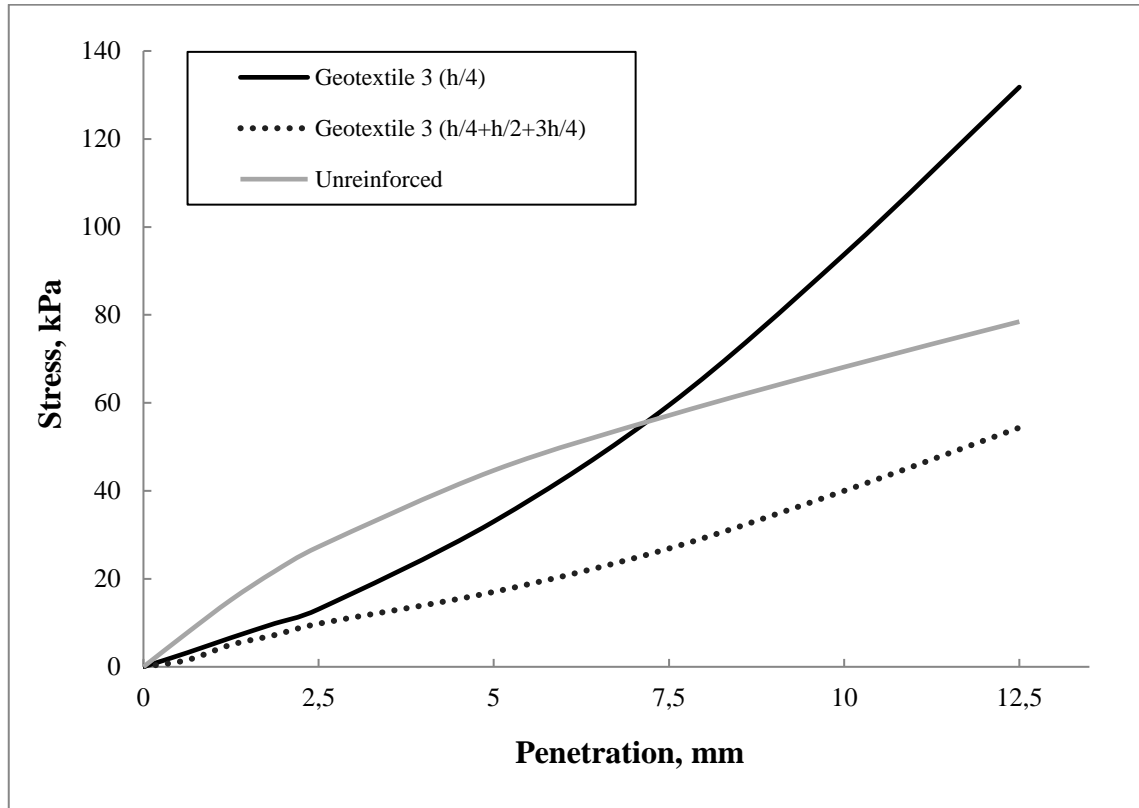


Figure 4.5 Comparison of the stress-penetration curves of Geotextile 3 reinforced pavements.

Table 4.8 Maximum stress values for Geotextile 3 at different penetration levels (kPa)

Reinforcement Placement Depths	Penetration Levels (mm)		
	2.5	5	10
h/4	13.11	33.03	93.74
h/4 + h/2 + 3h/4	9.80	17.03	40.00

As observed in Geotextile 1 and 2 tests, Geotextile 3 also showed similar behavior in single and three-layered model comparisons. Bearing capacity of single reinforced model

was higher than three-layered model. It was observed that geotextiles perform better under higher loadings and even at 10 mm penetration level bearing capacity ratio of single reinforcement was found higher. Bearing capacity ratios of single and three-layered Geotextile 3 models at 10 mm were found 1.38 and 0.59, respectively. Results that were obtained are shown in Table 4.9.

Table 4.9 Bearing capacities of reinforced sand with Geotextile 3

Penetration (mm)	Reinforcement Placement Depths	
	$h/4$	$h/4 + h/2 + 3h/4$
2.5	0.48	0.36
5.0	0.74	0.38
10.0	1.38	0.59

Up to this point, three different geotextiles were tested in single and multiple reinforced conditions. In each test, it was found that using three geotextiles in a pavement showed lower bearing ratios than single reinforced models. These results were found similar with the research of Azar & Dabiri (2015). They tested single and two-layered reinforced models and highlighted that, single geotextile reinforced model increased the bearing capacity where two-layered model decreased the bearing capacity and reduced the resistance of the samples. The reason of this behavior could be the discontinuity of the soil particles between geotextiles and placing one geotextile layer does not affect the natural structure of the specimens as researchers mentioned. This outcome supports the results of this test series as well. Vikram (2018) also noted that, in some cases, unreinforced pavements are even better than multiply reinforced pavements because of the separation of soil particles from each other. Same case was true for Geotextile 3 which decreased the bearing capacity of pavement in multiple usage. Naeini & Mirzakhani, (2008) mentioned about the effects of using multiple geotextiles can vary due to soil gradation. For the case of this study, using multiple geotextiles in one model was not found effective for this soil type. So, following geotextile reinforced tests were all conducted as one layered model.

CBR results of models reinforced with single Geotextile 1, 2, and 3 which were at h/4 depth, were compared to each other. The thickness values, weights and tensile strengths of these geotextiles increases in order as Geotextile 1, 2 and 3 as given in Table 3.3. However, CBR results of these models decreased as mentioned properties increased. Highest CBR result was obtained from the Geotextile 1 which had the lowest thickness and tensile strength value. Table 4.10 shows the stress comparison of h/4 depth placed Geotextile 1, 2 and 3.

Table 4.10 Maximum stress and CBR comparison of Geotextile 1, 2 and 3 at h/4 depth

Reinforcement Type	Max Stress at 2.5 mm (kPa)	CBR
Geotextile 1	62.46	88.3
Geotextile 2	57.81	81.8
Geotextile 3	13.11	18.5

Highest CBR value was obtained from the Geotextile 1 and Geotextile 3 reinforced model had the least CBR value. In fact, it was an important outcome that Geotextile 1 performed better than Geotextile 2, even if it had the lowest tensile strength which is detailed in Table 3.3. Microscopy analysis was performed to understand this behavior of geotextiles. Magnified images obtained under microscope are given as Figure 4.6.

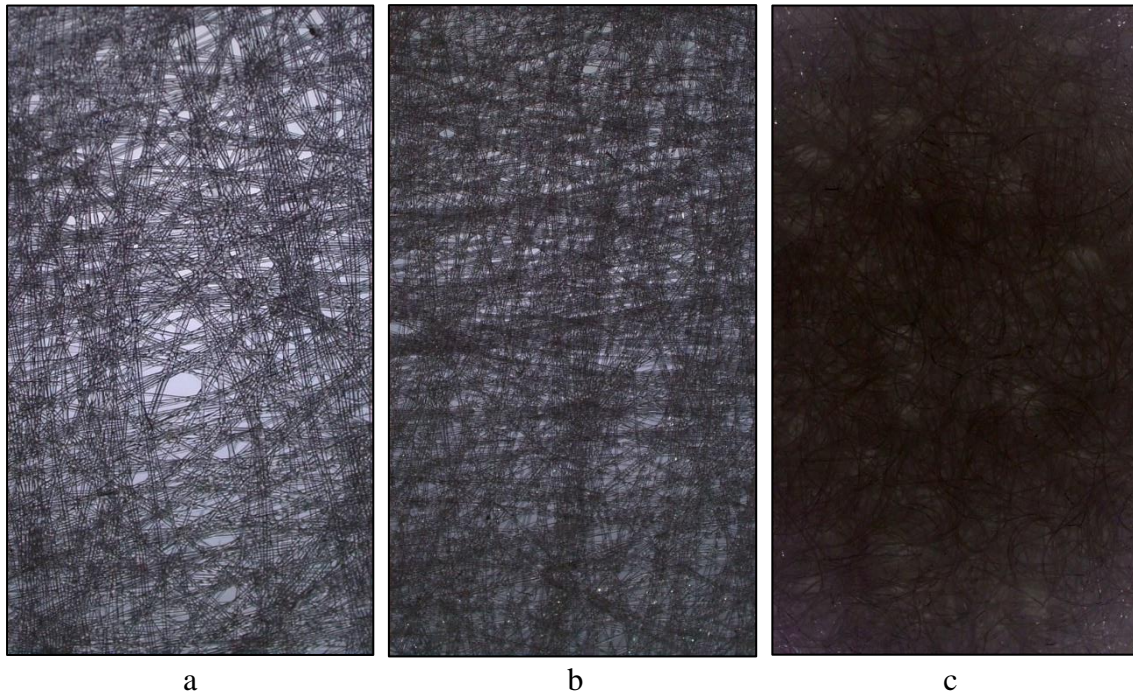


Figure 4.6 Microscope images for geotextiles; (a) Geotextile 1, (b) Geotextile 2, (c) Geotextile 3.

Since the backlight behind the reinforcements could pass through the voids, the places that appeared white in the images represented the gaps in the geotextiles. As can be seen from the microscopic images higher the geotextile thickness, more threads and less voids were observed. In contrast, thinner geotextiles which were knitted less, had more voids to let soil particles to fill. Geotextile 3 showed the least CBR value in tests even it had more threads and had higher strength than Geotextile 1 and 2. The reason of this behavior could be the knitting method of geotextiles. It was thought that there could be a significant amount of void areas required for soil to pass through and combine with geotextile naturally. Since Geotextile 3 had less voids, it separated the soil layers and prevent soil to work naturally.

On the other hand, Geotextile 1 which was produced with less threads, had more gaps and showed almost 5 times higher CBR results than Geotextile 3. In addition, these tests showed that, there must be a significant loading for each geotextile to start working completely. Since CBR values were taken into consideration at 2.5 mm penetration level, it did not represent the full potential capacity of geotextiles truly at 2.5 mm penetration level. So, the effect of geotextiles at 10 mm penetration level were discussed on following tests as well.

Figure 4.7 shows the results of the other geotextile group which consists Geotextile 4, 5 and 6. These reinforcements were tested only at $h/4$ depth and compared to unreinforced condition. Geotextile 6 shows different behavior than other geotextile types. Geotextile 4 and 5 have linear behavior for stress-penetration curve, but Geotextile 6 has different curve behavior and it increases with different slope. The thickness values, weights and tensile strengths of these geotextiles decreases in order as Geotextile 4, 5 and 6. However, CBR results increased in same order which means highest CBR was observed from Geotextile 6. CBR value of Geotextile 6 reinforced model was almost 2 times of unreinforced model. Relation between these properties and CBR values were found similar like the previous test series with Geotextile 1, 2, and 3. Stress values due to penetration levels which are detailed in Table 4.11.

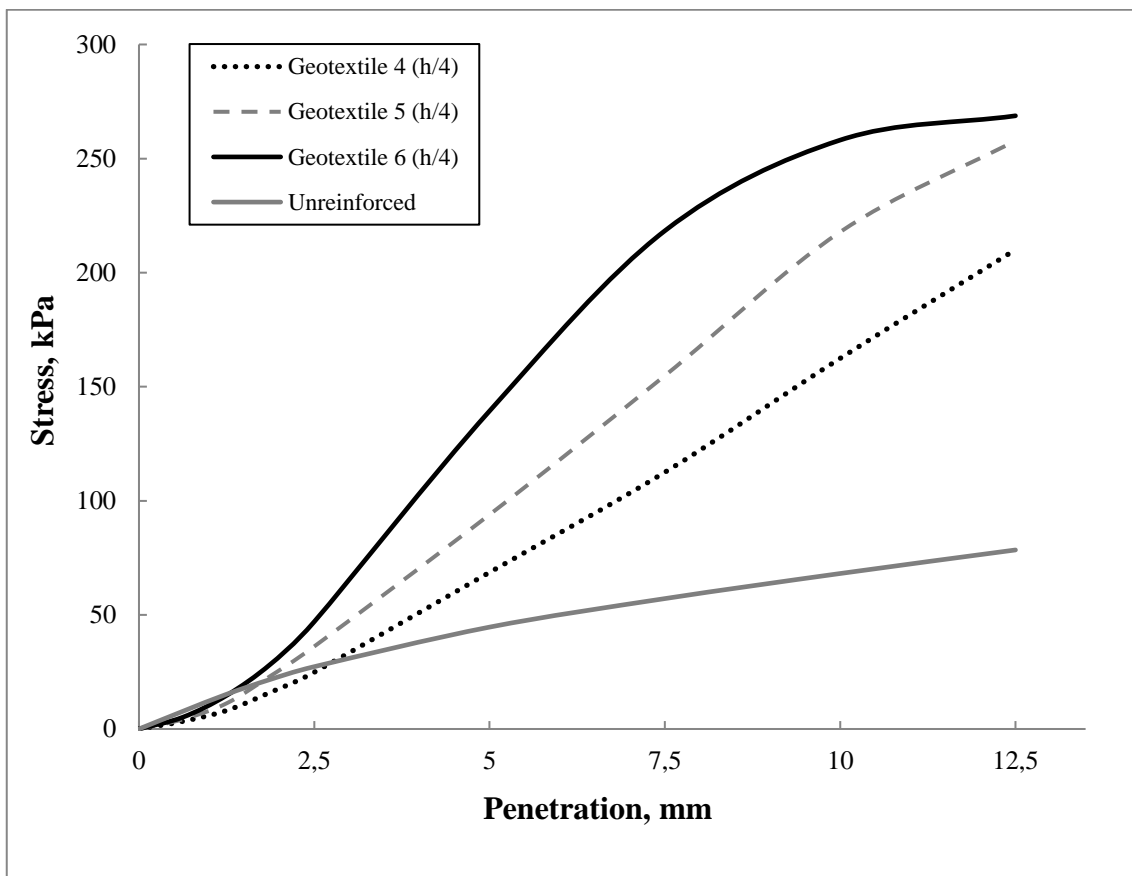


Figure 4.7 Comparison of the stress-penetration curves of Geotextile 4, 5 and 6 reinforced pavements.

Table 4.11 Maximum stress values for Geotextile 4, 5 and 6 at different penetration levels (kPa)

Reinforcement Type	Penetration Levels (mm)		
	2.5	5	10
Geotextile 4	24.88	68.65	162.45
Geotextile 5	36.18	93.95	217.83
Geotextile 6	47.02	139.37	258.10

Geotextile 4, 5, 6 were all polyester reinforcements. It was thought that there might be inverse proportional relation between the thickness and the bearing capacity. Increase of the thickness of this material caused the decrease of the bearing capacity. As shown in the Figure 4.7, Geotextile 6 showed the best performance among these geotextiles 4, 5, 6 and plotted a non-linear curve unlike Geotextile 4 and 5. Geotextile 4 could not able to perform up to 2.5 mm penetration like unreinforced condition. However, after 2.5 mm penetration, Geotextile 4 started to affect. Although Geotextile 4 showed the least bearing capacity between 4, 5 and 6 at 2.5 mm, it was still higher than unreinforced road condition on increasing stress values. It was observed that this group of geotextiles increased bearing capacity up to 2.38 to 3.79 times. Detailed bearing ratios of Geotextile 4, 5 and 6 over unreinforced model were compared in Table 4.12.

Table 4.12 Bearing capacities of reinforced sand with Geotextile 4, 5 and 6

Penetration (mm)	Reinforcement Type		
	Geotextile 4	Geotextile 5	Geotextile 6
2.5	0.91	1.33	1.72
5.0	1.54	2.10	3.12
10.0	2.38	3.20	3.79

Additionally, microscopic examinations in Figure 4.8 showed the textures of Geotextile 4, 5 and 6. It was thought that the spaces between fibers and knitting method of geotextiles could also affect CBR results. As can be seen in images, knitting frequent of weaving decreases from Geotextile 4 to 6 and the voids increases in this order as their tensile

strength. In contrast, CBR values were increased, respectively. Less woven geotextiles could let geotextile to mix in soil better than the geotextiles with more threads.

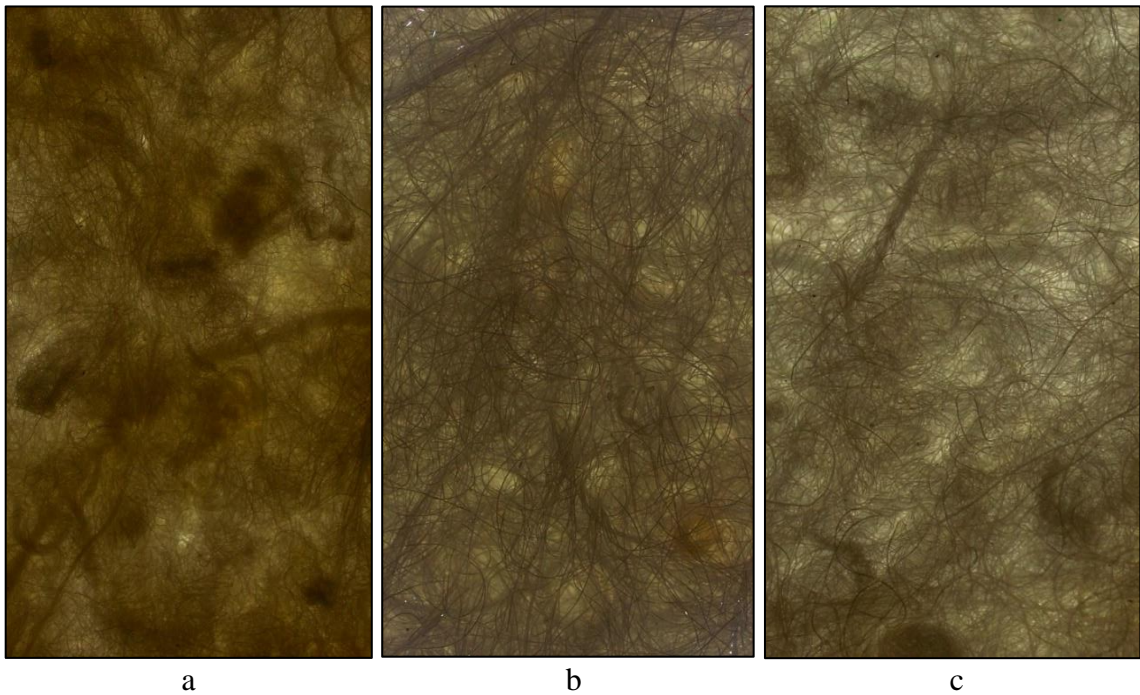


Figure 4.8 Microscope images for geotextiles; (a) Geotextile 4, (b) Geotextile 5, (c) Geotextile 6.

The comparison of models reinforced with Geotextile 7, 8, 9, 10, 11 can be observed in Figure 4.9. This experiment series also showed the relation between the thickness and bearing capacity because each reinforcement sample was made of identical material, recycled polyester. Differences between these geotextiles were thicknesses, textures, and tensile strengths which is given in Table 3.3. Stress-penetration values are detailed in Table 4.13. It was observed that, as the thickness of these geotextiles increases, CBR values of the pavement decreases relatively. Between these geotextiles, best result was observed from Geotextile 9 which was the thinnest material between Geotextile 7, 8, 10 and 11. Lowest CBR value was observed from Geotextile 8 that having more thickness. However, Geotextile 8 started to perform better than unreinforced condition after 2.5 mm penetration.

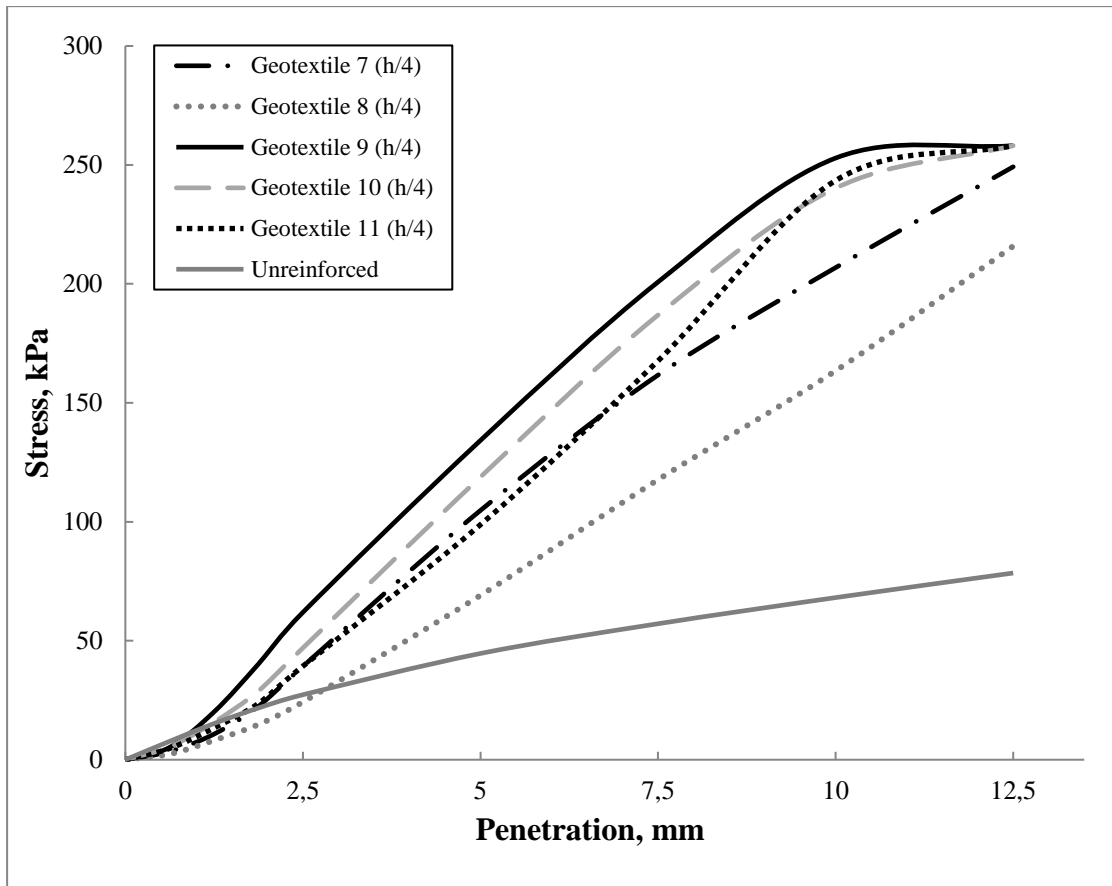


Figure 4.9 Comparison of the stress-penetration curves of Geotextile 7, 8, 9, 10 and 11 reinforced pavements.

Table 4.13 Maximum stress values for Geotextile 7, 8, 9, 10 and 11 at different penetration levels (kPa)

Reinforcement Type	Penetration Levels (mm)		
	2.5	5	10
Geotextile 7	39.23	104.79	206.84
Geotextile 8	24.26	69.07	163.48
Geotextile 9	61.94	134.21	252.88
Geotextile 10	46.97	118.83	240.24
Geotextile 11	39.33	98.80	243.44

These geotextiles increased the bearing capacity of unreinforced pavement between 2.40 and 3.71 times. Highest bearing capacity was observed from the thinnest geotextile (Geotextile 9). Even bearing capacity of Geotextile 8 at 2.5 mm penetration level was

lower than unreinforced pavement, Geotextile 8 started to perform at higher penetration levels and increased bearing capacity to 2.40. Again, it was thought that geotextiles should be loaded up to a significant point to unlock their full potential. Bearing ratios of these reinforcements over unreinforced case are given in Table 4.14.

Table 4.14 Bearing capacities of reinforced sand with Geotextile 7, 8, 9, 10 and 11

Penetration (mm)	Reinforcement Type				
	Geotextile 7	Geotextile 8	Geotextile 9	Geotextile 10	Geotextile 11
2.5	1.44	0.89	2.27	1.72	1.44
5.0	2.35	1.55	3.01	2.66	2.21
10.0	3.04	2.40	3.71	3.53	3.57

Furthermore, the performance of these geotextiles was related with the voids and the textures of the materials. The microscopic examination of Geotextile 8 and 11 showed that, they were woven more frequent than other geotextiles and they had highest tensile strengths as given in Table 3.3. Image of Geotextile 11 was too dark due to the woven method of the material and could not be captured clearly. On the other hand, Geotextile 9 was woven less and had tensile strength as 10% of Geotextile 8. But, CBR result of Geotextile 9 reinforced pavement was 2.55 times higher than Geotextile 8 reinforced pavement. Detailed microscopic images which showed the gaps on the Geotextile 7, 8, 9 and 10 are shown in Figure 4.10 and 4.11.

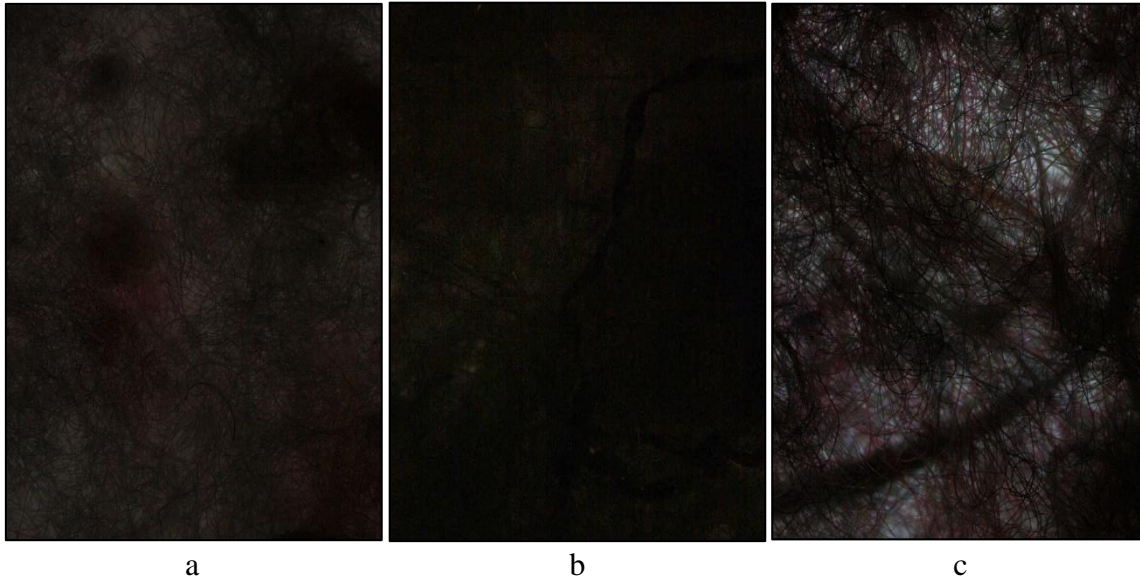


Figure 4.10 Microscope images for geotextiles; (a) Geotextile 7, (b) Geotextile 8, (c) Geotextile 9.



Figure 4.11 Microscope image for Geotextile 10.

As could be observed in microscopic images, less woven geotextiles (such as Geotextile 9 and 10) had more gaps which let them mix with soil efficiently and perform better than other geotextiles at 2.5 mm penetration level.

Another test series were conducted to examine the behaviors of Geotextile 12, 13, and 14. These geotextiles were made of identical raw material which was polypropylene. The thickness values, weights and tensile strengths of these geotextiles increases in order with Geotextile 12, 13, and 14 which are given in Table 3.3. Even if the tensile strength of the Geotextile 12, 13, and 14 increases respectively, CBR values were decreased in same

order. Figure 4.12 shows the detailed linear behavior of these materials under loading. Another supporting result was observed from this test series. Maximum stress values can be seen in Table 4.15. Highest CBR value was observed from Geotextile 12 and the smallest CBR value was examined from Geotextile 14. Additionally, CBR values of Geotextile 13 and 14 were less than unreinforced condition. However, under increased loading these geotextiles started to perform better than unreinforced test. At 4.0 mm penetration level, stress-penetration curve of Geotextile 13 got higher than unreinforced curve which was thinner than Geotextile 14, and performance increase occurred earlier than Geotextile 14. Especially around 9 mm penetration level, even slope of curve of Geotextile 14 reinforced model passed unreinforced test. As the compaction occurred, thickness of these geotextiles decreased and that could be the reason of the linear increase on their slope. As observed in previous results, this test series was supported the idea of the performance increase at the higher stress levels due to the compression on geotextiles which caused reduction on their thicknesses.

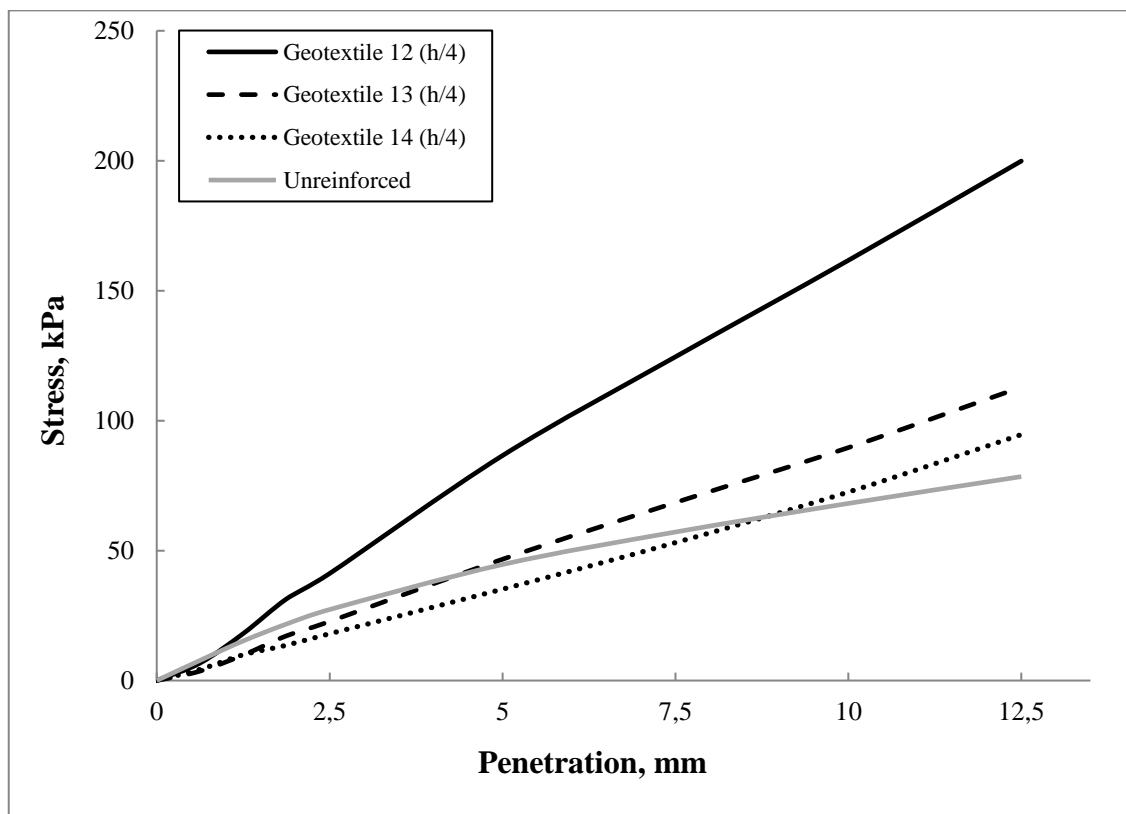


Figure 4.12 Comparison of the stress-penetration curves of Geotextile 12, 13 and 14 reinforced pavements.

Table 4.15 Maximum stress values for Geotextile 12, 13 and 14 at different penetration levels (kPa)

Reinforcement Type	Penetration Levels (mm)		
	2.5	5	10
Geotextile 12	41.19	86.57	161.67
Geotextile 13	22.71	46.66	89.61
Geotextile 14	18.01	35.15	72.52

As a result, the relation between CBR values and thickness of geotextile reinforcements was observed on these test series too. Highest CBR value was obtained from the thinnest geotextile which was Geotextile 12. Bearing capacity of unreinforced pavement were increased up to 1.51 times at 2.5 mm penetration and 2.37 times at 10 mm penetration level with Geotextile 12.

This test series also showed that, there must be a loading required for geotextiles to start performing in soil effectively. Geotextile 13 and 14 were not seem as effective as Geotextile 12 at 2.5 mm penetration level. Yet, when whole testing process taken into consideration, bearing capacities increased at 10 mm penetration, just as Geotextile 12 did. Bearing ratio comparison of Geotextile 12, 13 and 14 reinforced models over unreinforced model is detailed in Table 4.16.

Table 4.16 Bearing capacities of reinforced sand with Geotextile 12, 13, and 14

Penetration (mm)	Reinforcement Type		
	Geotextile 12	Geotextile 13	Geotextile 14
2.5	1.51	0.83	0.66
5.0	1.94	1.05	0.79
10.0	2.37	1.32	1.06

As could be observed in microscopy analysis, which is shown in Figure 4.13, gaps that soil could fill in the textile reinforcements decreases in Geotextile 12, 13 and 14,

respectively. Geotextile 14 was woven most frequent between these geotextiles. Detailed microscopic images of Geotextile 12, 13 and 14 are given below.

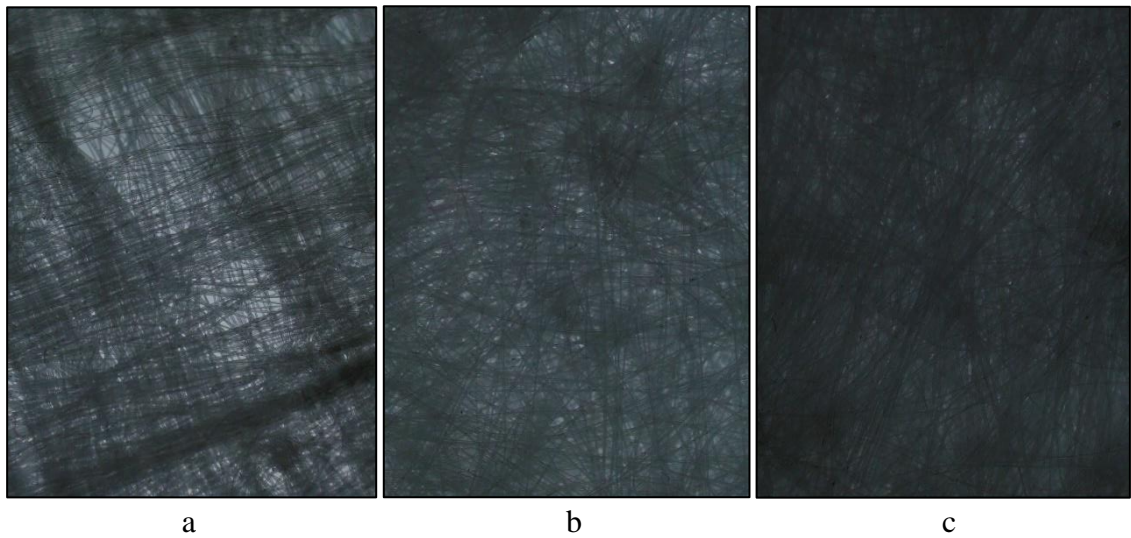


Figure 4.13 Microscope images for geotextiles; (a) Geotextile 12, (b) Geotextile 13, (c) Geotextile 14.

Final conditions of geotextiles were examined while emptying the testing molds. It was observed that none of the geotextile reinforcements tore. This could support the idea that geotextiles were not reach their maximum tensile limit under loadings. Figures 4.14 and 4.15 represents the final shapes of some geotextiles at the end of CBR tests.



Figure 4.14 Soil layers and geotextiles that were extracted from the mold after CBR Test.



Figure 4.15 Condition of a geotextile reinforcement after CBR Test.

As a result, highest values were obtained from the models when reinforcements were placed at $h/4$ depth. Top reinforcement was placed with a distance from surface which was equal to quarter of mold height. Then, effect of using multiple reinforcements were tested. Different models with single reinforcement showed higher results than multiple layered reinforced models. Using three geotextiles in models showed the lowest bearing capacity results. Model with two geotextiles showed higher bearing capacity and CBR results than model with three geotextiles. Azar & Dabiri (2015) were also supported this outcome on their research. They compared one geotextile in middle and two geotextiles which were distanced at one third of height. Geotextile that was used in their research is made of artificial fabric and un-weaved needled type. Their CBR tests were conducted with coarse granular material like in this study. Study highlighted that, using single geotextile in soil increased the bearing capacity, however, two layered model caused decrease in bearing capacity.

At the beginning of the tests, highest CBR values were expected from the geotextiles with higher tensile strengths. However, geotextiles which had lower tensile strength values performed better in pavement. So, geotextiles were all examined under microscope and it was observed that, less woven geotextiles could able to mix in soil better due to the gaps

which let soil to pass through. Geotextiles with higher thickness values caused a separation between soil layers which decreased pavement's bearing capacity. Because of that, geotextiles which were woven less frequent and had lower thickness and tensile strength values showed better results than heavier geotextiles in all experiments. CBR results of all geotextile reinforced experiments are given in Table 4.17.

Table 4.17 CBR results of geotextile reinforced models

Reinforcement Type	CBR
Geotextile 1 (at $3h/4$ depth)	60.7
Geotextile 1 (at $h/2$ depth)	97.3
Geotextile 1 (at $h/4$ depth)	88.3
Geotextile 1 (at $h/4+h/2$ depth)	65.0
Geotextile 1 (at $h/4+h/2+3h/4$ depth)	35.0
Geotextile 2 (at $h/4$ depth)	81.8
Geotextile 2 (at $h/4+h/2+3h/4$ depth)	46.4
Geotextile 3 (at $h/4$ depth)	18.5
Geotextile 3 (at $h/4+h/2+3h/4$ depth)	13.9
Geotextile 4 (at $h/4$ depth)	35.2
Geotextile 5 (at $h/4$ depth)	51.2
Geotextile 6 (at $h/4$ depth)	66.5
Geotextile 7 (at $h/4$ depth)	55.5
Geotextile 8 (at $h/4$ depth)	34.3
Geotextile 9 (at $h/4$ depth)	87.6
Geotextile 10 (at $h/4$ depth)	66.4
Geotextile 11 (at $h/4$ depth)	55.6
Geotextile 12 (at $h/4$ depth)	58.2
Geotextile 13 (at $h/4$ depth)	32.1
Geotextile 14 (at $h/4$ depth)	25.5

4.1.3. Geogrid Reinforced Pavement Tests

Three types of geogrids were used to increase the bearing capacity of the pavement. It was observed that all three of them showed similar deformation behavior (Figure 4.16). It can be thought that geogrids had not started to work yet to perform better results because of the size of the samples and scale of the geogrids. Larger test areas or plate load test models can be used for future research for this type of geosynthetics.

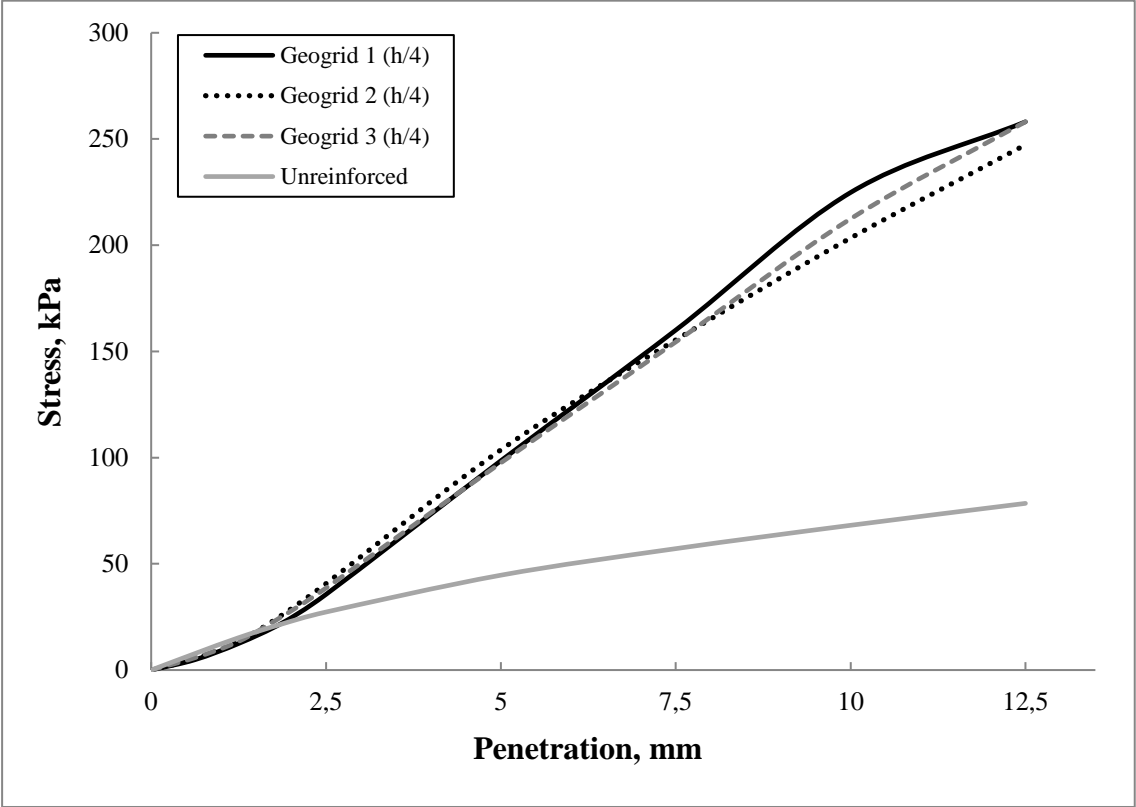


Figure 4.16 Comparison of the stress-penetration curves of Geogrid 1, 2 and 3 reinforced pavements.

As can be observed in Figure 4.16, stress-penetration curves of Geogrid 1, 2 and 3 were like each other and increased with almost similar slopes. Maximum stress values of all geogrids passed 200 kPa at 10 mm penetration level which were higher than most of the geotextile reinforced models. CBR values of geogrids were so close to each other and found as 50.4, 57.5 and 54.6 for Geogrid 1, 2 and 3, respectively. Detailed test results of geogrid reinforced soils are shown in Table 4.18.

Table 4.18 Maximum stress values for Geogrid 1, 2 and 3 at different penetration levels (kPa)

Reinforcement Type	Penetration Levels (mm)		
	2.5	5	10
Geogrid 1	35.62	98.54	224.80
Geogrid 2	40.67	103.65	203.38
Geogrid 3	38.61	97.56	212.41

In these tests, Geogrid 2 had the highest CBR value between geogrids at 2.5 mm and Geogrid 1 had the least value. However, as the penetration goes, Geogrid 1 started to perform better than other geogrids through 10 mm penetration. At the end of tests, Geogrid 1 showed the highest curve, which was the lightest geogrid between Geogrids 1, 2 and 3. Because of that, like geotextile reinforcements, gaps that soil could fill was thought to be important for geogrids as well. Tavakoli Mehrjardi & Khazaei (2017) reported that, one-fourth of medium grain size of soil is the optimum aperture size of geogrid. Medium grain size of soil material that was used in this research is around 1.30 mm. If these geogrids had less aperture sizes, CBR values could have been higher.

Besides, other physical properties like weight and tensile strength and of geogrids also affected the bearing capacity of the pavement which are given in Table 3.4. As can be seen from the results, highest bearing ratio was obtained from Geogrid 1 which had the largest aperture size. Bearing capacities of geogrid reinforced pavements are represented in Table 4.19 in details.

Table 4.19 Bearing capacities of reinforced sand with Geogrid 1, 2, and 3

Penetration (mm)	Reinforcement Type		
	Geogrid 1	Geogrid 2	Geogrid 3
2.5	1.30	1.49	1.41
5.0	2.21	2.32	2.18
10.0	3.30	2.98	3.12

These tests were also showed the bearing capacity could increase with geogrid reinforcements. Even at 2.5 mm penetration level, bearing ratio increased 1.30-1.41 times of unreinforced condition. Furthermore, on higher penetration levels performance of geogrid reinforced pavements were increased up to 3 times of unreinforced condition approximately.

Microscopy analysis for geogrids was performed in laboratory to understand the structure of geogrids. It was observed that Geogrid 1 had less and thinner threads than other geogrids. Fibers on Geogrid 2 and 3 were more frequent and wrapped from different angles which made them tighter. Since Geogrid 1 was more flexible than other geogrids it was thought that it adapted in soil better. Microscopic images of each geogrid are represented in Figures 4.17, 4.18 and 4.19.



Figure 4.17 Images of Geogrid 1 under microscope.



Figure 4.18 Images of Geogrid 2 under microscope.

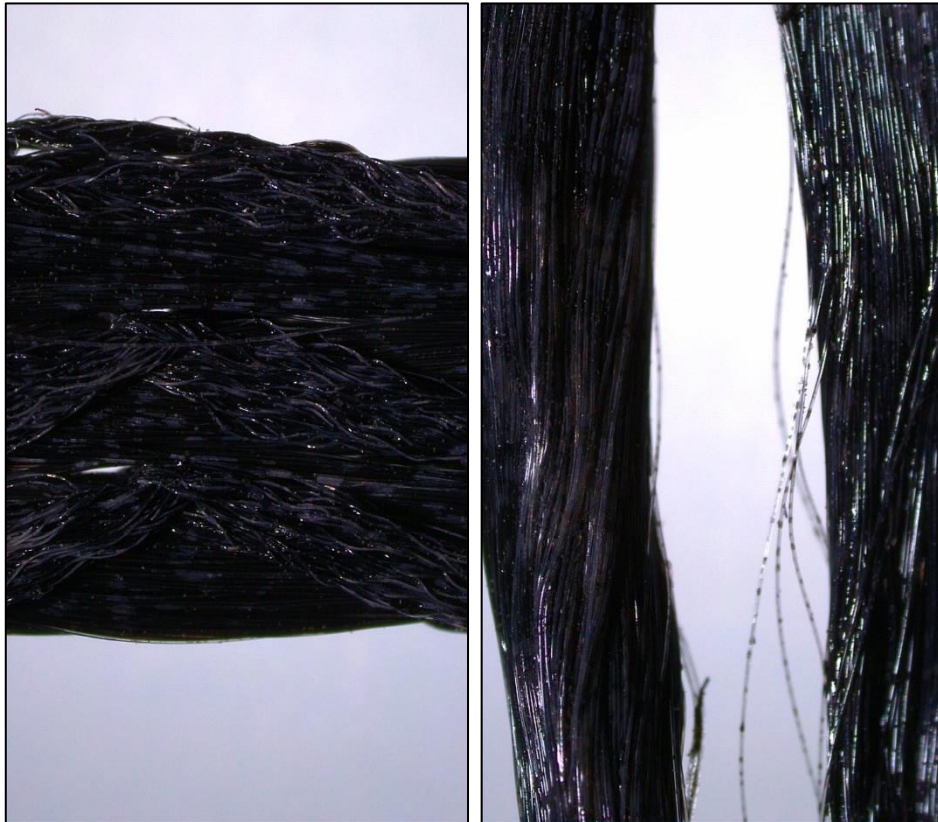


Figure 4.19 Images of Geogrid 3 under microscope.

4.1.4. Fiber Reinforced Pavement Tests

In this series of the tests, six types of fibers were examined by using two different methods. Firstly, fibers which were 1% content of the mass were directly laid between the soil layers without mixing and as a second method, same amount of fibers were mixed in whole soil. Figure 4.20 shows the stress-penetration behaviors of fibers for the first testing method. Highest result was obtained from Fiber 6 and lowest result was observed from Fiber 2 in CBR tests as shown in Table 4.20 and 4.21.

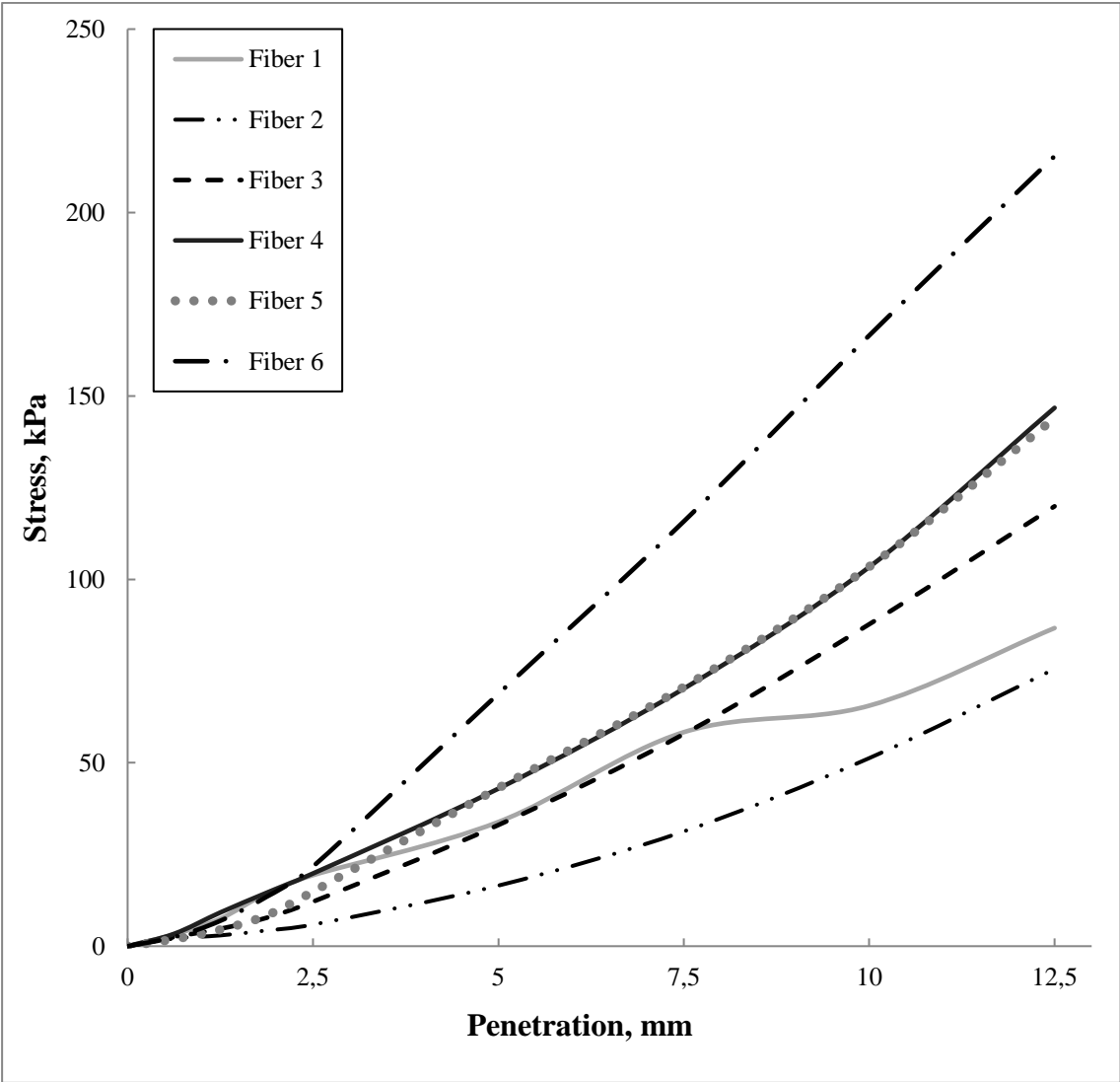


Figure 4.20 Comparison of the stress-penetration curves of Fiber 1, 2, 3, 4, 5 and 6 reinforced pavements as layer without mixing.

Table 4.20 Maximum stress values for laid fibers at different penetration levels (**kPa**)

Reinforcement Type	Penetration Levels (mm)		
	2.5	5	10
Fiber 1	19.35	33.86	65.56
Fiber 2	5.88	16.52	51.26
Fiber 3	12.13	33.03	87.75
Fiber 4	19.82	42.95	103.34
Fiber 5	14.86	43.10	103.45
Fiber 6	21.73	68.81	166.47

Table 4.21 CBR results of fiber reinforced models

Reinforcement Type	CBR
Fiber 1 (1% layered)	27.4
Fiber 2 (1% layered)	8.3
Fiber 3 (1% layered)	17.2
Fiber 4 (1% layered)	28.0
Fiber 5 (1% layered)	21.0
Fiber 6 (1% layered)	30.7

Fibers seemed to decrease CBR results on this testing method. CBR result of unreinforced soil was 38.6 which was higher than all laid fiber reinforced samples. On the other hand, bearing capacities of Fiber 3, 4, 5 and 6 were increased up to 1.29 to 2.44 times on higher penetration levels. Results are given in Table 4.22.

Table 4.22 Bearing capacities of reinforced sand with Fiber 1, 2, 3, 4, 5, and 6

Penetration (mm)	Reinforcement Type					
	Fiber 1	Fiber 2	Fiber 3	Fiber 4	Fiber 5	Fiber 6
2.5	0.71	0.22	0.44	0.73	0.54	0.80
5.0	0.76	0.37	0.74	0.96	0.97	1.54
10.0	0.96	0.75	1.29	1.52	1.52	2.44

It was thought that pressure on fibers made them to attach and perform like a single geotextile as the penetration increases. This could be the reason why fibers, which had high tensile strengths, concluded with lower values in CBR tests but provided higher bearing ratios at further penetration levels.

An important observation from this test was about the behavior of Fiber 1. Fiber 1 showed high performance almost like Fiber 6 around 2.5 mm penetration level. However, after 7.5 mm penetration level, stress-penetration curve of Fiber 1 changed pattern. Microscopy analysis was done to understand the behaviors of fibers. Magnified image of Fiber 1 can be seen in Figure 4.21 for example.

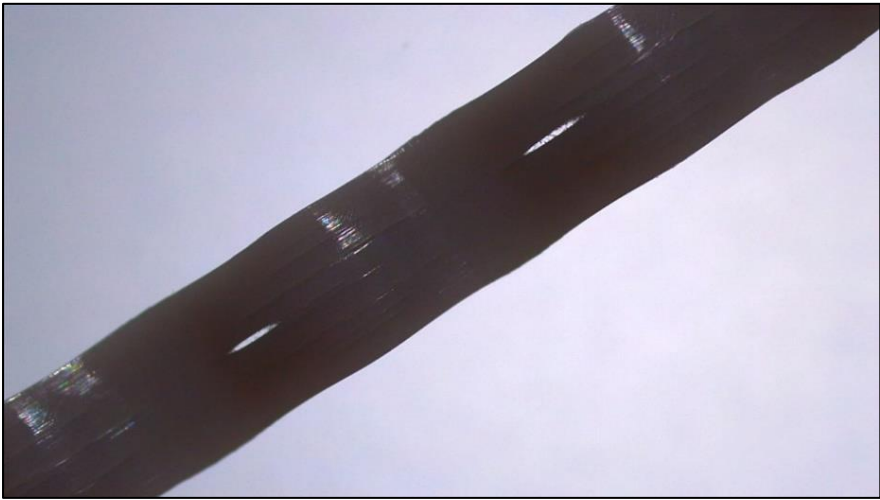


Figure 4.21 Image of Fiber 1 under microscope.

The stiffness of Fiber 1 caused to hardly mix in soil and under increased loading, fractures on fibers occurred. After 2.5 mm penetration level, Fiber 1 started to corrupt and other fibers showed higher bearing capacity. Another important point was observed at 7.5 mm penetration level. Fiber 1 and 3 were performing similar curves but at this point, a significant decrease on Fiber 1's performance was determined because of its structure. This could be the reason why Fiber 1 could not able to perform the highest stress-penetration curve at the end. And this showed that, performances of reinforcements could change under increasing loadings.

Besides, as the loading values increase, Fiber 6 showed the highest bearing capacity among all fibers. Bearing capacity of Fiber 6 was almost 1.5-3 times bigger than other fiber types at the 10 mm penetration. It was thought that Fiber 6 was shortest, thinnest, and able to reshape easier which caused it to mix better than other fibers. In fact, because of these physical properties of Fiber 6, it could behave like a geotextile when it was put as layer. As a result, Fiber 6 provided the highest bearing capacity. Detailed microscopy analysis that shows the structure of Fiber 6 which is given in Figure 4.22.



Figure 4.22 Image of Fiber 6 under microscope.

However, method of adding all fibers between two soil layers were concluded with less CBR results. All CBR values that were obtained from these tests were smaller than unreinforced test. As can be seen from the stress-penetration results, using fiber reinforcements with this method decreased the bearing capacity at 2.5 mm penetration level. On the other hand, bearing capacity of the pavement started to increase on higher

penetration levels for Fiber 3, 4, 5 and 6. Moreover, bearing capacity of some models increased up to 2.4 times of unreinforced condition at 10 mm penetration level, which are shown in Table 4.22. The reason of this behavior could be the compression of fibers due to higher loadings. CBR results were taken at 2.5 mm penetration level and fibers did not seem to be effective at first, but Fiber 3, 4, 5 and 6 adapted at higher loadings and performed like a geotextile reinforcement together.

Second method was to prepare fibers with 1% content of the total mass and properly mixing them with the soil. Different results were obtained from these tests (Figure 4.23). As can be seen in Figure 4.23, fibers performed linear stress-penetration curves. CBR values of this mixing method resulted in higher CBR values than first method. Detailed stress values and CBR results are given in Table 4.23 and 4.24. Fiber 6 had the highest curve among all fibers as in the previous testing method.

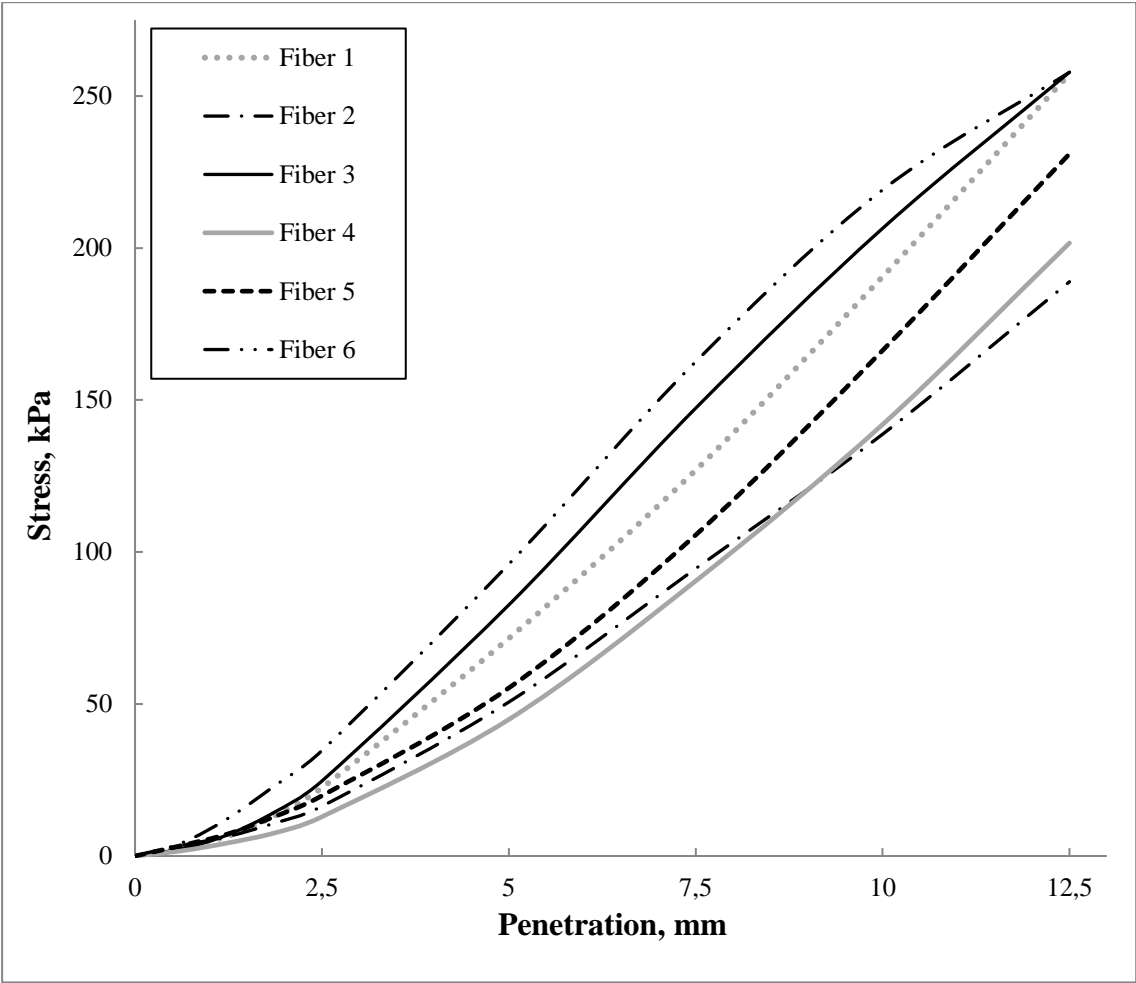


Figure 4.23 Comparison of the stress-penetration curves of Fiber 1, 2, 3, 4, 5 and 6 reinforced pavements with 1% content.

Table 4.23 Maximum stress values for fibers at different penetration levels (kPa)

Reinforcement Type	Penetration Levels (mm)		
	2.5	5	10
Fiber 1 (1% mix)	22.45	71.60	190.58
Fiber 2 (1% mix)	16.36	50.64	138.75
Fiber 3 (1% mix)	24.67	82.59	206.48
Fiber 4 (1% mix)	12.90	44.91	141.95
Fiber 5 (1% mix)	19.82	55.28	166.32
Fiber 6 (1% mix)	34.69	96.01	219.12

Table 4.24 CBR results of fiber reinforced models

Reinforcement Type	CBR
Fiber 1 (1% mix)	31.8
Fiber 2 (1% mix)	23.1
Fiber 3 (1% mix)	34.9
Fiber 4 (1% mix)	18.2
Fiber 5 (1% mix)	28.0
Fiber 6 (1% mix)	49.1

The tensile strengths and lengths of Fiber 1, 2, 3 and 4 were nearly close to each other but all fibers acted differently and showed different stress results under loading. In this case, it was thought that the reason that causes these differences could be another property rather than their tensile strength or lengths which are detailed in Table 3.5. Since Fiber 6 had smaller length and higher amount, it was thought that Fiber 6 was combined with soil better than other fibers. Figure 4.24 shows the internal structure of Fiber 6 with examining under microscope. Because of the structure type of Fiber 6, it was examined under different lighting which was used to observe the internal structure of geotextile reinforcements. As shown in Figure 4.24, Fiber 6 was almost had the similar structure like geotextiles under microscope and this could be the reason why it showed the highest

CBR value in tests that had been used as layer. Fiber 6 could behave like a geotextile under compressive loading.



Figure 4.24 Image of Fiber 6 under microscope.

After Fiber 6, best CBR result was obtained from Fiber 3. Fiber 3 was able to separate easily and little gaps between those fibers let soil to mix better. Another characteristic that Fiber 3 was to reshape easier than other stiff fibers and this could cause Fiber 3 to adapt in soil under increasing loadings better. Additionally, surface texture of Fiber 3 was rough which are given in Figure 4.25, could cause reinforcements to work better with soil.



Figure 4.25 Image of Fiber 3 under microscope.

On the other hand, model reinforced with Fiber 4 showed the least CBR value. Since surface texture of Fiber 4 was smooth, it could not work properly in terms of cohesion. Besides, Fiber 2 was almost similar with Fiber 4 but had fragments on surface which may have caused friction that increased CBR value. Tensile strengths of Fiber 4 and 2 were nearly close to each other and this supported the idea that physical properties could be more important than comparing tensile strength only as well. Microscopic images of Fiber 4 and 2 are given in Figure 4.26.

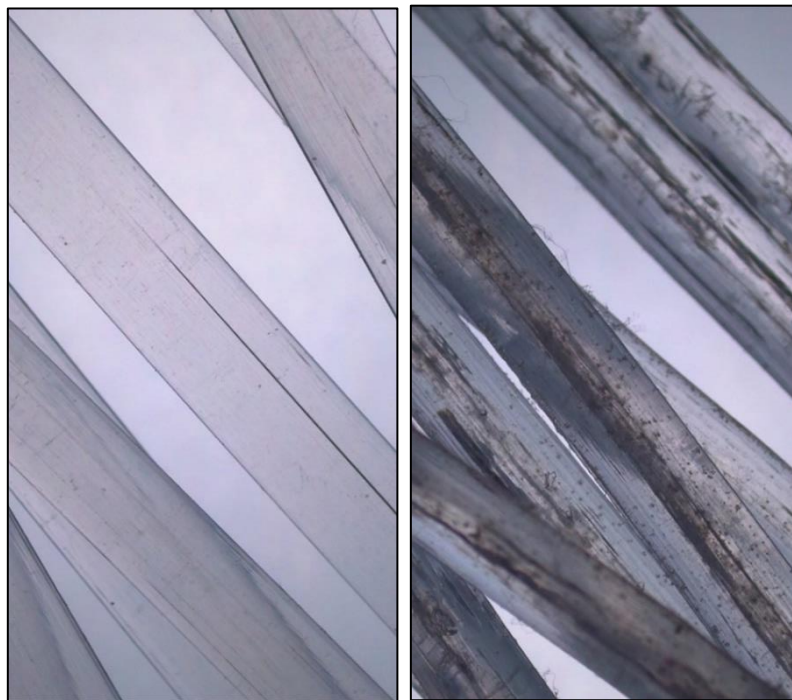


Figure 4.26 Surface textures of Fiber 4 and Fiber 2 under microscope, respectively.

Additionally, at 2.5 mm penetration level, stress value of Fiber 4 was smaller than Fiber 2 which caused Fiber 4 to show fewer CBR than Fiber 2. Fiber 2 seemed better than Fiber 4, however, Fiber 4 reached higher stress level after 9.0 mm penetration. It was thought that, performance of fibers could be related with the stress level, like observed in geosynthetic reinforcements.

When Fiber 1 was examined under microscope, there were spaces on its surface that could make soil to mix better than Fiber 2, 4 and 5. This could be the reason why Fiber 1 showed higher results than Fiber 2, 4 and 5 when comparing to the results on the layering method tests. Microscopic image of Fiber 1 is given in Figure 4.27.

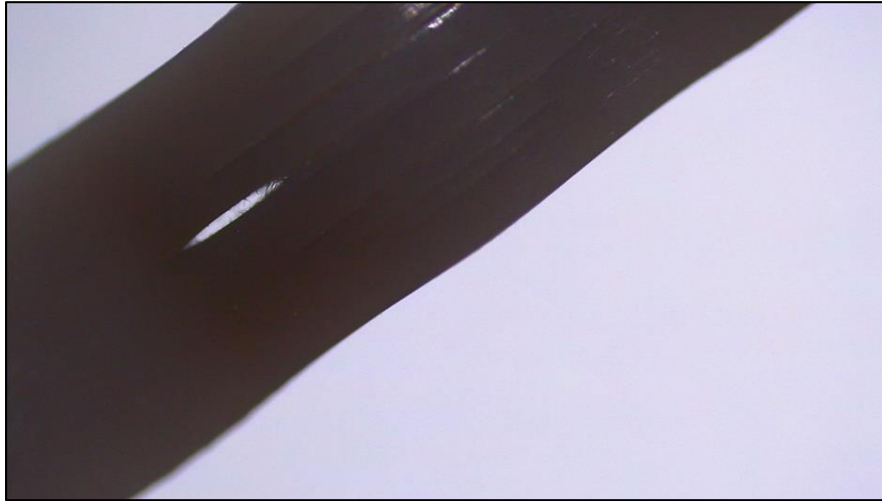


Figure 4.27 Closer view of spaces on surface of Fiber 1 under microscope.

It was thought that Fiber 1, 2, 3, 4 and 5 could not able to mix with the soil naturally like Fiber 6 did. These fiber reinforcements are used in concrete generally, but they were tested in pavement to observe their behaviors. Although these fibers behave well in concrete, the desired performance has not been achieved in pavement without binding material. This is why performance of other fiber reinforced models were less than Fiber 6 reinforced model.

In fact, using those fibers showed lower bearing capacity values than Fiber 6. Unreinforced pavement results were higher than using these fibers except Fiber 6 at 2.5 mm penetration level.

Though, it was observed that using fibers as reinforcement increased the bearing capacity for each case. Raju et al. (2018) reported that, tensile load soil acting on the soil can be carried by fiber reinforcements. Unreinforced soil was only able to reach around 80 kPa stress maxima. On the other hand, fiber reinforced models showed better performance and stress capacity of some fibers passed 250 kPa. Loadings at 2.5 mm and 5.0 mm were taken into consideration to calculate CBR values which could be the reason of lower CBR results of reinforced scenarios.

Another idea was to examine the effect of relation between the CBR values and number of fibers that were used in the mix. All fibers were applied by 1% proportion of total mass. Since each fiber had different weight per kilogram, amount that was used in all models

varied. Bearing capacity comparison of fibers with 1% mix content can be seen in Table 4.25.

Table 4.25 Bearing capacities of reinforced sand with %1 Fiber 1, 2, 3, 4, 5, and 6

Penetration (mm)	Reinforcement Type					
	Fiber 1 (1%)	Fiber 2 (1%)	Fiber 3 (1%)	Fiber 4 (1%)	Fiber 5 (1%)	Fiber 6 (1%)
2.5	0.82	0.60	0.90	0.47	0.73	1.27
5.0	1.60	1.13	1.85	1.01	1.24	2.15
10.0	2.80	2.04	3.03	2.08	2.44	3.22

The highest CBR value and the bearing capacity ratio values were seen for Fiber 6. It was observed that Fiber 6 was adapted soil better than other fiber types. Structure of Fiber 6 was smoother and make it able to reshape in soil better. Besides, length of Fiber 6 was shortest that it can separate into little pieces and mix naturally. Also, between all fiber types, Fiber 6 was the lightest reinforcement in weight. Therefore, amount that was applied to achieve 1% content in soil was higher than other fiber types. Although tensile strength of Fiber 6 was not the highest, it showed best results on CBR tests due to its physical advantages and amount of fibers used. Fiber 3 had same softness as well which could be the reason of Fiber 3 to perform as second-best reinforcement in the soil. Fiber 3 had gaps on it and was able to separate into smaller parts like Fiber 6.

In addition to this, when mixed in soil, Fiber 4 showed least performance on CBR tests even it had the highest tensile strength. It was thought that other physical properties of Fiber 4 affected its performance. Fiber 4 was stiffer and longer than other fibers which could cause it to deform in the compaction process. So, it was observed that, structural properties of fiber reinforcements can affect the bearing capacity more than their tensile strengths.

4.1.5. Geotextile and Fiber Combined Pavement Tests

For this test series, Geotextile 1 was chosen and put at h/4 depth and combined with different fiber types. Then, samples were prepared for CBR testing. Figure 4.28 shows the results.

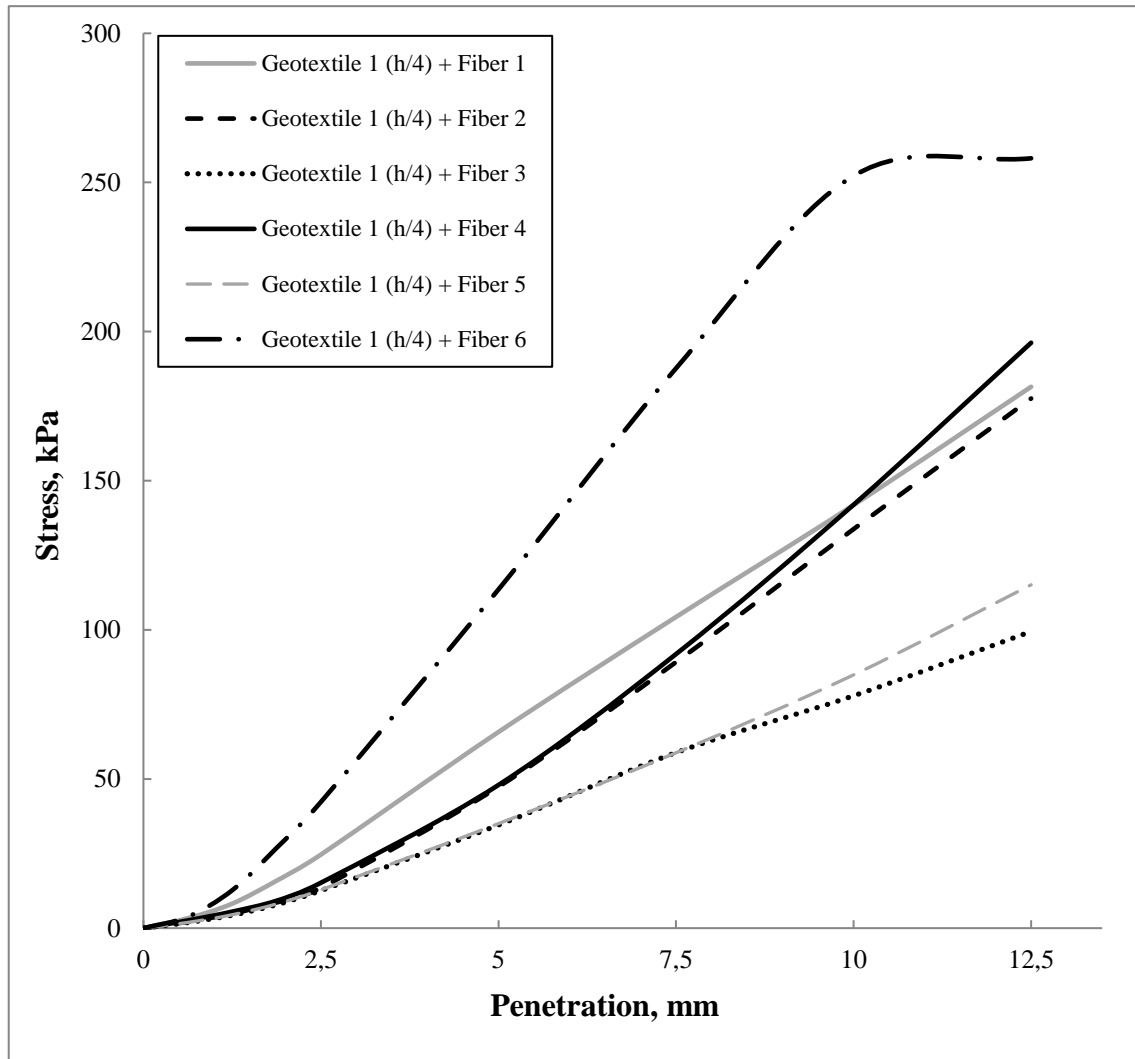


Figure 4.28 Comparison of the stress-penetration curves of Fiber 1, 2, 3, 4, 5 and 6 (1%) with combining Geotextile 1 reinforced pavements.

When using a Geotextile 1 and fibers in same samples, linear stress-penetration curves can be seen but Fiber 6 has different curve behavior. Fiber 2, 3, 4 and 5 combinations almost had the similar slopes at 2.5 mm penetration level. Highest CBR result was obtained from the Fiber 6 combined model and least CBR was observed from Fiber 3 combination. Results for Geotextile 1 and fiber combinations are detailed in Table 4.26 and 4.27.

Table 4.26 Maximum stress values for Geotextile 1 and fiber combinations at different penetration levels (kPa)

Reinforcement Type	Penetration Levels (mm)		
	2.5	5	10
Geotextile 1 + Fiber 1	24.67	65.76	141.85
Geotextile 1 + Fiber 2	13.52	47.39	133.80
Geotextile 1 + Fiber 3	12.59	34.58	77.89
Geotextile 1 + Fiber 4	15.22	48.00	141.95
Geotextile 1 + Fiber 5	12.85	35.05	84.91
Geotextile 1 + Fiber 6	42.33	113.56	252.21

Table 4.27 CBR results of Geotextile 1 and fiber reinforced models

Reinforcement Type	CBR
Geotextile 1 + Fiber 1	34.9
Geotextile 1 + Fiber 2	19.1
Geotextile 1 + Fiber 3	17.8
Geotextile 1 + Fiber 4	21.5
Geotextile 1 + Fiber 5	18.2
Geotextile 1 + Fiber 6	59.9

In general, combining fibers with a geotextile decreases CBR values. Combination of more reinforcements decreases the stress value at 2.5 mm penetration degree. And these CBR values were examined lower than the unreinforced condition. Only Fiber 6 could adapt to this combination and showed higher performance than unreinforced condition at 2.5 mm penetration level. The reason could be the length of Fiber 6. Since the weight of the Fiber 6 was the minimum between fibers, amount that was put in mixture to obtain 1% of soil mass was higher than all other fibers. High amount of this material could increase the bearing capacity and cause the result of this observation. Bearing capacity of each fiber type and Geotextile 1 combination over unreinforced soil are given in Table 4.28.

Table 4.28 Bearing capacities of reinforced sand with Geotextile 1 and Fiber 1, 2, 3, 4, 5, 6 combinations

Penetration (mm)	Reinforcement Type					
	Geo.1 + Fiber 1 (1%)	Geo.1 + Fiber 2 (1%)	Geo.1 + Fiber 3 (1%)	Geo.1 + Fiber 4 (1%)	Geo.1 + Fiber 5 (1%)	Geo.1 + Fiber 6 (1%)
	2.5	0.90	0.50	0.46	0.56	0.47
5.0	1.47	1.06	0.77	1.08	0.78	2.54
10.0	2.08	1.96	1.14	2.08	1.25	3.70

Since CBR values calculated at 2.5 mm penetration level, some combinations seemed to have lower bearing capacities than unreinforced condition. Though, on higher penetration levels it was observed that bearing capacities could increase up to 3.7 times higher than unreinforced condition. Especially after 10 mm penetration level, all reinforcements started to perform effectively. This test series showed that, fiber and geotextile combination started to activate on higher stress values as well.

In addition, Hossain et al. (2015) highlighted that combining fibers with geotextiles can be effective in soil. However, fiber that was mentioned on that research was natural jute fibers. Most polypropylene fibers that were used in this study were harder to mix in soil than jute and decreased CBR values at 2.5 mm penetration. But, Fiber 6 was the most like to jute in physical structure and combination with geotextile increased the CBR values as research mentioned. Besides, bearing capacity of the road increased for all cases at 10 mm penetration level. Especially Fiber 6 increased bearing capacity 3.7 times over unreinforced pavement when it was combined with Geotextile 1. On the other hand, Zornberg (2012) concluded that using one type of reinforcement in soil can provide better results than combining geosynthetics with different reinforcements. Same is true for geotextile and fiber combined model testing series. Single Geotextile 1 at h/4 depth reinforced model showed higher CBR value when compared to these models, which was 88.3.

For this research, fibers were used in soil with three methods. At first, fibers were prepared by 1% of soil mass and put together as layer in soil. Secondly, fibers were prepared by 1% of mass and mixed in soil. Thirdly, 1% of each fiber type was prepared and combined with Geotextile 1 and mixed in soil. Geotextile was placed with a distance of $h/4$ from top surface. Between all fiber testing methods, mixing fibers in soil was the found the most effective method to use as reinforcement in pavement, except for Fiber 6. For Fiber 6, highest result was obtained when it was combined with Geotextile 1 in soil. Except this case, all fibers with all methods showed linear stress-penetration curves. However, curve of Fiber 6 and Geotextile 1 combined test was non-linear and higher than all other fiber tests. Although stress-penetration curve of Geotextile 1 on $h/4$ model was above on all 1% fiber mixed test curves, geotextile and fiber combination curves were decreased for fibers, except Fiber 6. And for Fiber 3 and 5, test results with layering method was provided higher bearing ratios than fiber-geotextile combination. For Fiber 1, 2, 4 and 6, Geotextile 1 combined tests concluded with higher results than layering method. Detailed stress versus penetration curves that were obtained in CBR tests are represented between Figure 4.29.

To sum up, each geosynthetic and fiber type can exhibit unique behavior and sometimes the scale effect can also affect result. In this respect, whichever material will be used in a road project, it will be better to apply it in practice after fully investigated the behavior of that material in the pavement.

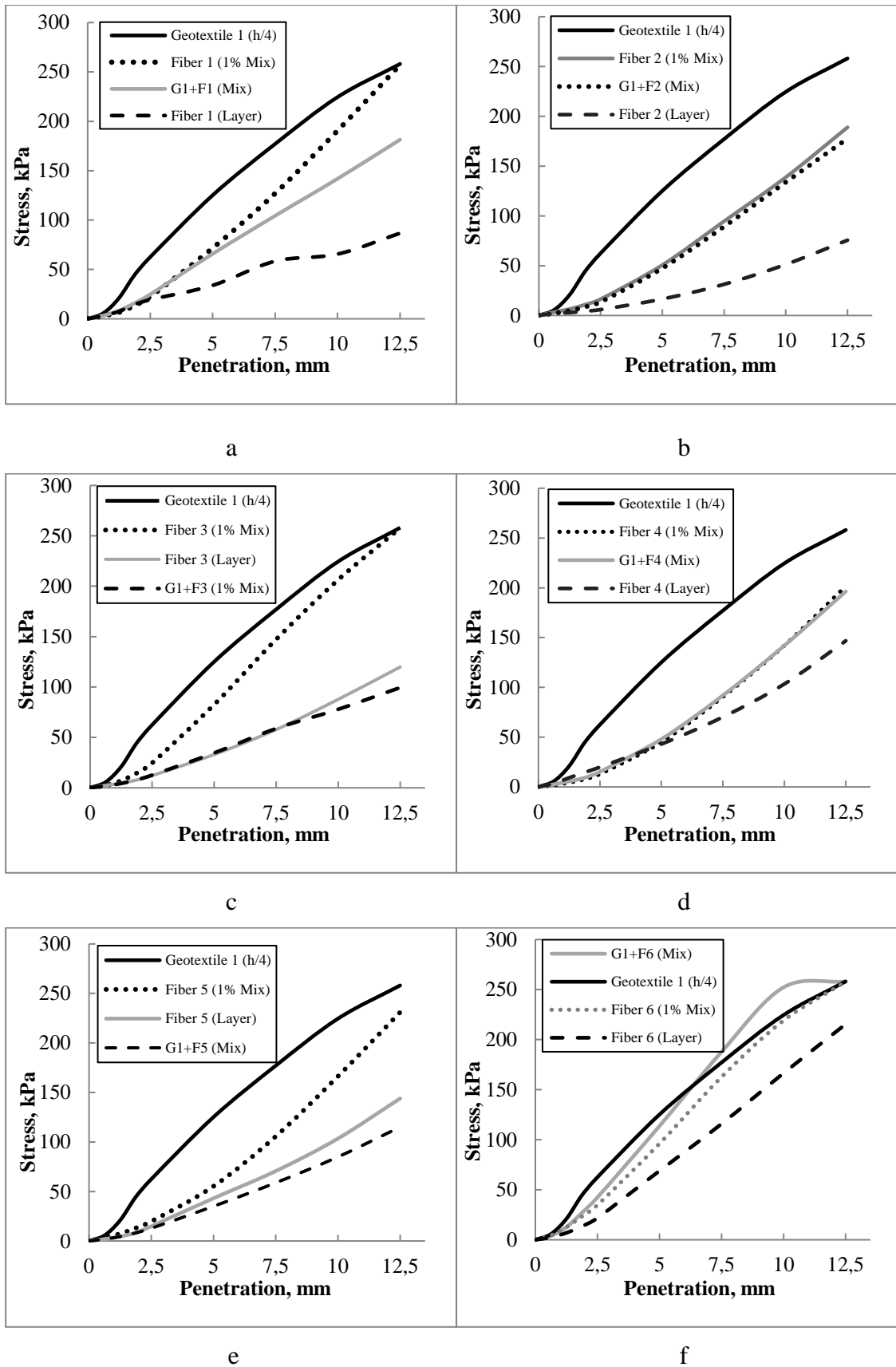


Figure 4.29 Comparison of the stress-penetration curves of fiber and geotextile reinforcement combinations (a) Fiber 1, (b) Fiber 2, (c) Fiber 3, (d) Fiber 4, (e) Fiber 5, (f) Fiber 6.

4.2. Pavement Thickness and Cost Analysis Results

Determining the effect on the pavement thickness and according to this value, calculating the cost analysis of pavement design are other important points of this study. Therefore, unreinforced, and reinforced pavement designs were made, compared with each other and then the most economic reinforced model was determined. Pavement thickness and cost analysis were conducted as following parts.

4.2.1. Pavement Thickness Results

In the study, a sample road was designed with using AASHTO Guide for Design of Pavement Structures (1993) and pavement thickness values were determined. As can be known, structural number (SN) for each scenario should be determined for thickness values of unreinforced and reinforced pavements. CBR values which were obtained at 2.5 mm penetration level were used for this exercise. Since this study focused on the relation between the CBR and SN, resilient modulus (M_R) of models were calculated with the Equation 3.15 which is detailed in Materials and Methods section. After that, with computing M_R into formula, structural number of all cases were found with Equation 3.14. M_R and SN values after computation are given in Table 4.29. Only higher results than unreinforced pavement on CBR tests were taken into consideration for cost analysis to have improved pavement models.

Table 4.29 CBR, M_R and SN results for unreinforced and reinforced pavement models

Reinforcement Name	Property	CBR	M_R	SN
Unreinforced	0	38.6	26478.987	3.26
Geotextile 1	1 (3h/4)	60.7	35353.661	2.93
Geotextile 1	1 (h/4)	88.3	44964.390	2.68
Geotextile 1	1 (h/2)	97.3	47838.884	2.62
Geotextile 1	2 (h/4 + 3h/4)	65.0	36940.209	2.89
Geotextile 2	1 (h/4)	81.8	42794.630	2.73

Geotextile 2	3 (h/4 + 3h/4 + h/2)	46.4	29762.193	3.13
Geotextile 5	1 (h/4)	51.2	31706.571	3.05
Geotextile 6	1 (h/4)	66.5	37495.703	2.87
Geotextile 7	1 (h/4)	55.5	33389.540	3.00
Geotextile 9	1 (h/4)	87.6	44726.585	2.69
Geotextile 10	1 (h/4)	66.4	37469.356	2.87
Geotextile 11	1 (h/4)	55.6	33445.749	2.99
Geotextile 12	1 (h/4)	58.2	34448.601	2.96
Geogrid 1	1 (h/4)	50.4	31387.242	3.07
Geogrid 2	1 (h/4)	57.5	34171.695	2.97
Geogrid 3	1 (h/4)	54.6	33051.164	3.01
Fiber 6	1%	49.1	30860.722	3.09
Geotextile 1 + Fiber 6	1 (h/4) + 1%	59.9	35053.437	2.94

After obtaining the SN values, pavement thickness for each model was calculated by AASHTO's design formula (Equation 3.16). Thickness values of wearing surface (D_1) and base (D_2) layers were fixed at the beginning of the assumption. So, subbase thicknesses (D_3) were required for the cost estimation. For design purposes, half numbers were rolled to higher numbers in determination of D_3 to be on the safer side. As Sharma et al. (2013) mentioned, using geosynthetic reinforcements reduced the thickness value of unreinforced pavement and increased bearing capacity in positive way. Additionally, fiber reinforcements decreased the thickness of pavement layer as Pandit et al. (2016) reported in their research. Detailed thickness values of unreinforced and reinforced models can be seen in Table 4.30.

Table 4.30 Calculated layer thickness values for subbase according to SN results (D_3)

Reinforcement	Testing Method	SN	D_3 (in)	D_3 (cm)	D_3 (m)
Unreinforced	0	3.26	8.04	20.42	0.21
Geotextile 1	1 (3h/4)	2.93	5.03	12.78	0.13
Geotextile 1	1 (h/4)	2.68	2.75	6.97	0.07
Geotextile 1	1 (h/2)	2.62	2.19	5.56	0.06
Geotextile 1	2 (h/4 + 3h/4)	2.89	4.60	11.68	0.12
Geotextile 2	1 (h/4)	2.73	3.20	8.14	0.09
Geotextile 2	3 (h/4 + 3h/4 + h/2)	3.13	6.79	17.24	0.18
Geotextile 5	1 (h/4)	3.05	6.13	15.57	0.16
Geotextile 6	1 (h/4)	2.87	4.46	11.32	0.12
Geotextile 7	1 (h/4)	3.00	5.60	14.23	0.15
Geotextile 9	1 (h/4)	2.69	2.80	7.11	0.08
Geotextile 10	1 (h/4)	2.87	4.46	11.34	0.12
Geotextile 11	1 (h/4)	2.99	5.59	14.19	0.15
Geotextile 12	1 (h/4)	2.96	5.29	13.44	0.14
Geogrid 1	1 (h/4)	3.07	6.23	15.83	0.16
Geogrid 2	1 (h/4)	2.97	5.37	13.64	0.14
Geogrid 3	1 (h/4)	3.01	5.71	14.49	0.15
Fiber 6	1%	3.09	6.41	16.28	0.17
Geo.1 + Fiber 6	1 (h/4) + 1%	2.94	5.12	13.00	0.13

4.2.2. Cost Estimation Results

Firstly, cost results were determined for pavement soil as follow:

Since pavement thickness values were determined, pavement costs of all cases were examined. To start with, the amount of the soil that was required for subbase layer was calculated. As designed pavement model's length and width were assumed 1000 and 3 meters respectively, multiplication of these values by pavement thicknesses showed the amount of soil that was necessary in meter cubes. Pavement costs for all cases are detailed in Table 4.31. As can be seen from the results, using reinforcement in pavement affected the amount of required thickness and cost of pavement layer. Some reinforcements reduced thickness values to almost half of the unreinforced soil which directly affected

to pavement cost. The most effective results were obtained from the geotextiles among all reinforcements, especially from the geotextiles with smaller thickness and tensile strength values.

Table 4.31 Cost of subbase soil for unreinforced and reinforced pavements for 1 km

Reinforcement	Layer Thickness (m)	Lane Width (m)	Road Length (m)	Total Soil Volume (m³)	Unit Price of Soil (\$/m³)	Cost of Soil (\$)
Unreinforced	0.21	3	1000	630	2.36	1486.80
Geotextile 1 (3h/4)	0.13	3	1000	390	2.36	920.40
Geotextile 1 (h/4)	0.07	3	1000	210	2.36	495.60
Geotextile 1 (h/2)	0.06	3	1000	180	2.36	424.80
Geotextile 1 (h/4+3h/4)	0.12	3	1000	360	2.36	849.60
Geotextile 2 (h/4)	0.09	3	1000	270	2.36	637.20
Geotextile 2 (h/4+3h/4+h/2)	0.18	3	1000	540	2.36	1274.40
Geotextile 5 (h/4)	0.16	3	1000	480	2.36	1132.80
Geotextile 6 (h/4)	0.12	3	1000	360	2.36	849.60
Geotextile 7 (h/4)	0.15	3	1000	450	2.36	1062.00
Geotextile 9 (h/4)	0.08	3	1000	240	2.36	566.40
Geotextile 10 (h/4)	0.12	3	1000	360	2.36	849.60
Geotextile 11 (h/4)	0.15	3	1000	450	2.36	1062.00
Geotextile 12 (h/4)	0.14	3	1000	420	2.36	991.20
Geogrid 1 (h/4)	0.16	3	1000	480	2.36	1132.80
Geogrid 2 (h/4)	0.14	3	1000	420	2.36	991.20
Geogrid 3 (h/4)	0.15	3	1000	450	2.36	1062.00
Fiber 6 (1%)	0.17	3	1000	510	2.36	1203.60
Geotextile 1 + Fiber 6 (h/4+1%)	0.13	3	1000	390	2.36	920.40

As for second step cost results were determined for reinforcements as follow:

The number of reinforcements for geosynthetics were determined with the surface area of the pavement. For example, required amount of reinforcement for single layered models were taken as 3000 m² and for two and three reinforcement layered models were 6000 m² and 9000 m², respectively. Since these materials are sold in square meters, their unit prices for meter square were obtained from the manufacturer firms and multiplied by the required area. Cost of geosynthetic reinforcements are given in Table 4.32.

Table 4.32 Costs of geosynthetics

Reinforcement	Unit Price of Geosynthetic (\$/m²)	Reinforcement Required (m²)	Cost of Geosynthetic (\$)
Geotextile 1 (3h/4)	0.60	3000	1800.00
Geotextile 1 (h/4)	0.60	3000	1800.00
Geotextile 1 (h/2)	0.60	3000	1800.00
Geotextile 1 (h/4+3h/4)	0.60	6000	3600.00
Geotextile 2 (h/4)	0.82	3000	2460.00
Geotextile 2 (h/4+3h/4+h/2)	0.82	9000	7380.00
Geotextile 5 (h/4)	0.54	3000	1620.00
Geotextile 6 (h/4)	0.40	3000	1200.00
Geotextile 7 (h/4)	0.22	3000	660.00
Geotextile 9 (h/4)	0.09	3000	270.00
Geotextile 10 (h/4)	0.15	3000	450.00
Geotextile 11 (h/4)	0.26	3000	780.00
Geotextile 12 (h/4)	0.49	3000	1470.00
Geogrid 1 (h/4)	3.08	3000	9240.00
Geogrid 2 (h/4)	3.45	3000	10350.00
Geogrid 3 (h/4)	5.42	3000	16260.00

As shown, choosing geotextiles as reinforcement was more cost effective than geogrids. In fact, thinner geotextiles were more affordable than thicker geotextiles. Since cost of geotextiles and geogrids were calculated, cost of fibers was calculated. Only the CBR result of Fiber 6 reinforced model was higher than unreinforced model so, Fiber 6 was examined as fiber reinforcement only. As required volume of pavement was determined above, mass of soil was calculated by multiplying pavement volume by mass per meter cube. For this calculation, an average mass of soil was taken as 1600 kg/m³ and multiplied with design volume which was 510 m³. Next, 1% of soil mass was calculated to determine required fiber amount. Then, fiber amount was multiplied by the unit price of Fiber 6 and cost of fibers were found. Result of this process is given in Table 4.33.

Table 4.33 Cost of fibers

Reinforcement	Unit Price of Fibers (\$/kg)	Mass of Soil (kg)	Total Fibers Required (kg)	Cost of Fibers (\$)
Fiber 6 (1%)	4.65	816000	8160	37944.00

Finally, cost of Fiber 6 and Geotextile 1 reinforcement combination was calculated. Cost of Geotextile 1 was found in previous section as 1800 dollars per one-kilometer pavement. However, cost of Fiber 6 changed because of the change in soil volume. So, it was found for 1% of new soil mass which is given in Table 4.34. Mass of soil was found by multiplying 390 m³ by 1600 kg/m³. Cost of Fiber 6 and Geotextile 1 was added and found as 30816.00 dollars per kilometer.

Table 4.34 Reinforcement cost of fiber and geotextile combination

Reinforcement	Unit Price of Fibers (\$/kg)	Mass of Soil (kg)	Fibers Required (kg)	Cost of Fibers (\$)	Cost of F6 + Geo. 1 (\$)
Geo. 1 + F6	4.65	624000	6240	29016.00	30816.00

As for total cost of reinforced pavements the results can be seen as follow: Reinforcement and pavement soil costs were combined to calculate total cost. Final costs of all reinforced pavements are compared in Table 4.35. Cost of unreinforced pavement

was determined as 1486.80 dollars per kilometer and CBR value of unreinforced pavement was 38.6. It was observed that CBR value of soil could be increased up to 97.3 with the help of these reinforcements, which was almost more than 2.5 times of unreinforced soil. Also, it was observed that soil cost could be reduced by almost half with adding reinforcements which provides better performance with decreasing pavement thickness.

For most cases, cost of reinforcements influenced total cost more than profit of reduced soil. However, Geotextile 9 and 10 reinforced pavement models were still found highly effective. Geotextile 9 and 10 increased CBR values of unreinforced pavement to 87.6 and 66.4, respectively and cost only 765.60 and 1299.60 dollars which are less than 1486.80 dollars.

Additionally, using other reinforcements in pavement such as Geotextile 7, could be calculated beneficial for bearing capacity but price could be different from others. Unreinforced pavement had 38.6 CBR and costs 1486.80 dollars. Preferring Geotextile 7 reinforced pavement has more CBR value as 55.5 and cost is as 1722 dollars, but it can be more effective for life span of pavement. In other words, it should not be forgotten that using reinforcements have also other advantages such as improvement and settlement reduction, so pavement design should be taken into consideration for long term.

Table 4.35 Total cost values of reinforced pavements

Reinforcement	Cost of Soil (\$/km)	Cost of Reinforcement (\$/km)	Total Cost of Pavement (\$/km)
Geotextile 1 (3h/4)	920.40	1800.00	2720.40
Geotextile 1 (h/4)	495.60	1800.00	2295.60
Geotextile 1 (h/2)	424.80	1800.00	2224.80
Geotextile 1 (h/4+3h/4)	849.60	3600.00	4449.60

Geotextile 2 (h/4)	637.20	2460.00	3097.20
Geotextile 2 (h/4+3h/4+h/2)	1274.40	7380.00	8654.40
Geotextile 5 (h/4)	1132.80	1620.00	2752.80
Geotextile 6 (h/4)	849.60	1200.00	2049.60
Geotextile 7 (h/4)	1062.00	660.00	1722.00
Geotextile 9 (h/4)	566.40	270.00	836.40
Geotextile 10 (h/4)	849.60	450.00	1299.60
Geotextile 11 (h/4)	1062.00	780.00	1842.00
Geotextile 12 (h/4)	991.20	1470.00	2461.20
Geogrid 1 (h/4)	1132.80	9240.00	10372.80
Geogrid 2 (h/4)	991.20	10350.00	11341.20
Geogrid 3 (h/4)	1062.00	16260.00	17322.00
Fiber 6 (1%)	1203.60	37944.00	39147.60
Geotextile 1 + Fiber 6 (h/4+1%)	920.40	30816.00	31736.40

Moreover, same procedure was repeated to understand the effects of reinforcements on total cost when they applied in base course (D₂). For this approach, top five reinforcements which provided highest CBR results were taken into consideration. Base thickness values before and after reinforcement application were given in Table 4.36.

Then, pavement costs for these models were analyzed according to thickness values which are represented in Table 4.37. Finally, total costs of reinforced and unreinforced base courses were compared with adding unit price of each material which are given in Table 4.38.

Table 4.36 Calculated layer thickness values for base according to SN results (D₂)

Reinforcement	Testing Method	SN	D₃ (in)	D₃ (cm)	D₃ (m)
Unreinforced	0	3.26	5.49	13.95	0.14
Geotextile 1	1 (h/4)	2.68	0.20	0.51	0.01
Geotextile 2	1 (h/4)	2.73	0.66	1.67	0.02
Geotextile 6	1 (h/4)	2.87	1.91	4.85	0.05
Geotextile 9	1 (h/4)	2.69	0.25	0.64	0.01
Geotextile 10	1 (h/4)	2.87	1.92	4.87	0.05

Table 4.37 Cost of base soil for unreinforced and reinforced pavements for 1 km

Reinforcement	Layer Thickness (m)	Lane Width (m)	Road Length (m)	Total Soil Volume (m³)	Unit Price of Soil (\$/m³)	Cost of Soil (\$)
Unreinforced	0.14	3	1000	420	2.36	991.20
Geotextile 1 (h/4)	0.01	3	1000	30	2.36	70.80
Geotextile 2 (h/4)	0.02	3	1000	60	2.36	141.60
Geotextile 6 (h/4)	0.05	3	1000	150	2.36	354.00
Geotextile 9 (h/4)	0.01	3	1000	30	2.36	70.80
Geotextile 10 (h/4)	0.05	3	1000	150	2.36	354.00

Table 4.38 Total cost values of unreinforced and reinforced base pavements

Reinforcement	Cost of Soil (\$/km)	Cost of Reinforcement (\$/km)	Total Cost of Pavement (\$/km)
Unreinforced	991.20	0.00	991.20
Geotextile 1 (h/4)	70.80	1800.00	1870.80
Geotextile 2 (h/4)	141.60	2460.00	2601.60
Geotextile 6 (h/4)	354.00	1200.00	1554.00
Geotextile 9 (h/4)	70.80	270.00	340.80
Geotextile 10 (h/4)	354.00	450.00	804.00

It was observed that using reinforcements in subbase layer were found highly effective. As can be seen from Table 4.38, adding reinforcements in base course could decrease total cost of pavement as well. The most efficient reinforcements to apply in pavement were found as Geotextile 9 and 10 in terms of both performance and economy. Costs of Geotextile 1, 2 and 6 reinforced models were calculated higher than unreinforced model. However, these reinforcements increased bearing capacity of soil almost 1.5-2 times than unreinforced condition. Therefore, benefits of adding reinforcements in soil in long run can be more important than their initial costs for overall design purposes.

5. CONCLUSION

In this study, effects of different reinforcements on the pavement's bearing capacity were examined. California Bearing Ratio (CBR) tests and microscopic analysis were conducted. Geotextiles, geogrids, and fibers were used as reinforcement materials. Geotextiles were used in different quantities to understand the most effective number of reinforcements and placements by CBR tests. Then, microscopy analyses were conducted for each reinforcement types and soil to see the convenience between reinforcement and soil. As a result, AASHTO pavement calculations and cost analysis for unreinforced and reinforced pavements were studied and effects were compared. Results of the study can be summarized as below:

- On CBR tests, reinforcement which was located at $h/4$ depth showed highest CBR value and effects. Then, the highest CBR values were obtained from $h/2$ and $3h/4$ reinforced models, respectively.
- The highest CBR result was observed from the single layer reinforced model when compared with multi layered models. It can be thought that using two and three reinforcements may cause separation of the aggregates in model and so CBR values decreases.
- Lighter geotextiles were found more effective than heavier geotextiles to improve the bearing behavior. In some cases, even unreinforced pavement showed higher CBR result than reinforced pavements due to thickness value of the reinforcements. It was thought that thicker and heavier geotextiles separated soil and caused each section to work independently, which deteriorated natural structure of soil and this can affect the bearing capacity as negatively. The spaces between the threads in geotextile layer could influence the performance of the reinforcements. It was thought that the spaces inside the geotextile could provide it to mix better with the soil particles. As aggregates fill inside the gaps, reinforcement may harmonize with soil more naturally. For geotextiles having thicker layer can have fewer spaces for soil to pass through, thus this could decrease the CBR values. Although thicker geotextiles showed fewer bearing capacities at 2.5 mm penetration level, they started to perform better for higher penetration levels. The reason of this behavior could be the pressure which caused them to be pressed, got thinner and

work better with soil like a lighter geotextile or after some penetration levels textiles start to behave as reinforcement by using their tensile strength. Highest CBR result was observed from the model reinforced with Geotextile 1.

- When different types of geogrids were tested, CBR results were obtained almost similar for each geogrid type. Therefore, it was thought that, geogrids could not be able to start to perform at applied pressure level yet. To see the behavior plate load tests by using larger scales can be conducted to see the effects. Highest CBR result was observed from the model reinforced with Geogrid 2.

- When fibers were directly laid at $h/4$ depth together like in geotextile models, highest effect was obtained from the thinnest and lightest polypropylene fiber with lowest tensile strength. It can be thought that, fiber pieces stuck to each other because of their physical advantages which caused fibers to act like a single geotextile reinforcement. Other fiber reinforced samples could not able to stick to each other because of their physical properties. They separated soil into different layers and negatively affected soil's natural structure which could cause the decrease in CBR values. Even unreinforced pavement model showed higher bearing capacity than this type of fiber placement for most cases.

- Putting fibers together like a layered reinforcement did not give efficient bearing ratios at 2.5 mm penetration level. However, on higher penetration levels few fiber types started to perform like a geotextile due to the pressure on them and increased the bearing capacity of pavement. For this test series, Fiber 6 reinforced model showed highest CBR value.

- When fibers were equally mixed in soil and CBR tests were conducted, the highest CBR result was observed from model reinforced with Fiber 6, which is smallest in length and weight. Since all fibers were tested at 1% content and applied weights were equal, Fiber 6 had more pieces than other fibers in soil. In addition to this, smallest and thinnest Fiber 6 adapted and reshaped in soil easier than other fiber types which observed in hand mixing process as well. In fact, fiber that showed the highest CBR, had the least tensile strength among fibers.

- This study showed that, the physical properties and amount of fibers could be more important than the tensile strength for achieving higher CBR results.
- When fibers used with a single geotextile as reinforcement in the pavement models, highest CBR result was observed from Geotextile 1 and Fiber 6 combination. However, CBR results at 2.5 mm penetration level were found less than unreinforced model for most fiber types. On the other hand, bearing capacities of all geotextile and fiber combined models were found higher than unreinforced model at 10 mm penetration level. It was thought that, this reinforcement combination starts to perform in soil better at higher stress levels.
- Bearing ratio of geotextile with smallest fiber reached up to 3.70 times of unreinforced pavement.
- When comparing the different reinforcement types, it can be seen that geotextile improve soil better than other reinforcement types. Then geogrids show better performance than fibers.
- When thicknesses of the pavements were calculated for unreinforced and reinforced conditions, it was observed that most of the reinforced pavements had less thickness values and higher bearing capacities than unreinforced model. As geosynthetics, Geotextile 1, 2, 6, 9 and 10 were the reinforcements which provided highest stress loads, increased CBR and decreased the thickness values most. As fiber reinforcement, best results were obtained from Fiber 6, in terms of performance and pavement thickness reduction.
- It was examined that reinforcements could decrease the cost of soil almost half by reducing the pavement thickness with providing higher bearing capacities.
- Although some reinforcements can increase costs in total like fibers, some thin and affordable geotextiles can increase bearing capacity remarkably when they are used in either subbase or base course. Among all types of reinforcements, Geotextile 9 and 10 were found highly effective in both economical and practical ways.

Consequently, behaviors of over twenty reinforcements and their alternative uses in pavement soil were examined in this research with conducting laboratory CBR tests and it was observed that, cost effective reinforcements can improve the bearing capacity of soil significantly. It is recommended that, other behaviors of same type of reinforcements on different testing methods can be investigated in further studies.

6. REFERENCES

- AASHTO Guide for Design of Pavement Structures, 1993 Volume 1; Volume 1993 of AASHTO Guide for Design of Pavement Structures, American Association of State Highway and Transportation Officials.
- AASHTO M 145-91 Standard Specification for Classification of Soils and Soil-Aggregate Mixtures for Highway Construction Purposes (2017).
- AASHTO T 180-19 Standard Method of Test for Moisture-Density Relations of Soils Using a 4.54-kg (10-lb) Rammer and a 457-mm (18-in.) Drop (2019).
- AASHTO T 193-13 Standard Method of Test for The California Bearing Ratio (2017).
- AASHTO T 88-19 Standard Method of Test for Particle Size Analysis of Soils (2019).
- Abbaspour, M., et al., Reuse of Waste Tire Textile Fibers as Soil Reinforcement, Journal of Cleaner Production, 207 (2019) 1059-1071.
- Ahmad, F. et al., Performance Evaluation of Silty Sand Reinforced with Fibres, Geotextiles and Geomembranes, 28-1 (2010) 93-99.
- Anggraini, V. et al., Effects of Coir Fibers on Tensile and Compressive Strength of Lime Treated Soft Soil, Measurement, 59 (2015) 372-381.
- ASTM C1444-00, Standard Test Method for Measuring the Angle of Repose of Free-Flowing Mold Powders, ASTM International, West Conshohocken, PA, 2000, www.astm.org
- ASTM D2487-06, Standard Practice for Classification of Soils for Engineering Purposes (Unified Soil Classification System), ASTM International, West Conshohocken, PA, 2006, www.astm.org
- ASTM D854-14, Standard Test Methods for Specific Gravity of Soil Solids by Water Pycnometer, ASTM International, West Conshohocken, PA, 2014, www.astm.org
- Ateş, A., Mechanical Properties of Sandy Soils Reinforced with Cement and Randomly Distributed Glass Fibers (GRC), Composites Part B: Engineering, 96 (2016) 295-304.
- Azar, K., Dabiri, R., The Effects of Geotextile Layers on Bearing Capacity of Gravel-Silt Mixtures, Trakya University Journal of Engineering Sciences, 16 (2015) 61-69.

- Baricevic, A. et al., Influence of Recycled Tire Polymer Fibers on Concrete Properties, *Cement and Concrete Composites*, 91 (2018) 29-41.
- Chang, L.C. et al., Effect of Mixing Conditions on the Morphology and Performance of Fiber-Reinforced Polyurethane Foam, *Journal of Cellular Plastics*, 51-1 (2014) 103-119.
- Cui, H. et al., Effect of Carbon Fiber and Nanosilica on Shear Properties of Silty Soil and the Mechanisms, *Construction and Building Materials*, 189 (2018) 286-295.
- Çelik, Ö., Geotekstil Donatılı Kum Zeminlerin Taşıma Gücünün Deneysel Olarak İncelenmesi, MS Thesis, Fırat University Institute of Science and Technology, Elazığ, 2020.
- Dhand, V. et al., A Short Review on Basalt Fiber Reinforced Polymer Composites, *Composites Part B: Engineering*, 73 (2015) 166-180.
- Dione, A. et al., Implementation of Resilient Modulus - CBR relationship in Mechanistic-Empirical (M. -E) Pavement Design, *Sciences Appliquées et de l'Ingénieur*, 1 (2014).
- El-Naggar, M., Kennedy, J.B., New Design Method for Reinforced Sloped Embankments, *Engineering Structures*, 19-1 (1997) 28-36.
- Erken, A., Torabı, M., Cyclic and Post Cyclic Static Behavior of Fibre Reinforced Sand, MS Thesis, İstanbul Technical University Institute of Science and Technology, İstanbul, 2011.
- Federal Highway Administration <https://highways.dot.gov/>
- Giroud, J.P., Han, J., Design Method for Geogrid-Reinforced Unpaved Roads. II. Calibration and Applications, *Journal of Geotechnical and Geoenvironmental Engineering*, 130-8 (2004) 775.
- Gökova, S. et al, Taşıma Gücü Düşük Taban Zeminine Sahip Karayolu Üsstyapılarında Geogrid Kullanımının Üstyapı Yapısal Performansına Etkisi, Sekizinci Ulusal Geosentetikler Konferansı, Boğaziçi Üniversitesi, İstanbul, 2019.
- Goodarzi, S., Shahnazari, H., Strength Enhancement of Geotextile-Reinforced Carbonate Sand, *Geotextiles and Geomembranes*, 47-2 (2019) 128-139.
- Green, J.L., Hall, J.W., Non-destructive vibratory testing of airport pavement: Experimental tests results and development of evaluation methodology and procedure, *Airport Research and Technical Reports*, Federal Aviation

Administration, Washington D.C., **1975**.

- Hazirbaba, K., Large-Scale Direct Shear and CBR Performance of Geofibre-reinforced Sand, *Road Materials and Pavement Design*, 19-6 (**2017**) 1350-1371.
- Hejazi, S. et al., A Simple Review of Soil Reinforcement by Using Natural and Synthetic Fibers, *Construction and Building Materials*, 30 (**2012**) 100-116.
- Heukelom, W., Klomp, A.J.G., Dynamic Testing as a Means of Controlling Pavements During and After Construction, *Proceedings, 1st Int. Conf. on Struct. Des. Of Asphalt Pavement*, University of Michigan, Ann Arbor, Mich., **1962**, p. 667-679.
- Hossain, A. et al., Improvement of Granular Subgrade Soil by Using Geotextile and Jute Fiber, *International Journal of Science, Technology and Society*, 3-5 (**2015**) 230-235.
- <https://images.app.goo.gl/9XVWbHuydHiyvUs18> (Date of access: **May 2020**).
- <https://images.app.goo.gl/aNFuWWG7y3tUm8cs7> (Date of access: **May 2020**).
- <https://images.app.goo.gl/FyTgiWTKwCjnGKH79> (Date of access: **May 2020**).
- <https://images.app.goo.gl/TQJot2x6kTWJhW5J7> (Date of access: **May 2020**).
- <https://images.app.goo.gl/VQRPY816XRTYum5KA> (Date of access: **May 2020**).
- <https://images.app.goo.gl/Xdtx7tCyscaAyCxaA> (Date of access: **May 2020**).
- <https://images.app.goo.gl/xjgTSZgETyDvTT3s7> (Date of access: **May 2020**).
- https://www.yapikatalogu.com/en/concrete-and-concrete-admixtures/concrete-reinforcement-materials/atlas-1-yapi-fibermesh-650s-macro-synthetic-fiber-reinforcement_25144 (Date of access: **May 2020**).
- Infante, D.J.U. et al., Shear Strength Behavior of Different Geosynthetic Reinforced Soil Structure from Direct Shear Test, *International Journal of Geosynthetics and Ground Engineering*, 2-17 (**2016**).
- Jayalath G. et al., in *Pavement Model Tests to Investigate the Effects of Geogrid as Subgrade Reinforcement*, Liu, H., Mills, P., Ruxton, N., & Mazengarb, C. (Eds.), *Proceedings of the 12th Australian and New Zealand Young Geotechnical Professionals Conference*, **2018**, Australian Geomechanics Society, Australia, p. 1-8.
- Kravchenko, E. et al., Performance of Clay Soil Reinforced with Fibers Subjected to Freeze-Thaw Cycles, *Cold Regions Science and Technology*, 153 (**2018**) 18-24.

- Kumar, P., Mir, F., Use of Jute Fiber in Improving Geotechnical Properties of Soil, *Geotechnics for Transportation Infrastructure*, 29 (2019) 487-494.
- Lavasan, A., Ghazavi, M., Behavior of Closely Spaced Square and Circular Footings on Reinforced Sand, *Soils and Foundations*, 52-1 (2012) 160-167.
- Leng, J., Gabr, M., Deformation-Resistance Model for Geogrid-Reinforced Unpaved Road, *Transportation Research Record*, 1975-1 (2006) 146-154.
- Leone, M. et al., Fiber Reinforced Concrete with Low Content of Recycled Steel Fiber: Shear Behavior, *Construction and Building Materials*, 161 (2018) 141-155.
- Li, Y. et al., Tensile Strength of Fiber Reinforced Soil under Freeze-Thaw Condition, *Cold Regions Science and Technology*, 146 (2018) 53-59.
- Masoumi, M. et al., Experimental Study of Geotextile Effect on Improving Soil Bearing Capacity in Aggregate Surfaced Roads, *International Journal of Civil and Environmental Engineering*, 11-1 (2017) 43 - 49.
- Meshram, K. et al., Application of Coir Geotextile for Road Construction: Some Issues, *Oriental International Journal of Innovation Engineering Research*, 1-1 (2013) 25-29.
- Moghal, A.A.B. et al., Effect of Polypropylene Fibre Reinforcement on the Consolidation, Swell and Shrinkage Behaviour of Lime-Blended Expansive Soil, *International Journal of Geotechnical Engineering*, 12-5 (2018) 462-471.
- Naeini, S.A, Mirzakhani, M., The Effect of Geotextile and Grading on the Bearing Ratio of Granular Soils, *Electronic Journal of Geotechnical Engineering*, 13 (2008).
- Nazia, N., Deepthy, B.L., Study on the Compaction Characteristics of Jute Reinforced Cohesive Soil, *International Journal of Engineering Trends and Technology (IJETT)*, 36-4 (2016) 198-202.
- Nazzal, M., Field Evaluation of in-situ Test Technology for QC/QA Procedures During Construction of Pavement Layers and Embankments, MS thesis, Louisiana State University, Baton Rouge, 2003.
- Pandit, P. et al., Experimental Analysis of CBR Value of Soil Reinforced with Jute and Coir Fiber for the Evaluation of Pavement Thickness., *International Journal of Civil Engineering and Technology (IJCIET)*, 7-5, (2016) 439-446.
- Powell, W.D., Potter, J. F., Mayhew, H. C., and Nunn, M. E., The structural design of bituminous roads, TRRL report, London, 1984.
- Raju, S. et al., Strength Behavior of Subgrade Soil mixed with Sand

- Manufacturing Dust and Fiber, *Journal of GeoEngineering*, 13 (2018) 79-84.
- Santoni, R.L. et al., Engineering Properties of Sand-Fiber Mixtures for Road Construction, *Journal of Geotechnical and Geoenvironmental Engineering*, Vol. 127-3 (2001).
 - Sayida, M.K. et al., Coir Geotextiles for Paved Roads: A Laboratory and Field Study Using Non-Plastic Soil as Subgrade, *Journal of Natural Fibers* (2019) 1-16.
 - Seed, H.B. et al., Resilience Characteristics of Subgrade Soils and Their Relationship to Fatigue Failures to Asphalt Pavements, *Proceedings 1st International Conference on the Structural Design of Asphalt Pavements*, (1962) p. 611-636.
 - Seed, H.B., McNeill, R.L., Soil Deformation in Normal Compression and Repeated Loading Tests in Pressure Deformation Measurements in Earth, *Bulletin Highway Research Board*, 141 (1956).
 - Sharma, B. et al., A Study of CBR Properties of Soil Reinforced with Jute Geotextile with reference to the road construction, *Proceedings of Indian Geotechnical Conference, Assam, 22-24 December 2013*.
 - Sharma, V. et al., Enhancing Compressive Strength of Soil Using Natural Fibers, *Construction and Building Materials*, 93 (2015) 943-949.
 - Tavakoli Mehrjardi, G., Khazaei M., Scale Effect on the Behaviour of Geogrid-Reinforced Soil under Repeated Loads, *Geotextiles and Geomembranes*, 45-6 (2017) p. 603-615.
 - Tran K. et al., Improvement of Mechanical Behavior of Cemented Soil Reinforced with Waste Cornsilk Fibers, *Construction and Building Materials*, 178 (2018) 204-210.
 - Uzuner, B.A., *With Solved Problems Fundamentals of Soil Mechanics*, 1st Edition, Derya Kitabevi, 2015.
 - Vikram, M.B., Effect of Geotextiles on CBR Values, *International Journal of Emerging Trends in Engineering and Development*, 1-6 (2018) 118-125.
 - Wasti, Y., in *Polymers in Construction*, Akovali, G. (Ed.), Chapter 5, 2005.
 - Wei L. et al., Mechanical Properties of Soil Reinforced with Both Lime and Four Kinds of Fiber, *Construction and Building Materials*, 172 (2018) 300-308.
 - Yashas, S.R., Muralidhar H.R., Improvement of CBR using Jute Fiber for the Design of Flexible Pavement, *International Journal of Engineering Research Technology (IJERT)*, 4-9 (2015).

- Yetimođlu T., Salbas O., A Study on Shear Strength of Sands Reinforced with Randomly Distributed Discrete Fibers, *Geotextiles and Geomembranes*, 21-2 (2003) 103-110.
- Yetimođlu, T. et al., A Study on Bearing Capacity of Randomly Distributed Fiber-Reinforced Sand Fills Overlying Soft Clay, *Geotextiles and Geomembranes*, 23-2 (2005) 174-183.
- Yılmaz, H.R., Compaction and Strength Characteristics of Fly Ash and Fiber Amended Clayey Soil, *Engineering Geology*, 188 (2015) 168-177.
- Yılmaz, H.R., Eskiřar T., Cost Considerations on the Economy of Using Geotextiles and an Improvement Application Example for İzmir – Melez Delta, *Nonwoven Technical Textiles Technology*, (2003) 28-33.
- Yılmaz, H.R., Eskiřar, T., Usage of Geosynthetic Products to Solve Geotechnical Problems and Their Advantages, 2. Geoteknik Sempozyumu, Adana, 22-23 November 2007, *Bildiriler Kitabı*, 2007, p. 433-447.
- Ziegler, M., Application of Geogrid Reinforced Constructions: History, Recent and Future Developments, *Procedia Engineering*, 172 (2017) 42-51.
- Zornberg, J.R. et al., Monitoring Performance of Geosynthetic-Reinforced and Lime-Treated Low-Volume Roads under Traffic Loading and Environmental Conditions, *GeoCongress 2012: State of the Art and Practice in Geotechnical Engineering*, 2012, p. 1310-1319.